Numéro National de Thèse : 2016LYSEN028

THESE de DOCTORAT DE L'UNIVERSITE DE LYON

opérée par

l'Ecole Normale Supérieure de Lyon

Ecole Doctorale N° 340

Biologie Moléculaire, Intégrative et Cellulaire

Spécialité de doctorat : Science de la Vie

Discipline : Infectiologie

Soutenue publiquement le 28/10/2016, par :

Axel ROSSI

Intracellular fate of AAV particles in human Dendritic Cell and impact on Gene Transfer

---

Devenir intracellulaire des vecteurs AAV dans les cellules dendritiques humaines et conséquences sur le transfert de gène

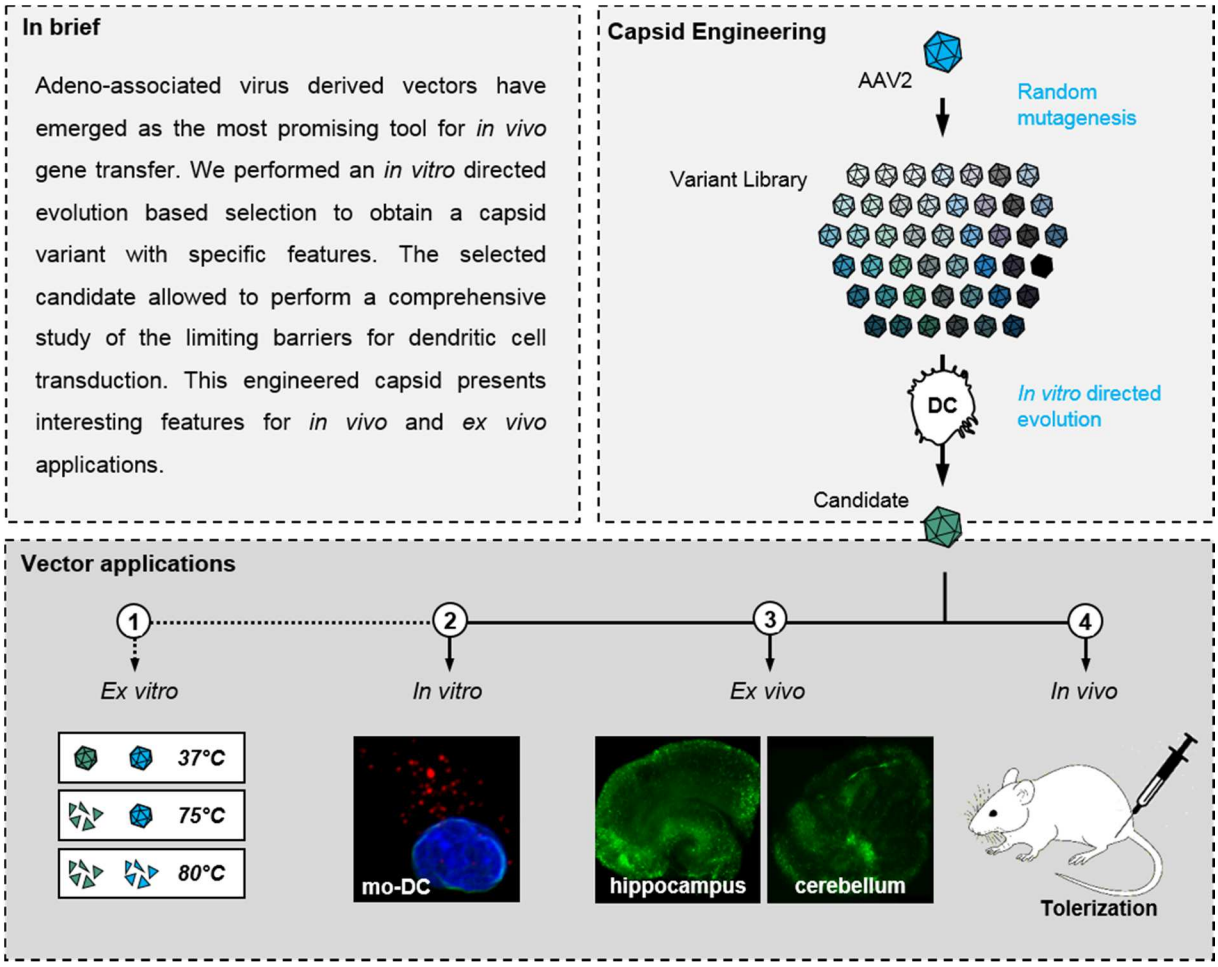
Devant le jury composé de :

ADRIOUCH,	Sahil	PhD	Université de Rouen	Examinateur
BÜNING,	Hildegard	PhD	Faculté de Médecine de Hanovre	Co-directrice
DAVOUST,	Jean	PhD	Université Paris Descartes	Rapporteur
DUTARTRE,	Hélène	PhD	Université de Lyon	Examinatrice
FAURE,	Mathias	PhD	Université de Lyon	Examinateur
GRIMM,	Dirk	PhD	Université de Heidelberg	Rapporteur
SALVETTI,	Anna	PhD	Université de Lyon	Directrice

Résumé

Les vecteurs viraux dérivés du virus adéno-associé (AAV) apparaissent depuis deux décennies comme des outils efficaces pour le transfert de gène *in vivo*. Cependant, malgré une faible immunogénicité et une absence de toxicité *in vivo*, leur optimisation requiert encore un effort important vers une meilleure compréhension de leur biologie et, en particulier, de leur interaction avec le système immunitaire. Au cours de ce travail de thèse, nous avons utilisé une méthode de sélection dirigée *in vitro* dans le but d'obtenir un variant de capside capable de transduire efficacement un type cellulaire non-permissif aux vecteurs AAV : les cellules dendritiques (DC). En effet, ces cellules jouent un rôle primordial dans l'établissement de la réponse immunitaire et, par conséquent, dans la persistance de l'expression du transgène *in vivo*. Cette technologie, très répandue dans la communauté AAV, a permis de sélectionner un variant de capside aux propriétés très intéressantes. La mutation sélectionnée, caractérisée *in vitro* comme induisant une instabilité de la capside, a permis d'identifier et de surmonter un point de blocage majeur dans le processus de transduction des DC par les vecteurs AAV, consistant dans l'étape de décapsidation du génome du vecteur dans le noyau cellulaire. De manière intéressante, le variant obtenu exhibe un avantage en terme de transduction, non seulement dans les DC, mais aussi dans différents modèles de cellules primaires humaines (*e.g.* HUVEC) ou animales (OBC), peu ou pas permissives à l'AAV. De plus, des expériences de transfert de gène *in vivo* réalisées dans un modèle murin, indiquent que le variant sélectionné conduit à une meilleure expression du transgène, possiblement due à la mise en place d'un processus de tolérisation. Les propriétés remarquables de ce variant de capside, font de lui un candidat intéressant pour des applications médicales.

Graphical abstract



Abstract

Vectors derived from the Adeno-associated virus (AAV) have emerged as an efficient system for *in vivo* gene transfer. However, despite their low immunogenicity and good tolerance *in vivo*, a better characterization of the host-AAV interaction is required to be able to fully exploit AAV potential for a gene therapy or gene vaccination. In this PhD project, we have used an *in vitro* directed evolution strategy to select an AAV capsid variant able to transduce human dendritic cell (DC), a non-permissive cell type which plays a critical role in the initiation of immune responses and, consequently, on the persistence of expression of the transgene *in vivo*. This procedure allowed us to identify an AAV variant characterized by a decreased stability of the capsid *in vitro*. The use of this mutant as a vector to transduce human DC resulted in an improved uncoating of the vector genome in the cell nucleus, thus identifying this step as major barrier toward DC transduction. Interestingly, the selected variant also displayed an increased transduction efficiency not only in DC but also in different primary human and animal cell types, poorly or non-permissive to AAV. Finally, when injected in mice, this AAV variant resulted in a higher expression of the transgene, associated to a low level of immune responses, suggesting the induction of a tolerant state. These remarkable features suggest that our selected variant capsid is a promising candidate for medical applications.

Table of content

Résumé 3
Graphical abstract 4
Abstract 4
Table of content 5
Abbreviations 8
List of figures 10
List of tables 11
I Introduction 12
I.1 The Adeno-Associated Virus: an atypical virus 12
I.1.1 Natural serotypes and variants 13
I.1.2 Genome organization 18
I.1.3 Structure of the viral capsid 20
I.1.4 Physical properties of the AAV virions 22
I.2 The viral cycle: a long winding road strewn with dangers and difficulties 25
I.2.1 Binding on the cell membrane 27
I.2.2 Entry into the target cell 28
I.2.3 Intracellular trafficking and degradation 29
I.2.4 Nuclear entry and genome release 32
I.2.5 Latent and productive phases 34
I.3 Recombinant AAV: a toolkit for gene transfer 35
I.3.1 rAAV mediated gene transfer for medical applications 36
I.3.2 AAV vectors improvements 40
I.4 AAV and Immunity: a challenging field of study for medical application 46
I.4.1 Innate immune responses against rAAV 47
I.4.2 Adaptive immune responses against rAAV capsids 48
I.4.3 Immune responses against the transgene product 51
I.5 Dendritic cells: a pivotal actor of the Immunity 52
I.5.1 Dendritic cells as the principal professional APC of the immune system 53
I.5.2 Maturation of the dendritic cells 53
I.5.3 Adeno-associated virus derived and dendritic cells 55
II. Materials and Methods 57
II.1 Adeno-associated virus derived vector production 57

II.2 Cell lines and infection procedures 58
II.2.1 Culture of monocyte-derived dendritic cells (mo-DC) 58
II.2.2 Cell Transduction 59
II.3 *In vitro* directed evolution of AAV particles 60
II.3.1 Overview of the selection procedure 60
II.3.2 Construction of AAV sub-libraries 61
II.3.3 Next generation sequencing 65
II.3.4 Production of rAAV with selected capsid 65
II.4 Analysis of intracellular AAV distribution 66
II.4.1 Fractionation assay 66
II.4.2 Western blot analysis 66
II.4.3 Quantification of AAV vector DNA by qPCR 68
II.4.4 Confocal microscopy analysis 68
II.4.5 *In vitro* uncoating assay 69
II.5 Analysis of capsid stability 69
II.6 *In vivo* experiments in mice 70
II.6.1 Quantification of rAAV mRNA in transduced muscles 70
II.6.2 IFNγ-ELISPOT assay 70
II.6.3 Anti-OVA IgG ELISA 71
II.6.4 Fluorescence-activated cell sorting analysis 71
II.7 Experiments on brain sections 72
II.8 Statistical analysis 72
III. Results 73
III.1 Presentation of the project and its objectives 73
III.2 Deciphering the interaction between AAV particles and human DC 73
III.2.1 rAAV particles enter DC but remain unable to transduce them 74
III.2.2 rAAV2 particles can reach the nucleus of DC 75
III.2.3 Selection of AAV capsid variants able to transduce DC 77
III.2.4 Identification of the rate-limiting steps for rAAV transduction of human DC 81
III.2.5 Analysis of the cell tropism of the selected AAV variants 91
III.3 Immune responses induced by the VSSTSPR variant *in vivo* 91
III.3.1 VSSTSPR presents interesting features *in vivo* 91
III.4 Analysis of AAV virions features by Atomic Force Microscopy 93
III.4.1 Atomic Force Microscopy 94
III.4.2 Quantitative analysis of the virions destabilization 95

III.4.3 Genome releasing 98
III.5 VSSTSPR, a powerful tool for research in brain 100
III.5.1 Organotypic brain culture as an elegant model to study MeV infection 101
III.5.2 Preliminary results 101
III.5.3 VSSTSPR in action in OBC 103
III.5.4 VSSTSPR has no effect on MeV replication *in vitro* 105
III.6 Conclusion 107
IV. Discussion 108
IV.1 Intracellular fate of AAV particles in human DC 108
IV.2 VSSTSPR: a bipolar candidate for gene transfer? 110
IV.3 New criteria for future selections 113
IV.4 Going beyond… 115
V. Popularization project on gene therapy using viral vectors 116
V.1 Project description 116
V.1.1 Project and members 116
V.1.2 A useful and challenging project 116
V.1.3 Concepts of biology 116
V.1.4 Method 117
V.1.5 Format 117
V.1.6 Target lectors 118
V.2 Resources 118
V.2.1 Estimated budget 118
V.2.2 Collaborators 118
V.2.3 Financial support (prospection in progress) 119
V.3 Extract of the comic 120
VI. References 123
VII. Acknowledgments 137
IX. Publications 139

Abbreviations

A.

αA:	Alpha helix
Å:	Angstrom (unit)
AAP:	Assembly-activating protein
AAV:	Adeno-associated virus
AAVR	AAV receptor (KIAA0319L)
AAVS:	AAV integration site
ADA:	Adenosine deaminase
AdV:	Adenovirus
AFM:	Atomic force microscopy
AID:	Autoimmun Diagnostika
APC:	Antigen presenting cell
APS:	Ammonium persulfate
ASR:	Ancestral sequence reconstruction
ATP:	Adenosine triphosphate
Atm:	Atmosphere (unit)

B.

βA:	β-strand A
βB-βI:	β-barrel
bb:	Baboon
BR:	Basic region
BSA:	Bovine serum albumin

C.

C-Term:	Carboxyl terminal domain
C2C12:	Mouse myoblast cell line
C57BL/6J:	C57 Black 6 laboratory mouse
$CaCl_2$:	Calcium chloride
CCP:	Clathrin-coated pit
CD:	Cluster of differentiation
Cdk-2:	Cyclin-dependent kinase 2
cDNA	complementary DNA
CEB:	Cytosol extraction buffer
CFTR:	cystic fibrosis transmembrane conductance regulator
Ch:	Chimpanzee
CLIC/GEEC	Clathrin-independent carriers/GPI enriched endocytic compartment
CMV:	Cytomegalovirus
CNS:	Central nervous system
CO_2:	Carbon dioxide
cOVA:	Cytosolic Ovalbumin
CsCl:	Cesium chloride
CSF:	Colony stimulating factor
CTL:	Cytotoxic response mediated by CD8+ T-cell
Cy:	Cynomolgus macaque

D.

DAPI:	4',6-Diamidino-2-phenylindole
DC:	Dendritic cell
DC-SIGN:	DC-specific intercellular adhesion molecule 3 grabbing non-integrin
DMD:	Duchenne muscular dystrophy
DMEM:	Dulbecco's Modified Eagle Medium
DMSO:	Dimethyl sulfoxide
DNA:	Deoxyribonucleic acid
DNase:	Deoxyribonuclease
dNTP:	Deoxy-nucleoside triphosphate
DPI:	Dibenziodolium chloride
ds:	Double strand
dsRNA:	double strand RNA
Dyn:	Dynamin

E.

e.g.	Lat. *Exempli gratia* (“for example”)
EC:	Endothelial cell
EE:	Early endosome
EGFR:	Epidermal growth factor receptor
ELISA:	Enzyme-linked immunosorbent assay
ELIspot:	Enzyme-linked immunospot
EMA:	European medical agency
epDNA:	Episomal DNA
ER:	Endoplasmic reticulum
etc.	Lat. *et cetera* (“and the rest”)

F.

FACS:	Fluorescence-activated cell sorting
FBS:	Fetal bovine serum
FCS:	Fetal calf serum
FGFR1:	Fibroblast growth factor receptor 1
FITC:	
FIX:	Coagulation Factor IX

G.

GFAP:	Glial fibrillary acidic protein
GPI:	Glycosylphosphatidylinositol (GPI anchor)
GTP:	Guanosine triphosphate
GFP:	Green fluorescence protein
GFP^+:	GFP positive (cell)
GM-CSF:	Granulocyte macrophage-CSF
GPI:	Glycosylphosphatidylinositol (GPI anchor)
GRAF1:	GTPase Regulator Associated with Focal Adhesion Kinase
GTP:	Guanosine triphosphate
GTPase:	GTP hydrolase enzyme

H.

H_2SO_4:	Sulfuric acid
HBV:	Hepatitis B virus
HCC:	Hepatocellular carcinoma
HCV:	Hepatitis C virus
HEK-293:	Human embryonic kidney cell line 293
HeLa:	Henrietta Lacks cell line
Hep:	Heparin
HEPES:	2-[4-(2-hydroxyethyl)piperazin-1-yl]ethanesulfonic acid
HGFR:	Hepatocyte growth factor receptor
HIV:	Human immunodeficiency virus
HLA-DR:	Human Leukocyte Antigen - antigen D Related
HPV:	Human Papillomavirus
HR:	Homologous recombination
HRP:	Horseradish peroxidase
HSPG:	Heparan sulfate proteoglycan
HSV:	Herpes simplex virus
Hu:	Human
HUVEC:	Human umbilical vein endothelial cell

I.

i.e.	Lat. *Id est* (“that is”, “in other words”)
iDC:	Immature monocyte derived dendritic cell
IFN:	Interferon
IgG :	Immunoglobuline G
IL:	Interleukin
IM:	Intramuscular
IP:	Inhibitor of protease
ITR:	Inverted terminal repeat

K.

kb	kilo base (unit)

L.

LamR: 37/67kDa laminin receptor
LCA: Leber's congenital amaurosis
LE: Late endosome
LPLD: Lipoprotein lipase deficiency
LPS: Lipopolysaccharides
LSM: Laser scanning microscopy
LYS: Lysosome

M.

mDC: Mature monocyte derived dendritic cell
mDCpi: Monocyte derived dendritic cell maturated post infection
MEB: Membrane extraction buffer
MEM: Minimum essential media
MeV: Measles virus
MF: Microfilament
MHC-I: Major Histocompatibility Complex class I
MHC-II: Major Histocompatibility Complex class II
MID: Multiplex Identifiers
Middle P: Middle Part
mo-DC: Monocyte derived dendritic cell
MOI: Multiplicity of infection
mRNA: Messenger RNA
MT: Microtubule
mutITR: Mutated ITR
MVM: Minute virus of mice
MyD88: Myeloid differentiation primary response gene 88

N.

N-Term: Amino terminal domain
NAb: Neutralizing antibody
NaCl: Natrium chloride
NEAA Non-essential amino-acid
NEB: Nuclear extraction buffer
NEBD: Nuclear envelope breakdown
NFκB: Nuclear factor κB
NGS: Next generation sequencing
NHP: Non-human primate
$NiCl_2$: Nickel Chloride
NIH: National Institutes of Health
3T3: Fibroblast cell line
NiV Nipah Virus
NK: Natural killer (cell)
NLS: Nuclear localization signal
NP: Nucleoplasm
NPC: Nuclear pore complex
Nts: Nucleotide (Unit)

O.

OBC: Organotypic brain culture
ORF: Open reading frame
OT-I: CMH-I OVA Immunodominant peptide
OT-II: CMH-II OVA Immunodominant peptide
OVA: Ovalbumin

P.

P/S: Penicillin-streptomycin
PAMP: Pathogen associated motif patterns
PBL: Peripheral blood lymphocyte
PBMC: Peripheral blood mononuclear cell
PBS: Phosphate buffer solution
PCR: Polymerase chain reaction
pDC: Plasmacytoid dendritic cell
PDGFR: Platelet-derived growth factor receptor
Pi (figure2): Pigtail macaque
Pi (figure18): Post infection
PL-8: Capsid immunodominant peptide
pN: piconewton (Unit)
PNRE: Perinuclear recycling endosome
Poly-A: Poly polyadenylation (Signal)
PPi: Inorganic pyrophosphate
PRR: Pattern recognition receptor

Q.

qPCR: Quantitative polymerase chain reaction

R.

R.U.: Relative Unit
rAAV: Recombinant adeno-associated vector
rab: G-protein rab (Ras superfamily)
Rac1: Ras-related C3 botulinum toxin substrate1
Raw 264.7: Murine macrophage cell line
RBS: Rep binding site
RC: Replication center
Rh: Rhesus macaque
RNA: Ribonucleic acid
RPMI: Roswell Park Memorial Institute medium
RT-qPCR: Reverse transcription- qPCR

S.

SA: Splice acceptor site
sc: Self complementary (AAV)
SCID: Deficient severe combined immunodeficiency
SD: Splice donor site
SDS: Sodium dodecyl sulfate
SDS-PAGE: SDS-Polyacrylamide gel electrophoresis
SEM: Standard error of the mean
SFU: Spot forming units
SH-5YSY: human neuron cell line
SIV: Simian immunodeficiency virus
SM: Skeletal muscle
SPN: Supernatant
ssAAV: Single strand AAV

T.

T: Triangulation number
T-CD8$^+$: Lymphocyte CD8 positif
T5: Phage T5
TAP: Transporter associated with Antigen Processing
tDNA: Total DNA
TG: Transgene (expression)
TGN: Trans-Golgi network
TIL: Tumor-infiltrating lymphocytes
TGN: Trans-Golgi network
TLR: Toll like receptor
Treg: Regulatory T cell
TRS: Terminal resolution site

U.

UPS: Ubiquitin protease system

V.

vg: Viral genome (Unit)
VP: Viral protein
VR: Variable region
VV: Vaccinia virus

W.

WGA: Wheat germ agglutinin
WHO: World Health Organization
wt: wild type

List of figures

Figure 1. Direct observation of AAV2 virions by electronic microscopy. 13
Figure 2. Phylogeny of AAV variants. 14
Figure 3. AAV2 genome organization. 19
Figure 4. AAV capsid organization. 21
Figure 5. Overview of AAV life-cycle. 26
Figure 6. Wild type and rAAV genomes. 36
Figure 7. Overview of gene transfer in clinical trials worldwide. 37
Figure 8. AAV vector applications. 38
Figure 9. Principle of gene therapy and gene vaccination using AAV vectors. 39
Figure 10. Trans-splicing of rAAV genomes 42
Figure 11. Self-complementary rAAV genomes 43
Figure 12. rAAV capsid engineering. 45
Figure 13. Maturation of DC. 54
Figure 14. Plasmids for rAAV production. 57
Figure 15. rAAV production. 58
Figure 16. Overview of the mo-DC production and control. 59
Figure 17. Cell culture, protocol outline. 60
Figure 18. Selection of AAV particles targeting mo-DC by directed evolution. 61
Figure 19. Cloning and sequencing of viral DNA extracted from AAV-transduced mo-DC. 63
Figure 20. New AAV library production. 64
Figure 21. Selected variants from three independent selections. 65
Figure 22. Fractionation procedure. 67
Figure 23. *In vitro* uncoating assay. 69
Figure 24. AAV vectors are unable to transduce iDC despite their entry. 75
Figure 25. Immunofluorescence analysis of scAAV2-GFP particles localization within iDC. 76
Figure 26. Intracellular fate of rAAV2 vector particles. 77
Figure 27. Mutagenesis of AAV capsid. 78
Figure 28. Mutations selected on iDC. 79
Figure 29. Transduction efficiencies of rAAV on human DC according to their maturation status. . 81
Figure 30. HSPG binding is required for efficient transduction of mDCpi with rAAV. 82
Figure 31. Intracellular distribution of AAV particles within mo-DC. 83
Figure 32. Effect of intra-vesicular acidification on AAV transduction of human DC. 85
Figure 33. The VSSTSPR mutation decreases the stability of the capsid. 86
Figure 34. The uncoating is inefficient in hDC in comparison to HeLa cells. 87
Figure 35. The uncoating is not influenced by the VSSTSPR mutation into HeLa cells. 89
Figure 36. VSSTSPR and DC maturation of DC enhance the uncoating efficiency. 90
Figure 37. Analyses of VSSTSPR induced immune responses in vivo. 92
Figure 38. Atomic Force Microscope. 94
Figure 39. Super resolution image of AAV2 full capsids obtained from AFM. 95
Figure 40. Analysis of AAV8 and AAV9 thermal stability by native dot blot. 96
Figure 41. AFM images of ssAAV particles submitted to increasing temperatures. 97
Figure 42. Destabilization behavior of AAV8 and AAV9 at different temperatures. 98
Figure 43. AAV8 genome release upon heating. 99
Figure 44. Comparative analysis of the transduction efficiency of rAAV2 vs VSSTSPR. 103

Figure 45. VSSTSPR is a better candidate than rAAV2 to transduce cells within OBC. 104
Figure 46. Transduction efficiency of OBC cell types by VSSTSPR. 105
Figure 47. Analysis of VSSTSPR impact on MeV replication in vitro. 106
Figure 48. Illustration of the binding step (p1). 120
Figure 49. Illustration of the binding step (p2). 121
Figure 50. Illustration of the binding step (p3). 122

List of tables

Table 1. Percentage of sequence homology in VP1 amino acid sequences of AAV1 to AAV9 15
Table 2. Origin of common AAV isolates, receptors and tissue tropisms 16
Table 3. Serological evaluation of AAV vectors 18

I Introduction

Adeno-associated virus (AAV) derived vectors appear today as one of the most promising gene delivery system for human gene therapy. Since AAV discovery, fifty years of an intense scientific exploration allowed vectorization and application of a number of its advantageous features [1], [2]. The best illustration of this success story is Glybera® [3]–[5]: the first gene therapy drug that has received marketing authorization in Europe is using AAV as a delivery tool. However, in order to optimize AAV vectors for clinical use and broaden their spectrum of application, AAV host interaction, in particular with immune cells, needs to be further characterized.

I.1 The Adeno-Associated Virus: an atypical virus

AAV, the first human parvovirus to be described [6], was isolated in 1965 as a contaminant of adenovirus (AdV) preparations [7]–[9] (**Figure 1**), and then identified in a wide range of mammals including human and non-human primates (NHP). AAV is composed of a non-enveloped icosahedral capsid, containing a single stranded deoxyribonucleic acid (DNA) genome. Due to its replication-defective phenotype, AAV defined the genus of *Dependovirus* within the *Parvovirinae.* Specifically, AAV requires the help of a non-related virus for efficient replication and progeny production. The first helper virus identified for AAV is AdV and this relationship explains its name of “Adeno-Associated Virus”. Later on several other viruses such as Herpes Simplex Virus (HSV) [10], [11], Vaccinia Virus (VV) [12], and Human Papillomavirus (HPV) [13] have also been described as able to promote AAV replication. In the absence of any helper virus, AAV is able to maintain its genome in the host cell, in a latent form as an integrated or episomal molecule (latent phase). Replication can be switched on after infection of the cell by a helper virus. The high prevalence of AAV in the human species [14], [15] and the absence of any associated disease lead to consider it as a non-pathogenic commensal virus in humans [16]. However, a recent controversially discussed study suggests a potential role for AAV genome integration in the development of hepatocellular carcinoma (HCC) [17].

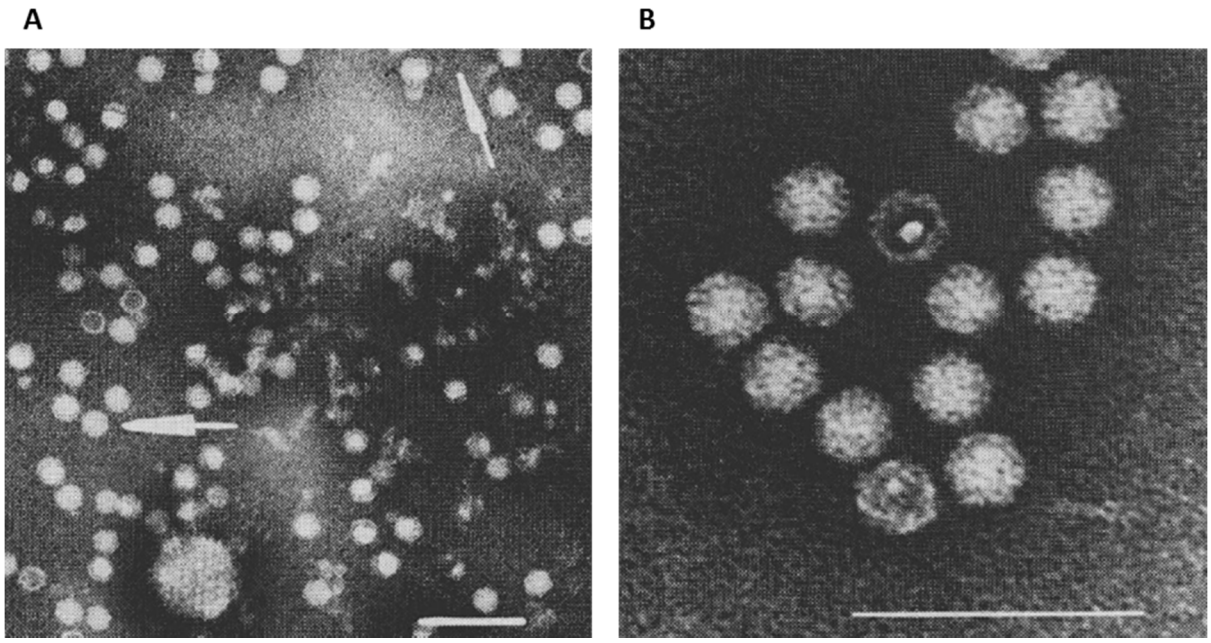


Figure 1. Direct observation of AAV2 virions by electronic microscopy.
A. AdV preparation purified by differential centrifugation. Several smaller AAV particles (arrows) surround the typical adenovirus capsid. **B.** Purified AAV particles obtained by membrane filtration. Units resembling capsomeres are visible on the surface of the capsid. Scale, 1000 Å. (figure from [7]).

I.1.1 Natural serotypes and variants

To date, more than one hundred AAV variants have been identified in human and NHP tissues [18], [19] (**Figure 2**), including thirteen serotypes which share 50 to 99% of sequence homology (**Table 1**). These variants have been divided in six clades according to their amino acid sequences. However, in addition to primates, AAV genomes have been also isolated from a large range of animal species such as horse, cow, chicken, lizard, goat and cat [20].

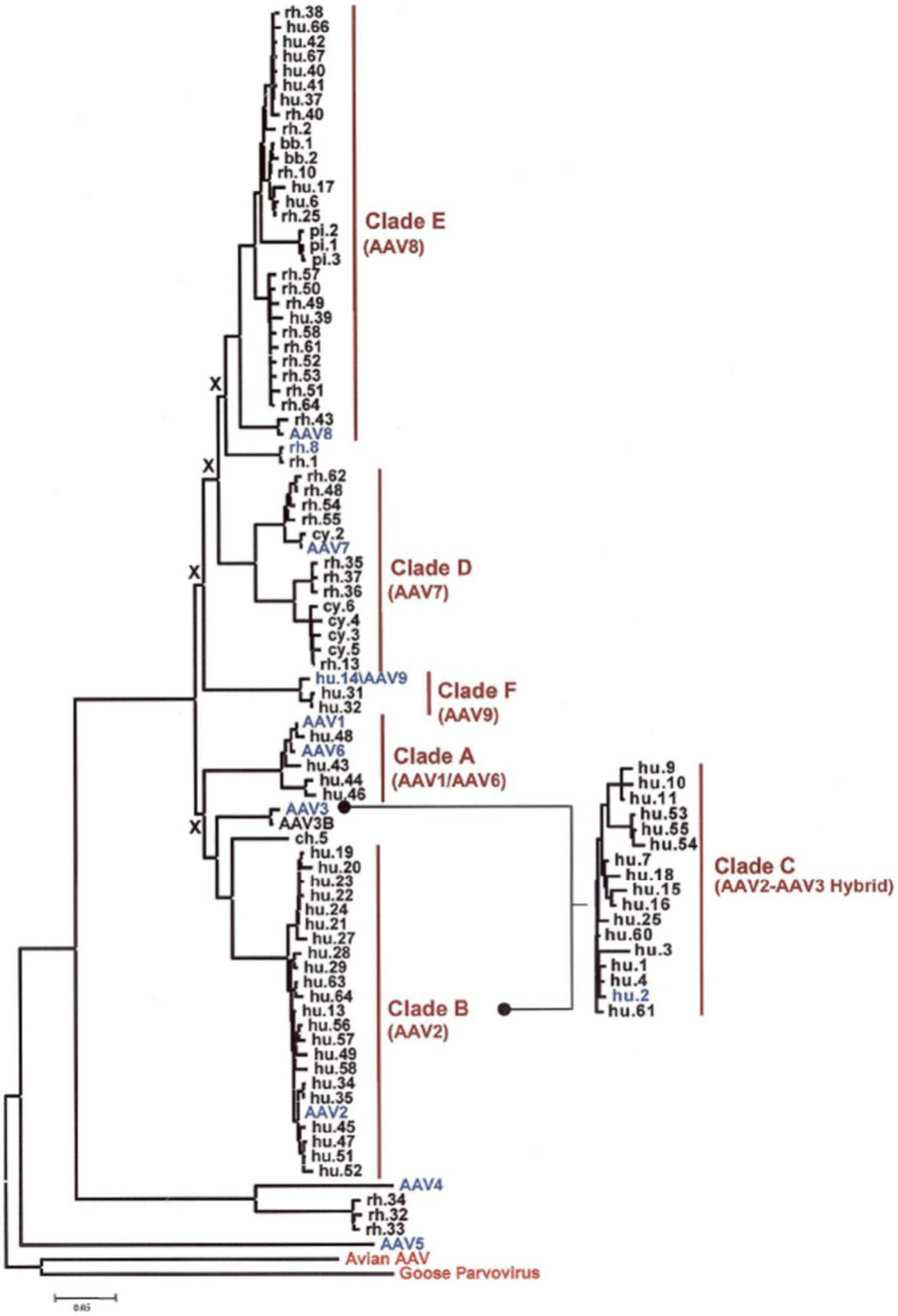


Figure 2. Phylogeny of AAV variants.

Neighbor-joining phylogenies of the VP1 protein sequences from primate AAV. Major nodes with bootstrap values < 75 are indicated with an "X." A goose parvovirus and an avian AAV were considered as an out group. Clades are indicated by their names and vertical lines on the right. The nomenclature for each taxa is either the serotype name or a reference to the species source (**hu,** human; **rh,** rhesus macaque; **cy,** cynomolgus macaque; **bb,** baboon; **pi,** pigtailed macaque; **ch,** chimpanzee), followed by a number indicating the order in which they were sequenced. The AAV2-AAV3 hybrid clade (clade C) originated from a recombination event, and its unrooted neighbor-joining phylogeny is shown [19].

This huge repertoire of AAV serotypes and variants has several advantages for gene transfer applications as in principle each variant can target a specific range of tissues according to its tropism. In addition, use of alternative serotypes can also allow, at least in experimental models, to overcome anti-AAV pre-existing immunity in the host [20].

Table 1. Percentage of sequence homology in VP1 amino acid sequences of AAV1 to AAV9

	AAV1	AAV2	AAV3	AAV4	AAV5	AAV6	AAV7	AAV8	AAV9
AAV1	**100**								
AAV2	83	**100**							
AAV3	87	88	**100**						
AAV4	63	60	63	**100**					
AAV5	58	57	58	53	**100**				
AAV6	99	83	87	63	58	**100**			
AAV7	85	82	85	63	58	85	**100**		
AAV8	84	83	86	63	58	84	88	**100**	
AAV9	82	82	84	62	57	82	82	85	**100**

(from [21])

AAV1 to AAV6 were isolated from AdV stock, except for AAV5 which was isolated from a human penile condylomatous wart. However, most of the other AAV serotypes and variants were identified directly *in vivo* using a PCR assay with primers that hybridize to conserved regions in the *cap* gene. Thereby, *cap* genes, differing in the variable region were isolated from various tissues. Based on the prevalence, it is currently assumed that AAV2, 3, 6 and 9 are of human origin, whereas AAV4, 7, 8, and 10 appear to have originated from monkeys (**Table 2**). The origin of the AAV1 is still controversial. Interestingly, AAV6 which displays a high capacity to transduce cells non-permissive to other serotypes, is considered to be a hybrid virus produced by a recombination event between AAV2 and AAV1, which occurred in cell culture or *in vivo* [22].

The initial reason for identifying new AAV variants was to develop vectors with specific tropisms. As AAV2, the first serotype used for gene transfer, most of the other AAV capsids are characterized by a wide tropism [22]. However, despite the difficulty to analyze results from studies conducted with a large range of experimental conditions such as multiplicity of infection (MOI), promoters, production methods or transgenes, it is commonly assumed that each serotype has a unique transduction profile (**Table 2**).

Table 2. Origin of common AAV isolates, receptors and tissue tropisms

Serotypes	origins	Receptors and co-receptors	Tissue tropisms
AAV1	Human or NHP	N-linked sialic acid, AAVR	SM[murine, NHP, canine,] CNS[murine, NHP,] airway[murine, NHP,] retina[murine,] pancreas[murine,] heart[murine, pig,] liver[murine.]
AAV2	Human	HSPG, FGFR1, HGFR, LamR, CD9, integrin αVβ5, α5β1, AAVR	SM[murine,] CNS[murine, monkey,] liver[murine,] kidney[murine,] retina[murine, canine, human, NHP]
AAV3	Human	HSPG, FGFR, HGFR, LamR, AAVR	HCC[human,] SM[murine]
AAV4	NHP	O-linked sialic acid	CNS[murine,] retina[murine, canine,] lung[murine, NHP,] kidney[murine]
AAV5	Human	N-linked sialic acid, PDGFR, AAVR	SM[murine,] CNS[murine, canine,] airway[murine,] retina[murine]
AAV6	Human	N-linked sialic acid, EGFR, AAVR	SM[murine, dog,] heart[murine, dog, sheep, pig,] airway[murine, dog, NHP]
AAV7	Rhesus macaque	?	SM[murine,] retina[murine,] CNS[murine,] liver[murine]
AAV8	Rhesus macaque	LamR, AAVR	Liver[murine, NHP, canine,] SM[murine,] CNS[murine,canine,NHP,] retina[murine, canine,] pancreas[murine,] heart[murine,] kidney[murine]
AAV9	Human	LamR, N-linked glycans, AAVR	Liver[murine,] heart[murine, NHP, porcine,] SM[murine, canine,] lung[murine,] pancreas[murine,] CNS[murine, NHP,] retina[murine, NHP,] testes[murine,] kidney[murine]
AAVrh10	Rhesus macaque	LamR	Liver[murine,] heart[murine,] SM[murine, canine,] lung[murine,] pancreas[murine,] CNS[murine, rat,] retina[murine] kidney[murine]

Abbreviations: AAV, adeno-associated virus; **NHP,** non-human primate; **AAVR,** AAV Receptor; **HSPG,** heparan sulfate proteoglycan; **LamR,** 37/67kDa laminin receptor; **FGFR1,** fibroblast growth factor receptor 1; **HGFR,** hepatocyte growth factor receptor; **PDGFR,** platelet-derived growth factor receptor; **EGFR,** epidermal growth factor receptor; **SM,** skeletal muscle; **CNS,** central nervous system; **HCC,** hepatocellular carcinoma.

(from [22])

The tropism of each AAV capsid was initially considered as closely linked to its ability to bind a different receptor; however this concept is currently debated. Indeed, many receptors have been identified for each AAV suggesting the existence of several mechanisms for AAV entry into the target cell [23]. Moreover, a recent work identified a new AAV receptor called

AAVR which is shared by at least AAV1, 2, 3b, 5, 6, 8 and 9 [24]. Recently, many reports clearly showed that post-entry steps have a major importance to determine the tropism of each AAV serotype. The importance of these early phases of the AAV life-cycle is discussed in detail later on in this manuscript. Moreover, it is important to note that the preclinical data summarized in **Table 2**, were not sufficient to predict the tropism of these serotypes in humans. A good example is provided by AAV8 which, although being highly efficient in hepatocytes from mice or NHP, only targeted a few percent of human hepatocytes in a clinical trial for FIX deficiency [22]. Thus, the selection of a capsid for clinical trials remains largely empirical and a comprehensive analysis of the tropism has to be performed to improve the efficiency of gene transfer in humans. Studies in optimized models more closely reproducing conditions in humans (*e.g.* human primary cells, mice engrafted with human cells [25], or *ex vivo* human tissue culture [26]) are currently privileged.

The second reason for identifying new AAV serotypes was to overcome preexisting immunity against AAV capsids which is strongly detrimental for medical applications. Serological studies report that approximately 40 to 70% of the human population has been exposed to AAV, and that the presence of neutralizing antibodies against AAV decreases its transduction efficiency, even at low titers [27]–[29]. The high prevalence of AAV in humans is one of the main obstacles for medical applications, and is an exclusion criterion in clinical trials. It also complicates vector re-administration in therapeutic as well as preventive vaccination approaches. Thus, the identification of new AAV serotypes displaying a low prevalence in the human population appeared as a good solution to overcome this problem. However, recent analyses clearly showed that most of the previously described AAV serotypes cross-react with sera obtained from animals pre-immunized with other serotypes (**Table 3**). Furthermore, it is assumed that the cross reactivity between these serotypes is dependent on the animal species and the administration routes. The mapping of the antigenic sites and the production of mutated vectors, able to escape recognition by anti-AAV neutralizing antibodies, currently appears as the most promising strategy to overcome this important obstacle for medical applications.

Table 3. Serological evaluation of AAV vectors

	Vectors								
Antisera	AAV1	AAV2	AAV3	AAV4	AAV5	AAV6	AAV7	AAV8	AAV9
AAV1	1/163840	No NAb	No NAb	No NAb	1/40960	1/40960	1/40	No NAb	No NAb
AAV2	1/80	1/81920	1/5120	1/20	No NAb	1/80	1/40	1/40	No NAb
AAV3	1/1280	1/2560	1/40960	1/20	1/40	1/2560	1/1280	1/1280	No NAb
AAV4	1/20	No NAb	No NAb	1/1280	1/40	No NAb	No NAb	No NAb	1/40
AAV5	1/20480	No NAb	1/80	No NAb	1/163840	1/5120	1/40	No NAb	No NAb
AAV6	1/81920	No NAb	1/640	1/40	1/40	1/327680	1/40	No NAb	1/40
AAV7	1/1280	1/640	1/1280	1/20	No NAb	1/1280	1/163840	1/5120	1/80
AAV8	1/20	1/1280	1/1280	No NAb	1/20	No NAb	1/640	1/327680	1/2560
AAV9	No NAb	No NAb	No NAb	No NAb	No NAb	No NAb	1/20	1/640	1/20480

Polyclonal antibodies against AAV serotypes 1 to 9 were generated in rabbits. Neutralizing and cross-neutralizing re-activities were evaluated by incubating each sera, at different dilutions, with AAV-CMV-EGFP vectors derived from serotype before transducing indicator cells. The transduction efficiency was measured 48 to 72 hours later. Neutralizing antibody (**NAb**) titers are reported as the highest serum dilution that resulted in 50% of transduction inhibition as with serum from a naive animal. (From [19]).

I.1.2 Genome organization

The various AAV serotypes share a common genome organization characterized by a single stranded (ss) DNA molecule of approximately 5 kb, containing three open reading frames (ORF) flanked by two palindromic sequences called inverted terminal repeats (ITR) (**Figure 3**). The ITR form a T-shaped structure containing a Rep binding site (RBS) and a specific cleavage site for bound Rep proteins, named terminal resolution site (TRS) [30]–[33]. These particular structures constitute an important *cis*-acting signal which serves for AAV genome replication, integration and packaging [34]–[36]. AAV genes share a unique polyadenylation signal (polyA) and their expression is under the control of three different promoters (**Figure 3**). The first ORF, *rep,* encodes for four regulatory proteins: Rep78 with its splice variant Rep68 and Rep52, with its splice variant Rep40 are expressed under the control of the p5 and p19 promoters, respectively. The alternative splicing responsible of the generation of the Rep78/68 and the Rep52/40 proteins is due to a splice donor site at position 1906 and a splice acceptor site at position 2228. These four proteins have several functions: the two larger proteins (Rep78/68), which display DNA binding, DNA helicase and site specific endonuclease activities, are involved in genome replication, transcription regulation and site specific integration. The two smaller proteins (Rep52/40), which lack the DNA binding domain, are not essential for virus replication

and have been described as important for packaging of the AAV genome into the capsid thanks to their helicase activities [37]–[40].

The second ORF, *cap,* encodes the structural viral proteins (VP) VP1, VP2 and VP3. These proteins are assembled to form an icosahedral capsid with a ratio varying between 1:1:10 and 1:1:20 according to the serotype. The p40 promoter regulates the expression of the *cap* and *aap* ORF. This latter ORF encodes the assembly activating protein (AAP) required for the assembly of the capsid in the nucleolus [41], [42]. The viral proteins VP2 and VP3 are synthetized from a spliced mRNA obtained using the same splice donor and acceptor sites than Rep68 and Rep40. However, VP1 and AAP are produced from a different mRNA which is generated using a different splice acceptor site at the position 2201. Interestingly, due to translation from three different in frame start codons, the VP1, VP2 and VP3 proteins are overlapping and have in common the VP3 region forming their carboxyl terminal regions (C-Term) but differ in their amino terminal regions (N-Term) [43], [44]. The overlapping VP1/VP2 domain, which is absent in VP3, contains two basic regions (BR) which serve as nuclear localization signal (NLS) during viral infection. Importantly, the VP1 unique region (VP1U), which also contains a NLS, exhibits a Phospholipase A2 activity domain which has a key role during the infection process [45]–[47].

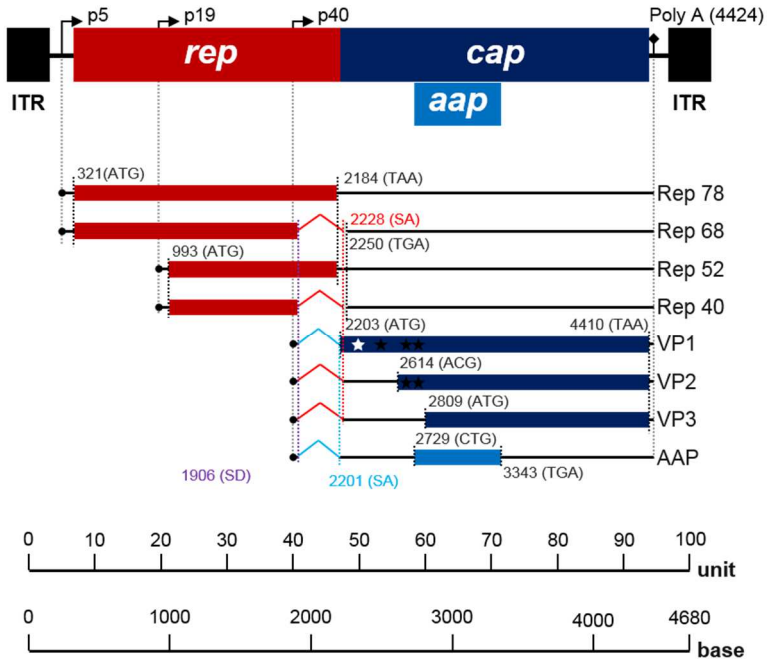


Figure 3. AAV2 genome organization.
The AAV genome of 4680 nucleotides (**nts**) is divided here in 100 units map (46.8 nts per unit). The genome is flanked by ITR. Three viral promoters (**p**) are located at units 5, 19 and 40 (p5, p19, p40). The polyA signal is at positon 4424. The viral ORF are shown as colored boxes, untranslated regions as solid lines and introns as peak lines. **Abbreviations: SA,** splice acceptor site; **SD,** splice acceptor site; **ITR,** inverted terminal repeats; **poly A,** polyadenylation signal; **VP,** viral proteins.

I.1.3 Structure of the viral capsid

As it is the case for all non-enveloped viruses, the AAV capsid constitutes the unique barrier protecting the viral genome from the environment. Moreover, the AAV capsid plays also a key role for entry and trafficking of the particle toward the cell nucleus, where the viral genome is released. Before describing the AAV life-cycle in more details, we will first describe the AAV capsid structure (**Figure 4**).

Like the other members of the *Parvovirinae*, the AAV capsid is one of the smallest amongst animal viruses. It is composed of three structural proteins: VP1, VP2 and VP3, which are arranged as an icosahedral lattice of approximately 25 nm in diameter, with T=1 symmetry (60 structurally equivalent subunits). The tridimensional structure of several AAV serotypes has been resolved by cryo-electron microscopy and/or X-ray crystallography [48]–[54]**.** The analyses revealed that AAV capsids show a similar surface topology, characterized by the presence of a canyon at the two-fold axis of symmetry and a depression surrounding a cylindrical channel at the five-fold axis. The three-fold axis is surrounded by three protrusions described as the most external regions of the capsid (**Figure 4A**) [55]. Capsids analyzed in these studies are constituted exclusively by the VP3 common region. VP3 is composed of a conserved eight anti-parallel β-barrels (designated βB-βI), one β-strand A (βA) that forms the contiguous capsid shell, one alpha helix (αA), and large loops inserted between the β- strands at the surface of the capsid (**Figure 4C**). The most highly conserved regions of the capsids amongst the different AAV serotypes are those known to be required for capsid stability. In contrast, the loops observed at the surface of AAV capsid contain variable regions (VR) at their apex, designated VR-I to VR-IX which determine the viral tropism and are responsible for the immunogenicity observed for the different AAV serotypes (**Figure 4B and C**) [56]–[58].

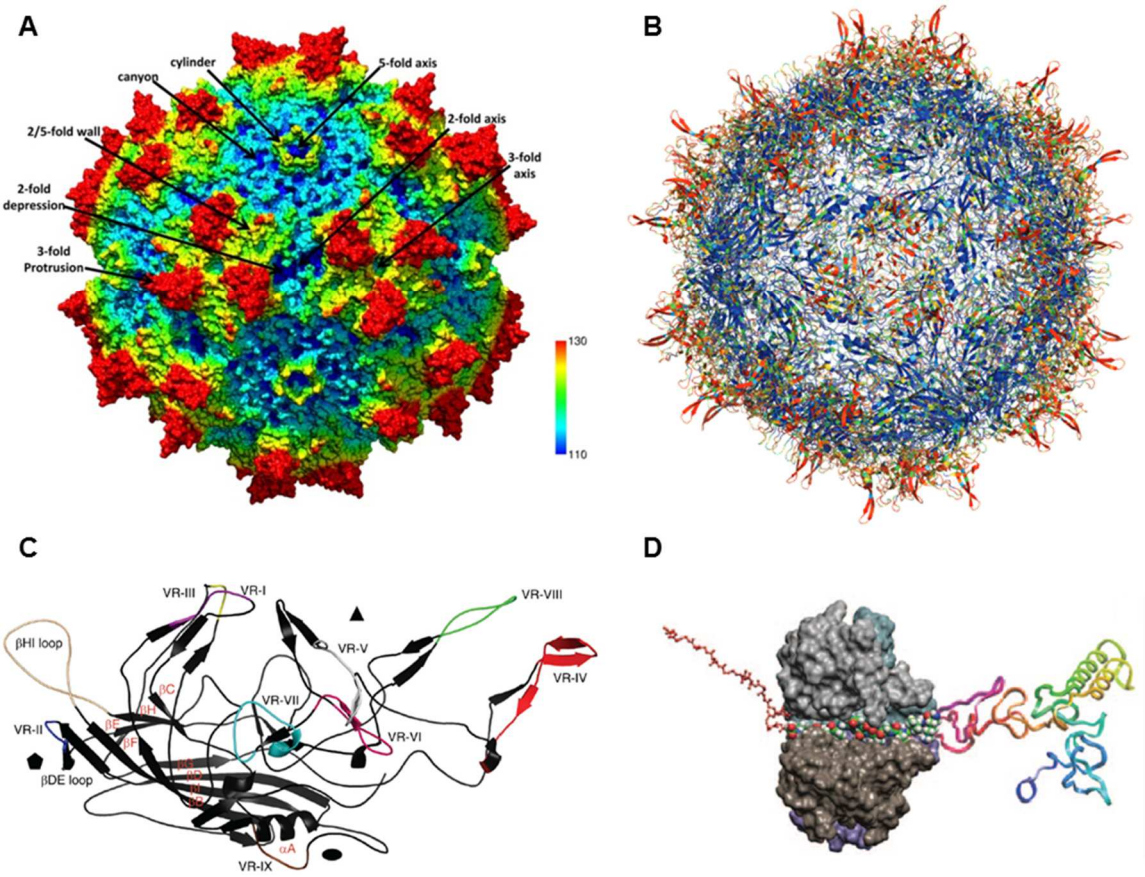


Figure 4. AAV capsid organization.

A. Radially color-cued (from capsid center to surface: blue-green-yellow-red; ~110-130 Å) AAV1 capsid generated from 60 VP monomers (RCSBPDB#3NG9). The approximate icosahedral two-, three-, and five-fold symmetry axes are as well as the AAV capsid surface features are indicated by the arrows and labeled (from [55]). **B.** Amino-acid variability plotted on the full AAV2 capsid. Blue end of the spectrum represents more conserved positions while the red end represents more variable positions. Variability was calculated using the Shannon-entropy statistic on a multiple sequence alignment of the sequences of different AAV serotypes (from [58]). **C.** A VP3 monomer is shown with the conserved core region consisting of eight antiparallel β-sheets (βB–βI) and an α-helix (αA). Loop insertions between the β-sheets vary among the AAV serotypes. Nine VRs (defined in [49]) are present on the capsid surface, and are color coded and denoted with roman numerals (I: purple; II: blue; III: yellow; IV: red; V: gray; VI: hot pink; VII: cyan; VIII: green; IX: brown; βHI loop: tan) (from [57]). **D.** The partially unfolded VP1 domain was fitted into the channel at the five-fold axis of symmetry. The backbone of residues is represented as a ribbon and coded with blue (residues 1 through 10) to red (residues 160 through 170) colors. The atoms of residues within the channel (amino acids 169 to 185) are shown using an atom color code (green, carbon; white, hydrogen; blue, nitrogen; red, oxygen). The backbones of residues inside the capsid (amino acids 186 to 209) are colored in red and represented by a ball and stick model. The solvent-accessible surface of the four VP3 units forming the channel is depicted in various grey tones. The fifth VP3 domain is not displayed to enable a view of how the unfolded VP1 strand into the channel (from [47]).

The VP1U and VP1/2 domains of the N-termini of VP1 and VP2, respectively, are more flexible than the rest of the capsid. During the viral life-cycle, the virus needs to externalize these regions through the channel at the five-fold axis of symmetry (**Figure 4D**). This process designated as "capsid maturation" is a key step during the transduction process [45]. Indeed, it is required for the endosomal escape of the particle by the action of the phospholipase A2 activity, and for nuclear entry via the presentation of the NLS to the nuclear import machinery of the cell (for more details see next chapter in this thesis). Because of their flexibility, the structures of the VP1U and VP1/2 domains proved difficult to resolve by X-ray crystallography. When analyzed by cryo-electron microscopy, these regions appear as a fuzzy globule on the internal surface of AAV capsid, located at the two-fold axis of symmetry [59].

I.1.4 Physical properties of the AAV virions

The physical properties of viral capsids or particles on virus biology constitute a research area which has recently emerged and is gaining an increasing interest in the virology field [60]. Before reaching their final destination, the viral particles must travel among a wide range of environments, both outside and inside the cell. Thus, the capsids have evolved to protect the viral genome against several physical constrains which can be thermal, chemical or mechanical. Besides their function in genome protection, the physical properties of the capsid can highly influence the viral life-cycle at many critical steps including viral genome packaging and release (uncoating). For example, in the case of bacteriophages it was shown that the genome is packaged into the capsid by an ATP-dependent molecular motor helping the compaction of the double stranded DNA into the capsid [40]. This high internal pressure allows to efficiently release the genome into the target cell without using any molecular motor. Indeed the internal pressure inside the capsid is approximately 5 atmospheres (atm) (as that in a bottle of Champagne), and the DNA can be compared to a compressed spring in a box, with a high energetic potential for release [61], [62]. The compaction of the viral genome is also influenced by its interaction with the capsid. In addition, the nature of the genome (DNA or RNA, single stranded or double stranded, length, *etc*.) with its own physical properties, and the environment, which can influence both capsid and genome physical properties, have an important impact on the biological properties of the virus. For example, ssDNA molecule does

not have the same compaction capacity in comparison with a dsDNA molecule that exhibits a higher steric hindrance (elastic bending) which is also dependent on the length of the genome. Furthermore, various secondary structures, created by the sequence and/or the ions present in the environment, can influence the compaction of the genome and impact on its release. This explanation was proposed to explain the variable efficiency of HSV-1 in neuronal cells in different ionic intracellular environments [63].

The minute virus of mice (MVM), a member of the Parvovirus family, shares several common features with AAV, in particular a small icosahedral capsid of 25 nm in diameter with T=1 symmetry, and a cylindrical channel at the five-fold axis of symmetry which is used to package the genome. In addition, as observed for AAV, internal domains of the MVM capsid have to be externalized across the pore present at the five-fold axis of symmetry to complete MVM life-cycle. The analysis of the physical properties of MVM capsids using atomic force microscopy (AFM), revealed that the genome packaged in the capsid can be considered as a structural element [64], [65]. Indeed, the capsid stiffness is significantly modified by the presence of the genome in a non-isotropic manner, thanks to its interactions with the internal capsid wall, at specific locations. These interactions result in an important increase of the capsid stiffness at the two- and the three-fold axis of symmetry (140% and 42% respectively), whereas the stiffness observed at the five-fold axis is only weakly increased by the presence of the genome (only 3%). This anisotropy may be explained by the fact that the five-fold axis, which is associated with a pore, plays an important role in the communication between the external and the internal environments. The authors suggest that a strong steric hindrance at this position may negatively influence the infectious process. Indeed, the pore at the five-fold symmetry axis was described as the exit gate for the N-terminus of VP1.

These examples illustrate well how important it is to increase our knowledge on the physical properties of viruses to better understand their biology and to optimize their use as viral vectors.

AAV vectors are currently considered as the most promising nanoparticles for gene transfer, and a better knowledge of their physical properties should allow the improvement their biological activities, in particular if one considers that several innovative strategies,

aiming to modify the capsid or the genome of the vectors are currently developed. Therefore, a transdisciplinary work at the interface between biology and physics may contribute to optimize the efficiency of the modifications introduced on the wild type capsids.

AAV stability, in different experimental conditions, is usually evaluated using biochemical assays with antibodies recognizing intact or denatured capsids. This kind of assay showed that AAV8 was more thermostable than AAV2 [66]. More recently, an elegant procedure evaluated the impact of the genome (size and nature) and the pH on the thermal stability of AAV2 particles [67]. This study clearly showed that the thermal stability of the capsid is highly influenced by the size of the genome. Indeed, the authors showed that an increase in the length of the genome renders the capsid more fragile and sensitive to heat treatment. In addition, this study showed that an acidic environment increased the stability of AAV2. Interestingly, acidification of the intracellular environment, which is required for AAV infectivity, triggers a conformational change of the capsid. Indeed, studies performed by X-ray crystallography have identified particular capsid domains which are sensitive to the pH and able to undergo a conformational change in acidic conditions [68]. These biophysical data suggest that the AAV capsid may have evolved to become more resistant during its passage in the late endosomes, where the pH is very low, to protect the viral genome and prevent its premature release in the cytosol, before the particle has reached the nucleus. Indeed, the exposure of the genome at this step may trigger unwanted antiviral innate responses. Interestingly, some studies performed with AAV vectors have shown that infection of plasmacytoid DC (pDC) at a very high MOI (more than 10^4 vg per cell) results in the activation of a TLR9-dependent innate responses which might have been induced by misfolded or immature capsids that do not sustain their passage in the late endosome (LE) [69], [70]. Recently, a study aiming to develop a new AAV capsid variant using an ancestral sequence reconstruction (ASR) method based on the analysis of a broad range of AAV variants and serotypes, provided an interesting observation about the physical properties of the AAV capsid [71]. Besides confirming the higher stability of AAV8 in comparison to AAV2, it also showed a high thermal stability of AAV9. More interestingly, common AAV ancestors of AAV8 and 9 also displayed a gradual reduction of thermal stability, further indicating the importance of the physical properties of the capsid.

I.2 The viral cycle: a long winding road strewn with dangers and difficulties

The first step of AAV infection requires cellular attachment factors which differ amongst serotypes. Attachment to these receptors involves amino acid residues on the surface of the viral capsid. The subsequent cell entry of AAV requires activation of a cellular co-receptor. Upon binding to its receptor and its co-receptor, AAV is internalized into the vesicular system from which it later escapes in order to reach the nucleus. As already outlined, the intra-nuclear fate of the AAV is critically influenced by the presence of a helper virus in the same host cell. In the absence of any helper virus, the AAV genome is maintained in the nucleus in an inactive (latent) form that can be either integrated or episomal. However, in the presence of a helper virus, AAV is able to replicate by exploiting both the cellular machinery and the factors provided by the helper virus. The replication of the AAV genome occurs in replication centers, within the nucleoplasm. Empty capsids are assembled in nucleoli, but the region in which empty capsids are filled with genomes (packaging) is presently unclear. AAV has no cytopathic effect, and it is currently accepted that new AAV virions are released from the cell following the cytopathic effect induced by the helper virus (**Figure 5**) [23], [72].

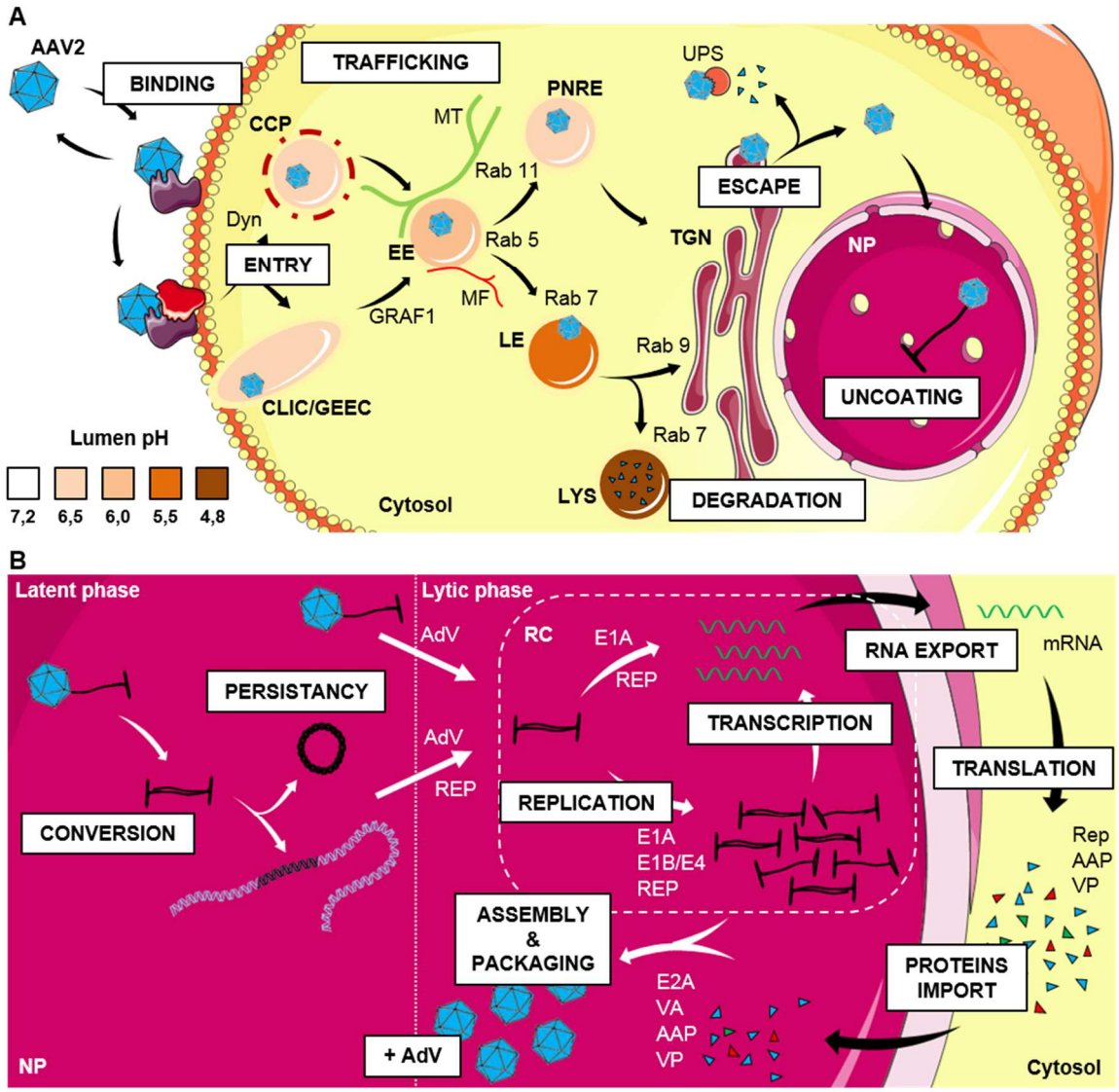


Figure 5. Overview of AAV life-cycle.

A. Early phases (adapted from [23]). The AAV life-cycle starts with its contact with the receptor/co-receptor complex. Then, the virions enter the target cell via the vesicular system. Different entry mechanisms are described, such as clathrin coated (**CCP**) or **CLIC/GEEK** endocytoses. Virions are retrograded-transported toward the cytoplasm via early endosome (**EE**), late endosome (**LE**) and perinuclear recycling endosomes (**PNRE**), leading to the accumulation of intact capsid in the perinuclear area. The endosomal escape of AAV capsids occur in this region, may be from the trans-Golgi network (**TGN**). AAV capsids can be degraded during their trafficking, in lysosomes (**LYS**) or by the ubiquitin protease system (**UPS**). Intact capsids cross the nuclear membrane through the nuclear pore complex (**NPC**) and the viral genome is released in the nucleoplasm (**NP**). **B.** Late phases. i) latent phase: in absence of a helper virus, the AAV genomes persist within the target cell integrated or as episomes; ii) replicative phase: in presence of a helper virus, such as AdV, the helper functions (such as E1A, E1B, E2A, E4 and VA I RNA for AdV) allow transcription and replication of the AAV genomes in viral replication centers (**RC**). After synthesis of the AAV VP proteins, new particles are assembled in the nucleus where packaging of the genome also occurs.

I.2.1 Binding on the cell membrane

The cell membrane is the first barrier that a virus has to overcome in order to infect a cell. In the case of AAV, this initial step implicates one or more proteoglycan conjugates as attachment factors together with proteinaceous receptor as a facilitator for the entry step. Most of the variable regions (VR) preferentially located at the external surface of the AAV capsids are implicated in this first interaction with the target cell, and they constitute a critical parameter which determines the serotype tropism (**see Table 2**). It was previously assumed that the abundance of known receptors and co-receptors correlated with the transduction efficiency of AAV vectors, but despite the key role of the binding step, gene delivery by AAV vectors is further limited by several post-entry barriers.

In order to describe the binding procedure of AAV, I focused my attention on AAV2 which is the most studied serotype and exhibits a broad tropism. The ubiquitous heparan sulfate proteoglycan (HSPG) was the first primary receptor described [73]. Indeed, HSPG with its high density of negative charges is able to bind the capsid on different residues, as described by a mutagenesis study [74]. The most important residues are two arginines located at positions 585 and 588 (VP1 numbering). The destruction of this motif may lead to non-HSPG binder capsid variants [56]. However, many studies identified several putative proteinaceous co-receptors, such as fibroblast growth factor receptor 1 (FGFR1) [75], integrin $\alpha V\beta 5$ [76], $\alpha 5\beta 1$, laminin receptor (LamR) [77] or hepatocyte growth factor (HGFR) [78]. Further analyses allowed to precise the nature of these interactions. A study performed using a single molecule tracking method showed that the virions decelerate when they approach the cell, then perform a series of touching events which end when the particles enter into the cell [79]. These touching events, which result from the charge interaction between the capsid and HSPG, induce a conformational change of the capsid [80]. Once the “active” conformation of the capsid has been gained, the interaction with the co-receptor is facilitated. This process was clearly described for the $\alpha 5\beta 1$ co-receptor of AAV2 [81]. Moreover, the Büning laboratory found that, if the interaction of the capsid with HSPG is too strong, the mutated capsid loses its infectivity and that it is also possible to reduce the touching time by mutating the binding site with HSPG (PhD thesis of Sebastian Rhode 2002, H. Büning PhD director). Further studies

are required to determine if this “priming” event of the capsid plays a role for the subsequent steps of the viral cycle.

This model of interaction between AAV and the target cell is now debated. Indeed, some studies failed to confirm the role of αVβ5 [82], FGFR1, HGFR [83] as a co-receptors, and more recently a genetic screen identified a new transmembrane protein as a common receptor of several AAV serotypes, provocatively called AAVR [24]. In addition, naturally occurring AAV2 variants recovered from humans do not use HSPG as an attachment receptor [74], [84], suggesting that AAV2, as several other virus using HSPG, has evolved in laboratory to adapt itself to the cell culture conditions.

I.2.2 Entry into the target cell

The internalization of extracellular components is essential for several biological processes. Indeed, the cell has distinct internalization mechanisms to interact with its environment or to recycle its membrane components to maintain cellular homeostasis [85]–[87]. To infect a target cell, viruses are able to use the cellular machinery to be internalized.

The AAV internalization pathway has been intensively studied since three decades, but remains debated and controversial. The AAV entry seems to be fast, since less than 100 ms are required to cross the plasma membrane since its first contact with the cell [79]. Moreover, this step is considered as very efficient, since all the virions bound on the cell membrane are internalized in the cell in less than 30 min. However, AAV uptake is largely influenced by the target cell type, the serotype and the MOI used for the transduction assays. It is assumed that AAV is internalized by the cell into the vesicular compartment as described for other non-enveloped viruses such as AdV. The complex formed between the virus and its receptors triggers an intracellular signaling pathway that stimulates the invagination of the plasma membrane and the formation of intracellular vesicles by membrane scission. Several studies described a clathrin or caveolin coat-mediated endocytosis, implicating a small GTPase protein called dynamin, as the major entry pathway for AAV2 [88]. However, experimental evidences showing only a partial inhibition of transduction by a dynamin dominant negative mutant indicate that AAV2 can use an alternative entry pathways independent of dynamin. Moreover, the first interaction between HSPG and the virions, which can be different according to the

HSPG binding features of the AAV capsid, can also influence the entry pathway, [89]. Macropinocytosis was proposed as an alternative pathway since overexpression of Rac1, the major effector of this process, increased gene delivery efficiency of AAV2 vectors [90]. More recently, the endocytic pathway called CLIC/GEEK (for clathrin-independent carriers/GPI enriched endocytic compartment), described as an entry route of HSPG, was proposed as the principal pathway for AAV2 internalization [91]. This variability in the entry process, initially described for AAV2, was also observed for AAV5, which uses several internalization pathways. In addition, it was shown that AAV4 and 8 (but not AAV2 and 6) can cross epithelial cells by transcytosis [92], [93]. Interestingly, inhibition of transcytosis can induce an increase of AAV transduction efficiency. Moreover, several cells or organs, are described as able to uptake AAV but remain non-permissive [94], [95]. These observations indicate the existence of important redundancies in the AAV entry mechanisms able to lead to an efficient transduction.

I.2.3 Intracellular trafficking and degradation

Following internalization into the target cell, virions have to cross the cytoplasmic compartment in order to reach and enter in the nuclear area. The intracytoplasmic trafficking of the AAV particles is currently recognized as being slow, rate-limiting, and intricately linked to the transduction efficiency. Only a small fraction of the input AAV particles appear to lead to transduction [72]. Moreover, due to the high amount of AAV particles used to transduce cells in culture, the identification of the infectious pathways appears difficult and remains intensively debated. However, understanding the limiting step of the AAV life-cycle appears as one of the most challenging objectives to be able to overcome the transduction barriers and to optimize the efficiency of gene delivery using AAV vectors.

The endosomal processing of AAV is an indispensable step for AAV transduction. Indeed microinjection of AAV particles directly in the cytosol did not result in transgene expression [96]. Following their entry, the endosomal environment induces a conformational change of AAV capsids. Capsid maturation results in the externalization of VP1U and VP1/VP2 domains, and allows the disruption of the endosomal membrane by the VP1 phospholipase A2 (PLA2) catalytic activity (lipolytic pore formation), followed by the endosomal escape of the virions. Moreover, basic regions (BR) harbored on the externalized regions seem to be important for

the nuclear translocation. Several *in vitro* studies suggest that the acidification occurring in late endosome is required to change the conformation of the capsid, but the decrease in intraluminal pH did not seem to be sufficient. In particular, endosomal proteases may also play a role in capsid maturation. AAV2 and 8 can, for example, be processed by cathepsins in a serotype specific manner. These latter enzymes, however, are not involved in AAV5 maturation [97]. These observations show the importance of capsid maturation, but also suggest that the maturation mechanisms are not conserved among all AAV serotypes. The impact of the conformational change of AAV capsids on subsequent steps, such as genome release, are poorly studied and understood, but recent work suggesting that the AAV2 capsid may have a role in the viral genome transcription provides a new important information to re-evaluate the role of AAV capsid processing during the AAV life-cycle [68].

Currently, it seems clear that for various AAV serotypes (currently shown for AAV2, 5, 8), virions must pass the trans-Golgi network (TGN) or the Golgi apparatus in order to reach the nucleus. The mammalian cells can transport specific proteins or lipids from the plasma membrane to the perinuclear endocytic compartments as TGN, Golgi or endoplasmic reticulum (ER) by a retrograde transport. This mechanism is selective and highly regulated by a large family of small GTPase proteins, named Rab proteins [98], [99]. These proteins regulate endosomal budding, sorting, transport and fusion, acting as “zip codes” to facilitate endosomal movements (**Figure 5**). The retrograde system is typically divided into two main routes, which allow to transport some cargos from the early endosome (EE), characterized by Rab5 protein, to the TGN. In the first one, the cargo goes to the late endosome (LE), characterized by Rab7 protein able to transport/deliver the cargo to the lysosome (LYS) for degradation or to the TGN via Rab9. The second route requires the perinuclear recycling endosome (PNRE, Rab 11) to conduct the cargo to the TGN. The Rab11 vesicles can also fuse with LYS during this pathway. During their travel, the cargos are confronted with various intra-vesicular environments, which differ in protease activities and intraluminal pH. These mechanisms, which are complex and dynamic, also vary according to the cell type. Several toxins or viruses, such as AAV, hijack these mechanisms to move inside the cell. Interestingly, AAV virions are observed in the different endosomal compartments of the retrograde system as into EE, LE, PNRE, and TGN, and the distribution is influenced by the MOI used to transduce a given cell or by the cell type itself [22], [23], [100]. Moreover, several studies confirmed the

importance of the route implicating LE and/or PNRE in the intracellular AAV trafficking. More recently one study showed that AAV can use Syntaxin-5 dependent retrograde transport to join the TGN [101]. It was also demonstrated, during the discovery of AAVR, that AAV particles can join the TGN using different pathways in the same cell [24]. Despite the required passage of AAV virions in the TGN, the exact localization of the endosomal escape is not clearly identified yet. Indeed, several studies indicate that endosomal escape occurs following the acidification of the endosomes and the conformational change of the capsid. But, it was shown that AAV can also escape from the early endosome [102], and single molecule tracking assays showed different kinds of motion for AAV particles in the cytoplasm. Indeed, diffusion of free AAV particles or endosomes containing AAV has been described. However, directed motion implicating molecular motors have also been shown and several studies revealed the importance of the microfilament (MF) and microtubule (MT) networks in the AAV transduction process [103].

Among all the particles internalized into the cell, only few of them succeed at reaching the nucleus. Two main degradation pathways were described for AAV particles during their trafficking into the cell. The particles can be sequestered in the lysosomal compartment that triggers their complete degradation. In addition, different studies have shown that the mature capsid can also be degraded by the ubiquitin proteasome system (UPS) [23]. The degradation mediated by the UPS requires either i) the externalization of the VP1U and the VP1/2 N-Term domains to induce the presentation of some lysine residues able to be conjugated to ubiquitin, or, ii) the phosphorylation of some tyrosine residues which can then be ubiquitinated [104]–[107]. Accordingly, the use of proteasome (such as MG132, MG101) or ubiquitin ligase inhibitors strongly increases AAV transduction efficiency. Similarly, mutation of tyrosine residues was shown to improve the transduction efficiency. These observations suggest that degradation of the AAV capsid mediated by the UPS is an important barrier for cell transduction. However, the proteasome inhibitor MG132 was also shown to be able to increase the transduction efficiency by another obscure mechanism which improves AAV nuclear translocation [83], [108]. All these observations show that AAV trafficking is complex and poorly understood. The endosomal machinery seems quickly saturated, and the rate-limiting effect of this step obviously suggests the presence of different dead end pathways which sequester the majority of the AAV virions.

However, these studies should be further completed by examining AAV entry in the presence of one of its helper viruses. Indeed AAV is not an autonomous parvovirus but a dependovirus, which implicates that it may have co-evolved with its helper viruses. Therefore, it is reasonable to think that the helper functions provided from the helper virus are not confined to the nuclear processing of the AAV genome. The initial steps of co-infection with AAV and a helper virus are extremely poorly studied. However, it is clearly recognized that AdV can help AAV to escape from the endosome, despite a very low co-localization in the same endosomes [109]. Interestingly it is known that AdV escapes from early endosome quickly after the cell entry and before their acidification. Therefore, it would be extremely interesting to determine if AdV can help AAV particles to traffic through the cytoplasm, and what is the maturation status of the capsid of these “helped” AAV particles.

I.2.4 Nuclear entry and genome release

After endosomal escape, and in order to complete the viral life-cycle, AAV capsids have to deliver their genome into the nucleus. Nuclear entry is considered as one of the main barrier against AAV transduction since only a low amount of intracellular viral DNA is delivered in this cell compartment [110], [102]. Moreover, the mechanism underlying nuclear entry is still unclear and at least two different pathways have been described [22], [23]: either i) intact AAV capsids reach the nucleoplasm by crossing the nuclear pore, or ii) intact AAV capsids cross the nuclear membrane via nuclear envelope breakdown (NEBD). For both these mechanisms, genome uncoating takes place in the nucleus. Before detailing these different pathways, it is also important to note that at least two reports have shown that AdV can facilitate AAV nuclear entry [102], [111].

The AAV capsid proteins present three basic regions (BR) described as a non-classical NLS domains. BR1 is localized on the VP1U domain, and is poorly implicated in the infectious process, whereas BR2 and 3, located on the VP1/2 domain seem to be implicated in nuclear entry of the AAV2. Indeed, a mutation of the BR2 or BR3 domain induces a moderate or important reduction of the transduction efficiency, respectively [107], [112]. Both these regions are externalized during the maturation of the capsid. Consequently, they are accessible when the capsid reaches the cytosol [96], and may interact with the NPC via the

karyopherins. Indeed, importin-β has been described as playing an important role in AAV nuclear entry [113]. Interestingly, AAV is also able to interact with a broad range of importins-α. A recent study, has succeeded at tracking AAV particles during their entrance in the nucleus, and confirmed that this step is rate-limiting since less than 20% of AAV virions bound on the NPC cross the nuclear envelope [114].

Interestingly, as described for other parvoviruses such as MVM [115], the interaction between the NPC and the AAV capsid was described to trigger NEBD similar to that observed during mitosis [116]. The interaction between AAV capsids and the NPC triggers the release of Ca^{2+} from the area between the inner and the outer nuclear membrane. This leads to the destabilization of the nuclear skeleton composed of lamins and to the breakdown of the nuclear envelope by cellular proteins implicated in mitosis or apoptosis (*i.e.* Cyclin-dependent kinase 2 *(*cdk-2) and caspase-3). Even if this mechanism was not entirely understood, the authors of this study interestingly demonstrated that incubation of AAV capsids at low pH was required to induce NEBD. Moreover, the interaction between the NPC and AAV induces a conformational change of the capsid, leading to the externalization of the VP1U domain. This result is really interesting because it proposes for the first time an alternative/rescue mechanism for capsid maturation, occurring after the endosomal escape. However, further studies are required to better understand the implication of this NPC-mediated maturation process during AAV infection.

In contrast, an older study has shown that AAV can enter into purified nuclei independently of the NPC [117]. In this study, the NPC was blocked with a specific anti-NPC antibody (p62) or with wheat germ agglutinin (WGA). This blockage had no impact on AAV nuclear entry, which could not be saturated. In this study the integrity of the nucleus was confirmed. However, no control was provided to verify the effective blockage of the NPC. Furthermore, NPC-independent entry of AAV occurred with a similar efficiency for nuclei isolated from permissive (human embryonic kidney cell line (HEK-) 293) or low permissive cells (NIH3T3), thus suggesting for the first time the importance of the post nuclear entry steps for transduction. The importance of these steps was also suggested later [107].

Several studies have indicated that AAV uncoating occurs inside the nucleus. Indeed, nuclear injection of an anti-capsid antibody (A20) inhibits the transduction efficiency [96]. However, the efficiency of nuclear uncoating was described as serotype and cell type-dependent, and in many cases inefficient and rate-limiting [118], [119]. Recent studies, such as the analysis of the physical properties of the AAV capsid [67], or the *in silico* reconstruction of the AAV evolutionary lineage [71] have suggested a link between uncoating efficiency and capsid stability but, up to date, this mechanism remains unclear. Interestingly, within the nucleus, AAV uncoating appears to be restricted to the nucleoplasm, whereas nucleoli appear as a retention nuclear sub-compartment preventing genome release [107], [120]. In these studies, the authors suggest that AAV capsids, which have been described as able to directly interact with some nucleolar components [82], [121], are retained in nucleoli in a dormant state, which can be rescued by the presence of an helper virus or a stress of the host cell, triggering more favorable conditions to uncoat.

I.2.5 Latent and productive phases

AAV is classified as a dependovirus because replication of its genome can take place only when the cell is co-infected with a helper virus. This atypical feature results in a biphasic life-cycle (**Figure 5B**) [122], [123]. After nuclear release of the AAV genome, the viral ssDNA is converted into a dsDNA molecule, the transcriptionally active form of the viral genome [124]. Two mechanisms allow this conversion: i) cell polymerases which can synthesize the complementary DNA strand of AAV using ITR as primers; ii) the conversion of the ssDNA into a ds molecule can also result from the hybridization of two ssDNA molecules with opposite polarities. Indeed, both positive and negative ssDNA molecules can be packaged into the capsid, with the same efficiency [6], [125]. This conversion process, which also takes place with AAV vectors, is considered as one important rate-limiting step during transduction that hampers vector gene expression. In the absence of any helper function, the ds DNA molecule persists in a silent form that is either maintained as a circular episome or integrated in cellular chromosomes. The AAV genome was initially thought to almost exclusively integrate within a specific locus of human chromosome 19, called AAVS1; however several other preferential sites were recently described [126]–[128]. These integration sites may contain many AAV genome copies. The integration is mediated *in cis* by the ITR, and *in trans* by the Rep78/68

proteins themselves. Rep proteins are expressed in the early phase of the latent phase, but rapidly inhibit the transcription of the AAV genome (negative feedback loop) [129], [130]. The persistence of the AAV genome as an integrated or an episomal form is dependent on the cell type and on the cell cycle. If the cell infected with AAV is superinfected with a helper virus such as AdV, AAV enters into a productive life-cycle: AAV uses the AdV proteins for its own benefit leading to a decreased replication of AdV [131]. AdV proteins play important roles in different steps of the AAV productive cycle. AdV increases the efficiency of single- to double-strand DNA conversion of the AAV genome; moreover, it strongly induces the transcription of the AAV genes [132]. Several AdV proteins are identified as helper factors for AAV: E1B which forms a complex with E4 (orf6) and helps Rep and the cellular polymerase to replicate AAV genomes in the replication center, and VAI RNAs and E2A which helps the translation of AAV mRNAs. The most important AdV factor is E1A, a multifunctional protein, which activates *rep* gene transcription. Replication of the AAV genome leads to the synthesis of several ss and ds AAV DNA molecules. Single-stranded AAV genomes are packaged into AAV capsid with the help of Rep helicase activities, and dsDNA molecules provide new templates for replication and transcription [16], [133].

I.3 Recombinant AAV: a toolkit for gene transfer

Viral vectors are an efficient system to deliver exogenous genes into cells or tissues. Derived by genetic modification of wild type viruses, they encode for heterologous or homologous genes and allow efficient gene transfer. To be efficient, a vector has first to be able to transfer the transgene into the cell and to lead to a specific and sufficient expression in the target tissue. Second, it has to avoid unwanted secondary effects, often linked to the properties of the virus from which the vector was derived (such as immunogenicity or detrimental genome integration). Finally, engineering and production of the viral vector have to follow an easy and scalable protocol to enable large-scale clinical applications. This last condition is one of the most limiting for viral vectors in comparison to synthetic vectors [20], [134], [135].

Due to their interesting properties, AAV vectors have rapidly gained popularity as tools for gene transfer. Indeed, as previously described, AAV infection in humans is not associated with any disease and its genome is relatively simple and easily genetically modified to produce

recombinant AAV (rAAV). The ITR, which are required *in cis* for replication and packaging of the genome in the producer cells, are the only viral sequences kept in the AAV vector genome. The other viral sequences, *rep, aap,* and *cap,* are replaced by the sequence of interest which can be either i) a transgene expression cassette allowing production of the transgenic protein in the target cell, ii) or a particular DNA sequence used, for example, as a template for homology-directed repair. In this manuscript we are focusing only on the first strategy. In this scenario, the expression cassette contains the transgene, encoding the protein of interest, placed under the control of a promoter and a polyA signal (**Figure 6**). AAV2 was the first serotype to be developed into a recombinant vector. Initially, for production of AAV vectors, the *rep* and *cap* genes were transfected in the producer cell and the helper functions were provided by the infection of cells with AdV. However, this protocol resulted in the production of rAAV particles contaminated with AdV. To avoid this problem, later on, the AdV helper functions were isolated and directly provided by transfection, thus, preventing the formation of infectious AdV particles [18].

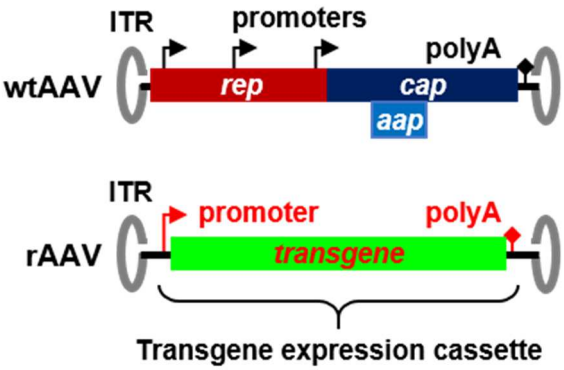


Figure 6. Wild type and rAAV genomes. rAAV genome are obtained by removing the *rep*, *aap* and *cap* genes and replacing them with the transgene cassette including at minimum a promoter, a cDNA and a polyA signal. Only the ITR sequences are conserved in the rAAV genome. The ITR are required for replication and packaging of the rAAV genome during AAV vector production. The size of the rAAV genome cannot exceed that of the wild type AAV genome.

I.3.1 rAAV mediated gene transfer for medical applications

Gene transfer was defined by the European medical agency (EMA) as the transfer into human cells of an engineered genetic material, mediated or not by a vector, which allows to develop a large range of therapeutic applications against various disorders. The nucleic acids are delivered with the objective to regulate, repair, replace, add or delete a genetic sequence triggering therapeutic, prophylactic or diagnostic effects [136]. The first human gene transfer trial was approved in 1989 [137], [138]. Its aim was to transfer the neomycin gene in tumor-infiltrating lymphocytes (TIL) by *ex vivo* transduction with murine retroviral vectors. This

human gene therapy trial was the first to document the feasibility of this approach. In 1990, the adenosine deaminase (ADA)-deficient severe combined immunodeficiency (SCID) was the first monogenic disorder treated by gene therapy in a clinical trial [139]. The authors performed an *ex vivo* retroviral-mediated ADA gene transfer into T cells of SCID children. These trials, which were successfully repeated some years later, illustrated the high potential of this strategy for medical applications in terms of efficiency and safety [140].

Up to date, more than 2300 gene transfer clinical trials have been conducted around the world. Most of them aimed to treat cancer (60%), monogenic disorder (10%) or infectious diseases (8%) (**Figure 7A**). This large number of clinical trials provided an important knowledge which allowed to refine gene transfer strategies [141]. In order to deliver the foreign gene into the target cell, different strategies were developed such as viral vectors, synthetic vectors or naked DNA (**Figure 7B**). Viral vectors appear as the most popular tool in these different clinical trials, mostly due to their elevated capacity to transfer their genome into the target cells, a property acquired after a long co-evolution process with their hosts.

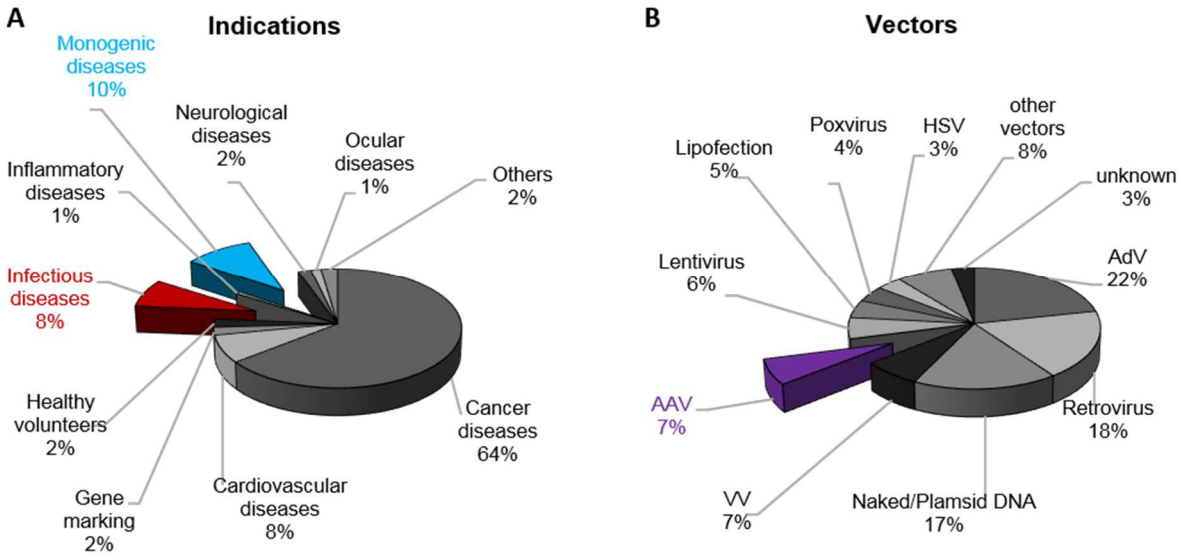


Figure 7. Overview of gene transfer in clinical trials worldwide.
A. Percentage of clinical trials according to the indications. **B.** Number of clinical trials according to the vectors used. **Abbreviations: AAV,** Adeno-associated virus; **VV,** Vaccinia virus; **AdV,** Adenovirus; **HSV,** Herpes simplex virus. Data upload at July 2016 from The Journal of Gene Medicine, Wiley and Sons (http://www.wiley.com//legacy/wileychi/genmed/clinical/).

As noted before, AAV vectors are currently considered as one of the most promising systems for these applications. Indeed, they are derived from a virus known to be non-pathogenic, persistent, ubiquitous and poorly immunogenic. These remarkable features led to an intense and exponential development of rAAV mediated gene transfer strategies. AAV entered the gene therapy field, in the 90's for the treatment of two monogenic disorders: i) cystic fibrosis, an autosomal recessive disorder due to a mutation in the cystic fibrosis transmembrane conductance regulator (CFTR) gene, and ii) hemophilia B, a recessive X-linked disorder (also known as Christmas disease) due to mutation of the coagulation factor IX (FIX) gene [142]. For these clinical trials, AAV2 vectors encoding for the transgene (CFTR or FIX) were delivered *in vivo* into the pulmonary epithelium (for cystic fibrosis) or intra-muscularly (for hemophilia B). These studies showed, for both treatments, a transient expression of the transgene coupled with partial phenotypic correction, which strongly suggested the high feasibility of rAAV mediated gene transfer.

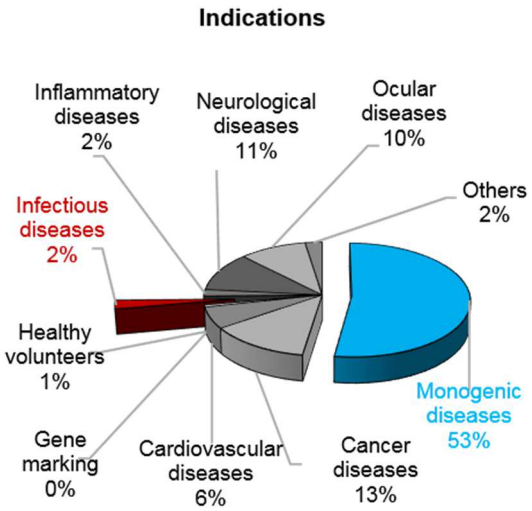


Figure 8. AAV vector applications.
Graphical presentation of indications addressed by gene transfer in clinical trials using AAV vectors. Data upload at July 2016 from The Journal of Gene Medicine, Wiley and Sons (http://www. wiley.com/ /legacy/ wileychi/ genmed/ clinical/).

Up to date more than 150 clinical trials using AAV vectors have been approved and provided several promising results. AAV vectors were mainly tested in a broad range of monogenic diseases affecting many tissues, such as Leber's congenital amaurosis (LCA) in the eye, Parkinson's disease in the central nervous system (CNS), or Duchenne muscular dystrophy (DMD) in muscle (**Figure 8**) [143]. In addition, even if initial trials were conducted exclusively with AAV2 derived vectors, newly discovered AAV serotypes rapidly entered in the clinics as illustrated by Glybera® – a rAAV derived from the AAV1 used to treat a Lipoprotein lipase

deficiency (LPLD) – which has received the first marketing authorization as a gene therapy medicine in Europe.

However, despite several successes and/or encouraging results, the advancement in clinical trials rapidly revealed that the host immune responses against the transgene product and/or the capsid could strongly impact the gene transfer efficiency by clearing transduced cells, and that pre-existing or induced humoral immunity against AAV (mediated by neutralizing antibodies) can strongly inhibit AAV vectors entry into the cells by binding to the injected particles. Even if these problems were not observed in all the trials and indications, immune responses against rAAV remain one of the most challenging problems that needs to be solved in order to expand the use of these vectors in *in vivo* applications (see next chapter for more details) [27], [144].

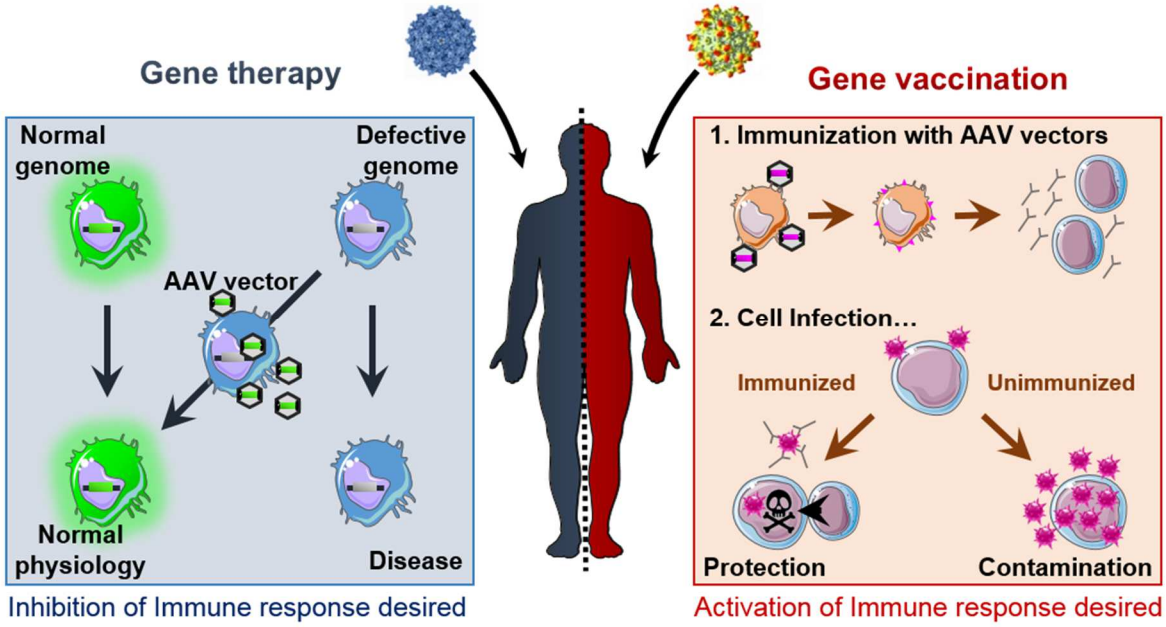


Figure 9. Principle of gene therapy and gene vaccination using AAV vectors.
Gene therapy aims to restore a physiological function by addition of a transgene able to restore the normal function (*e.g.* a monogenic diseases such as Hemophilia B [145]). The success of this strategy requires that the host tolerates the transgene product, implying a control of the host immune responses. Gene vaccination aims to immunize the host against an antigen by transfer of the antigen gene (*e.g.* for infectious diseases such as infection with NiV [146]). The success of this strategy requires that the host develops strong immune responses against the transgene product, implying an activation of the immune system.

The capacity of AAV vectors to induce immune responses against the transgene product *in vivo* also triggered the analysis of their potential for vaccination [147]. A study published in 1997 first indicated that it was possible to use AAV2 vectors to immunize mice against a viral infection [148]. In this study, HSV-2 glycoprotein B gene transfer mediated by rAAV induced strong cytotoxic and humoral responses against the transgene product and an effective immunization of mice. Later on, this application of AAV vectors was further studied in preclinical trials, and provided promising results (*e.g.* immunization against henipaviruses in rodents [146], human immunodeficiency virus (HIV) in mice [149], and simian immunodeficiency virus (SIV) in macaques [107]). Currently, 2% of the approved clinical trials use AAV vectors for therapeutic vaccination to treat infectious diseases, *e.g.* induced by Human Immunodeficiency virus and hepatitis C virus (HCV) (**Figure 8**).

These two applications of AAV vectors, gene therapy and gene vaccination, require opposite immune responses to be efficient **(Figure 9)**. Indeed, the correction of defective phenotypes such as LPLD or Hemophilia requires the absence of activation of immune responses against the transgene product to allow its sustained production. In contrast, in the case of gene vaccination, active immunization is critically linked to the detection of the antigen by the host immune cells to lead to a strong immune response. Several parameters such as the administration route, the AAV serotypes and the target tissue can largely influence the fate of the transgene product and the consequences on immune responses. An intense study is ongoing to optimize AAV vectors in order to improve the efficiency of the gene transfer according to the indication, and to overcome several biological challenges.

I.3.2 AAV vectors improvements

Gene transfer using viral vectors is a complex strategy strongly influenced by the interaction between the vectors and the target hosts. These two protagonists, with their own biological properties, interact at several levels leading to many consequences in the clinical outcome [150]. Thus, the advantages and the drawbacks of a vector are defined according to the aim of the gene transfer strategy, and the vector can be optimized by modulating its intrinsic features. Similarly, AAV vectors derived from AAV2 allow an efficient transduction of several tissues *in vivo*, but further analysis of their biological properties identified several

limiting barriers for efficient gene transfer. The engineering of AAV vectors aimed to overcome these limiting barriers by introducing specific modifications in the vector or capsid components. In this part, we provide an overview of the strategies developed to improve the efficiency of AAV vectors.

I.3.2.1 rAAV genome engineering

The low packaging capacity of AAV vectors (less than 4.5 kb) appeared quickly as an important barrier limiting their application to the transfer of small transgenes. Two main approaches were developed to overcome this limitation: i) split AAV vectors, taking advantage of the intrinsic features of the wt AAV genome which undergo inter-molecular tail – to – head concatemerization via recombination through the ITR; and ii) reassembly of fragmented AAV genomes, based on the capacity of AAV to package heterogeneous single strand genome fragments (less than 4.5 kb) of both polarities when using long transgene (more than 4.5 kb) [151]. In the first approach, the transgene is split in a proximal and distal part which are packaged into two independent AAV vectors. The co-infection of the target cell with these two vectors leads to the production of a functional transgenic protein. This may occur via homologous recombination (HR) in the case of overlapping transgene portions, or by splicing of the messenger RNA in the case of the *trans*-splicing strategy (**Figure 10**) [152]. For the second approach, the incubation of the target cell with the heterogenic vector population allows an intracellular reconstruction of the complete transgene by HR of overlapping sequences or directly by hybridization of negative and positive strands of the vector genomes [153]. Several evidences of the efficiency of these strategies have been provided in different tissues and the choice of the best strategy remains debated [21], [154]. Both these strategies require that each portion or fragments of the transgene is present and accessible in the same target cell. This has several consequences on the transduction efficiency, which appears to be lower in comparison to conventional AAV vectors containing a complete transgene cassette.

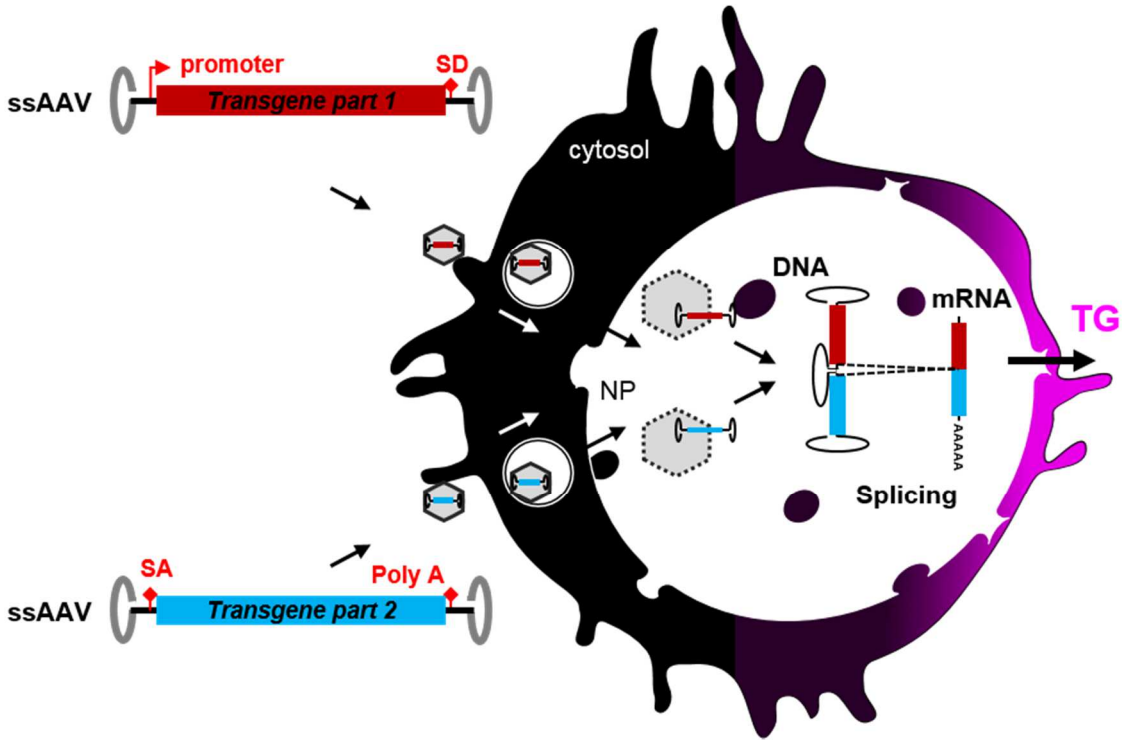


Figure 10. Trans-splicing of rAAV genomes
To transfer a transgene longer than 4.5 Kb using rAAV, the cassette is split into two vectors containing a splice donor site (**SD**) or acceptor site (**SA**) site flanking an intron. Co-transduction of cells with these two vectors leads to their concatemerization via the ITR. The DNA molecule is then transcribed into a long mRNA linking the two cassettes parts through the ITR which is then spliced out to provide the final mRNA corresponding to the transgene triggering transgene expression (**TG**) (modified from [21]).

As described before, the single-stranded to double-stranded conversion of the AAV genome mediated by the host DNA synthesis machinery is rate-limiting for transgene expression. Self-complementary (sc) AAV vectors were developed to overcome this phenomenon and resulted in a faster and higher transgene expression in several target tissues [21], [155]. Indeed, the scAAV genome contains two complementary sequences of the transgene on the same DNA molecule. (**Figure 11**). This complementary rAAV genome molecule is able to self-hybridize, resulting in a double-stranded transcriptionally competent vector. This mechanism is fast and independent of the host DNA synthesis machinery. The design of scAAV genomes further limits the packaging capacity of the vector, which is reduced by 50% as compared to ss AAV vectors (*i.e.* 2,3 Kb instead of 4,5 Kb, respectively [156].

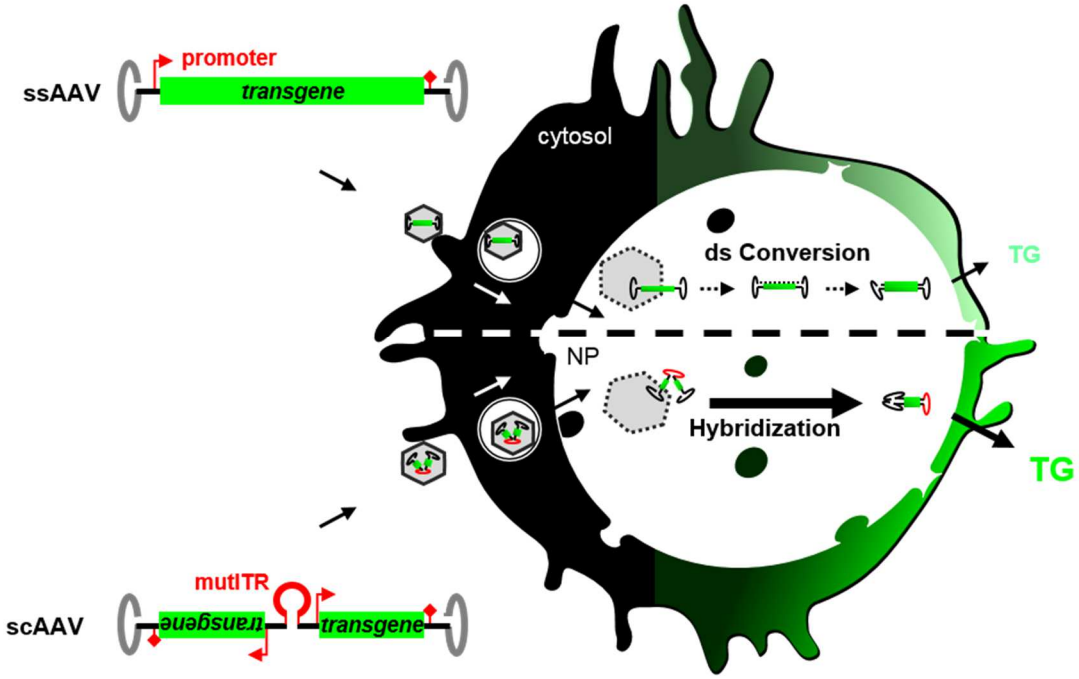


Figure 11. Self-complementary rAAV genomes
A rAAV with a sc genome results in an improved transgene expression (**TG**) by shunting the ss to ds conversion step required before transcription. scAAV vectors are obtained by mutating the TRS site within one of the two ITR resulting in a mutated ITR (**mutITR**), which will not be cut by Rep proteins during replication. This leads to the production of a sc molecule which is packaged within the capsid (modified from [21]).

In order to optimize the transduction efficiency of the AAV vectors, one strategy consists in modulating transgene expression using tissue-specific promoters. Indeed, promoters are key *cis*-elements in regulation of gene expression [157]. Thus, the transgene expression cassette can be placed under the control of different kinds of promoters which are able to improve and/or to target transgene expression [158]–[160]. The use of such promoters is also an efficient strategy to modulate the tropism of AAV vectors at a transcriptional level.

I.3.2.2 Capsid engineering

Given the importance of the capsid in the interaction with the host, various strategies have been developed to modify the properties of the wt AAV capsid and overcome different obstacles in gene delivery applications [20], [134], [135]. Different modifications have been introduced in order to respond to several challenges such as transduction of refractory cell types, overcoming preexisting immunity directed against wt AAV capsid, or identifying and characterizing the capsid domains implicated in life-cycle of the AAV. In the following section, we summarized different strategies developed to design new AAV capsids (**Figure 12**).

As described before, AAV serotypes present various interesting properties in term of tissue tropism, prevalence in the human population or immunogenicity. In order to use this wide range of properties for gene transfer applications, pseudotyped rAAV particles have been rapidly developed. Due to the high degree of sequence homology among AAV serotypes, it is possible to package a rAAV genome containing the ITR of AAV2 within a capsid derived from another serotype (**Figure 12A**). This technique presents the advantage to allow the production of a large spectrum of pseudotyped AAV vectors derived from various natural serotypes. However, these vectors are limited by the natural properties of the different capsids, and the development of new gene transfer strategies required the engineering of AAV vectors with original properties that are not found in nature yet.

Mosaic AAV vectors are particles containing a transgene cassette packaged in a capsid formed with a mixture of VP units derived from several AAV sources (**Figure 12B**) [20]. This strategy aims to combine several properties from the different natural capsids. To generate this kind of vectors, the producer cells are transfected with a mixture of helper constructs encoding for the capsid subunits derived from sources of interest. As an example, this technique was used to produce mosaic AAV vectors containing subunits from AAV1 and AAV2, and combining the ability to efficiently transduce the liver and the muscle [161]. The sources and the ratio of the helper constructs used to generate these mosaic vectors have an important influence on the properties of the final vectors. Interestingly, this technique can also lead to the production of AAV vectors with new properties absent in the parental sources. Although the mechanism is not understood, this technique allowed to generate mosaic AAV particles able to transduce C2C12 muscle cells from a combination of AAV2 and AAV1, whereas none of these parental serotypes could efficiently transduce this cell type [162]. This technique was also interesting to better understand the role of the capsid in the different steps of the AAV life-cycle but it presented a critical disadvantage linked to the experimental conditions. Indeed, the amount of each subunit in the final capsid was evaluated theoretically from the ratio of helper constructs used for the production but it could not be confirmed experimentally. It is reasonable to think that this kind of production leads to a very heterogeneous population of particles.

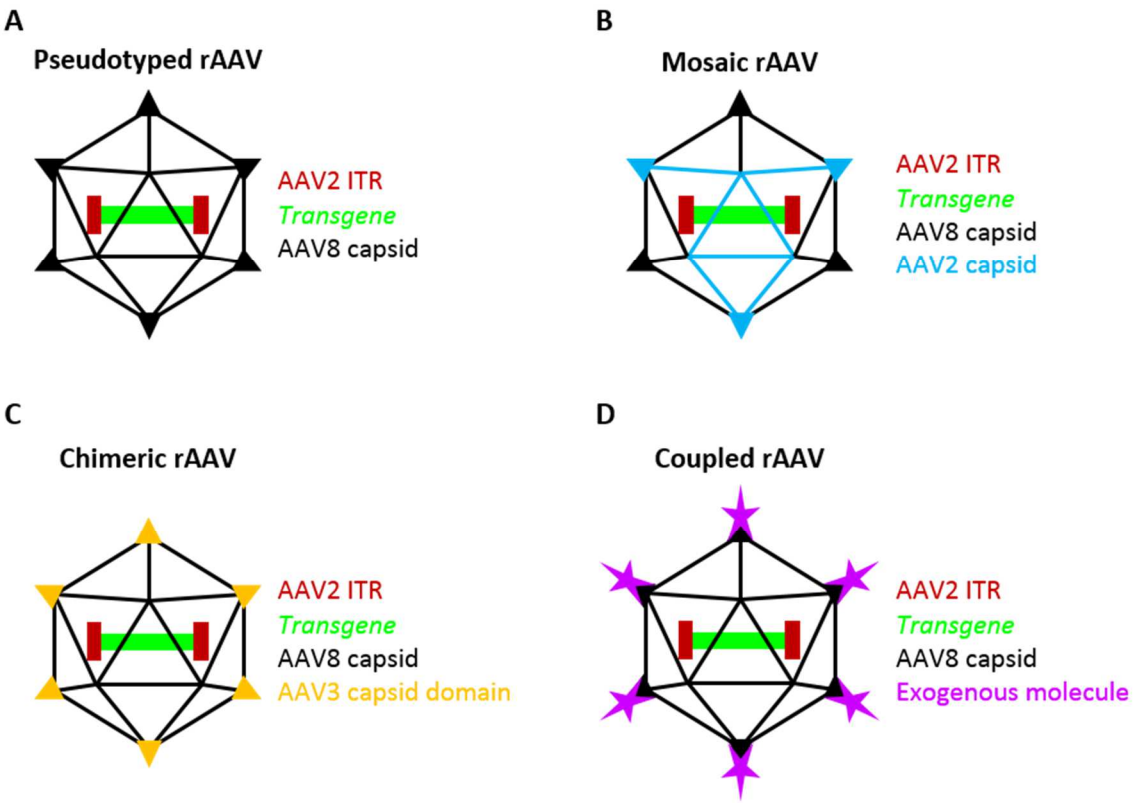


Figure 12. rAAV capsid engineering.
A. To produce a pseudotyped rAAV, the AAV2 ITR are used to package the transgene into the capsid derived from another serotype. **B.** Mosaic rAAV are composed of VP proteins derived from different serotypes. **C.** Chimeric rAAV are assembled with hybrid VP proteins derived from different serotypes. **D.** rAAV particles can be coupled with an exogenous molecule.

Another strategy to combine features of various AAV serotypes consists in the development of chimeric AAV capsids. These particles contain capsid domains that are swapped between serotypes (**Figure 12C**). The best-characterized domains of AAV capsids are those involved in cell binding. Consequently, several studies used chimeric particles to modify the binding profiles of capsids and to retarget AAV vectors [56], [163]. However, besides modifying the binding step, swapping specific capsid protein domains from one serotype for a similar region of another one, may also improve other steps such as intracellular trafficking, nuclear entry, uncoating or packaging. Therefore, a better knowledge of the different AAV serotypes is required to optimize this strategy. Technically, the production of chimeric AAV capsids can be performed in two different manners: the first one exploits the sequence homology between serotypes to serve as a crossover point for HR events mediated by cellular DNA repair proteins. The second one is performed by direct or random mutagenesis. This strategy allowed the identification of the AAV1 domain responsible for its strong muscular

tropism. However, several other parameters may control the tropism of AAV vectors: as an example, chimeric AAV5 particles containing the AAV2 HSPG binding motif were unable to efficiently transduce cells normally targeted by AAV2 [20], [164], [22].

Despite the high efficiency of these methods to obtain new attractive AAV vectors, other procedures were developed to add on the AAV capsid surface artificial motifs or elements such as fluorescent molecules or targeting ligands (**Figure 12D**). In particular, cell surface targeting is done to: i) improve transduction efficiency by exploiting a novel non-AAV receptor for cell infection, and ii) to re-direct AAV towards a known receptor. Furthermore, another process which allows to produce AAV capsids with original properties consists in performing a random mutagenesis on the *cap* gene by DNA shuffling or error-prone PCR. This strategy allowed to generate libraries of mutated AAV capsids potentially presenting several interesting properties [165], [166]. These libraries can be screened with various criteria, in order to select AAV variants with specific properties [135], [167], [168].

I.4 AAV and Immunity: a challenging field of study for medical application

The safety and the efficiency of gene delivery with viral vectors is intricately linked to the induction of host immune responses against both the particle and the transgene product. In this part, we will focus our attention on the response against AAV vectors and their transgene product.

The human immune system, which has evolved to avoid pathogen infections, can be subdivided in three different compartments that foreign organisms have to cross to successfully infect their targets: physical barriers, innate immune responses and adaptive immune responses. These obstacles, which define a functional gradient of specificity, speed and efficiency, compose the defense mechanism of the host. Indeed, physical barriers such as skin or the acidic environment of stomach lumen can block a large spectrum of microorganisms. In gene delivery strategies, this first barrier is mainly overcome by a direct administration (injection into muscle or intravenous) of the vector into the organism. The innate immunity is activated when microorganisms successfully cross the physical barriers and enter into the organism. It is mediated by several sensors, molecules and cell effectors such

as pro-inflammatory cytokines or various cell types, such as macrophages. These responses are induced quickly after the first interaction between pathogen and host, and are able to clear a large range of pathogens. If the clearance is not complete, the organism uses the adaptive immune response which is able to specifically target the pathogen. This latter barrier is highly specific and induces a memory immunity permitting to react quicker and stronger in case of a secondary interaction with the same pathogen.

I.4.1 Innate immune responses against rAAV

Innate immunity is based on sensors, called Pattern Recognition Receptor (PRR), which are able to recognize various pathogen associated motif patterns (PAMP). The best-characterized PRR are the Toll-like receptors (TLR). They are either localized on the cell membrane at the cell surface, and/or in the vesicular system. After recognition of the PAMP, the majority of these TLR activate the MyD88 pathway, triggering activation of NFκB and Map kinase pathways, and resulting in expression and secretion of several pro-inflammatory cytokines such as interleukin (IL)-1 and IL-6, or type 1 interferon (IFN-I) [70], [169]. According to the released cytokine cocktail, various cell effectors such as macrophages or granulocytes are recruited at the infection site. This inflammatory mechanism aims to clear the pathogen at the infection site. The clearance is helped by complement molecules that are able to opsonize various pathogens, resulting in an increase of the neutralization of the pathogen and/or its uptake by phagocytic cells. These responses start few hours after infection and are sometimes sufficient to stop or control the acute infection before the onset of adaptive immune responses. In parallel to the inflammation process, antigen presenting cells (APC), such as dendritic cells (DC), plasmacytoid DC (pDC), and macrophages activate T lymphocytes and trigger an adaptive immune response [87], [170], [171].

Several studies provided strong evidences that despite being unable to induce any acute inflammatory reaction, AAV vectors can interact with the innate immune system [172]. AAV capsids are able to bind directly the IC3b complement molecules which facilitate the phagocytosis of AAV particles by macrophages, and activate the expression of several pro-inflammatory genes [173]. This mechanism is described as essential to trigger anti-AAV B cell responses in mice. AAV capsids are also able to be detected directly by TLR-2, on the surface

of liver sinusoidal endothelial cells, Kupffer cells and activated endothelial cells, triggering the MyD88 pathway [174]. Moreover, the vector genome may be also detected by the innate immune system, via TLR-9, similarly resulting in the activation of MyD88 pathway [69]. The nature of the genome also influences innate immune response induced by rAAV. Indeed, scAAV vectors appear more immunogenic in mice, and the mechanism involved in this higher immunogenicity seems to be mediated by TLR-9 [175].

I.4.2 Adaptive immune responses against rAAV capsids

During intracellular trafficking, AAV capsid-derived peptides can be presented to the immune effectors lymphocytes by the major histocompatibility complex type I and II (MHC-I, -II). Indeed, after the endosomal escape, AAV capsids can be degraded by the proteasome and the peptides resulting from this degradation can be transported to the MHC loading compartment via the transporter associated with Antigen (TAP). As expected, this presentation event strongly correlated with the vector dose used and proteasome inhibitors were able to block antigen presentation. There are no evidences that the mode of presentation of AAV peptides onto the MHC differs among serotypes, but surprisingly empty capsids seem to be unpresented on the cell surface [176]. However, several studies performed with AAV2 and AAV8 suggest that these serotypes differ in the kinetics of induction of T cell responses. This presentation is required for the development of an adaptive immune response against the capsid [150], [177]–[179].

I.4.2.1 Humoral immunity

As described before, humoral immunity against the AAV capsid is one of the most important obstacles that can limit the efficiency of medical applications of AAV vectors. The natural exposure to wt AAV occurring early in life, leads to the production of neutralizing antibodies against AAV capsids in up to 70 percent of the human population [14], [28], [180]–[182]. Moreover, maternal antibodies directed against AAV capsid were found in newborns defining a very narrow window of time during which most humans are naive to these antibodies. During the first clinical trial for Hemophilia B, it was shown, and then confirmed in murine and NHP models that even low titers of neutralizing antibodies can efficiently block vector transduction. The presence of these antibodies in the human population leads to select

patients according to their serological status and to avoid vector re-administration [27], [28]. Several solutions have been proposed to overcome this pre-existing immunity such as plasmapheresis to remove most antibodies in the serum of the patient, or pharmacological drugs which target B cells during AAV treatment, or empty capsids to sequester anti-AAV antibodies [183]. This latter solution although less invasive, may however have important consequences on the immune response developed by the host. Moreover, several reports have shown a decrease of transduction efficiency using empty AAV capsids. The most elegant strategy to overcome humoral immunity is capsid engineering [48], [55]. Indeed, the identification of neutralizing antibodies binding motifs on capsids have made lot of progresses these last years, and the development of artificial AAV capsids able to escape pre-existing immunity is an important challenge for AAV capsid engineers.

I.4.2.2 T cell responses against the capsids

In humans, the presence of AAV capsid reactive T cells appears important, and variable according to the serotype. It has been shown that two-third of adults (more than 25 years old) present T cells able to produce IFN-γ after stimulation with AAV2 capsid peptides, whereas less than one-third react against peptides from AAV1 [150]. This difference can be explained by the variable exposition to these two serotypes and/or by their variable immunogenicity, but also by the variability of the protocols used to measure this response. As described for the humoral immunity, the important conservation of the AAV sequence among the broad range of serotypes leads to a high level of cross reactive T cells. Interestingly, the T- and B-cells responses seems to be uncoupled, suggesting that after the first contact with the AAV capsid, the host may develop either a Th1 or Th2 response. A better knowledge of the natural infection by AAV is required to identify the mechanisms leading to the development of these two kinds of responses.

In the first clinical trial aiming to treat Hemophilia B with AAV vectors, liver injection of AAV2 vectors led to a transient expression of the transgene, which was quickly decreased likely after clearance of the transduced hepatocytes mediated by a cytotoxic $CD8^+$ T-cells (CTL) [184]. Similar results were obtained in another clinical trial using AAV8 vectors [145]. The subjects enrolled in this clinical trial were selected for having a low titer of neutralizing antibodies against AAV, and for never having been pre-exposed to HCV or hepatitis B virus

(HBV), which can strongly influence the hepatic environment. Furthermore, transduction of hepatocytes was optimized by using a scAAV vector, a hepatocyte-specific promoter, and a codon-optimized FIX gene. Interestingly, in this study the administration of immune suppressive drugs (*i.e.* steroid) shortly after the appearance of T-cell responses against the capsid prevented, in most cases, the decrease in transgene expression. Immune responses observed in these studies are likely due to an expansion of a pre-existing pool of $CD8^+$ memory T-cells generated after a previous infection of the subject with wt AAV [185]. It is currently accepted that this kind of response is mediated by the presentation of the capsid antigens by MHC-I molecules on the surface of transduced cells, after degradation of the capsid by the UPS [176]. Because previous assays performed on animal models such as mice, dogs or NHP failed to reproduce the events observed in humans, an intensive work is currently performed to generate an animal model [186] allowing to improve our knowledge on the establishment of such responses. This T-cell response was also observed after intramuscular injection of rAAV in clinical trials [150]. It is closely linked to the rAAV doses and it was also observed for other serotypes [177], [187]. Interestingly, different immuno-privileged tissues, such the eye or the brain do not develop these responses [150], [188].

An intense work is ongoing to overcome the T cell response directed against the AAV capsid to prevent the elimination of rAAV-transduced cells. Three main strategies are currently being developed: i) the reduction of the capsid antigen dose, ii) the administration of immune suppressive drugs and, iii) the tolerization against the AAV capsid [150]. In order to reduce the amount of capsid antigens presented by transduced cells, vectors were designed to increase the transduction efficiency (allowing a reduction of the vectors doses in medical applications), or to escape the UPS [186], [189]. UPS inhibitors have also been tested [178]. The quality of the rAAV preparations has to be improved to avoid the presence of empty or non-infectious particles which obviously increase the amount of capsid antigens. The administration of immune suppressive drugs to reduce the immune response is also efficient but presents different drawbacks such as an increased sensitivity of the subject to pathogens, and the inhibition of tolerization which can be useful or required for gene therapy. In addition, the preventive use of such drugs in all patients compromises immune-monitoring during the clinical trial, thus limiting the comprehension of the interaction between rAAV and the immune system. The last strategy which exploits the natural ability of the immune system to

control the T cell reactivity against self-antigens by tolerization appears as the most elegant. This strategy based on the use of particular peptides (*e.g.* Tregitopes derived from MHC-II epitopes) allows to artificially induce a specific tolerization process based on the expansion of the regulatory T cells (Treg) and the inhibition of the Th-1 and Th-2 responses [190], [191].

I.4.3 Immune responses against the transgene product

Besides reacting against the viral constituents (the capsid and the vector genome), the immune system can also react against the transgene product. The type and the extent of this reaction vary according to several parameters including, notably, the nature of the transgene (homologous or heterologous protein), and its site and level of expression. In gene therapy applications, a tolerance against the transgene product is desired in order to induce a long term expression in the host. In contrast, in the case of gene vaccination, the transgene product, coding for an antigen, which can be derived from various pathogens, has to be recognized and to trigger a strong immune response in order to immunize the host against the pathogen. The low pro-inflammatory profile of AAV and its inability to efficiently transduce APC make AAV vectors very attractive for gene therapy. However, immune responses against the transgene products have been observed in several occasions during preclinical gene therapy experiments [179]. In addition, recent studies using rAAV for genetic vaccination have highlighted the high potential of AAV vectors to induce a strong and efficient immune response against viral and bacterial antigens, in particular in terms of humoral immunity [147].

The transgene product may be recognized as a foreign antigen, especially if the recipient of gene transfer does not express it naturally. A foreign protein can be presented to T cells by APC on MHC-I leading to a cytotoxic response mediated by $CD8^+$ T cells. It can also be presented on the MHC-II to trigger the activation of $CD4^+$ T cells, resulting in the activation of humoral immunity mediated by B cells. In APC, the peptides derived from endogenously expressed proteins can be directly presented on MHC-I after proteasome degradation. Exogenous proteins can be cross-presented on MHC-I or MHC-II after endocytosis. Due to its low efficiency to transduce APC, it is assumed that peptides derived from the AAV-encoded transgene products are not presented on MHC-II by direct presentation, but rather cross-presented by MHC-I and MHC-II after endocytosis [179].

The development of an adaptive immune response against the transgene product is critically linked to the administration routes and the target tissue for gene delivery. For example, in the liver, an organ of choice for gene therapy, several studies have shown a lack of responsiveness against factor IX (FIX) encoded by AAV, in small and large animal models [192]–[195]. This absence of response is due to a tolerance mechanism mediated by Treg. Indeed, given its role in the organism, the liver is an important tolerogenic organ [196]. The tolerance induced by Treg was confirmed in preclinical studies with several other transgene products [193], [197], [198]. In humans, the clinical studies conducted on Hemophilia B patients do not allow to draw this conclusion since the patients were selected for the presence of point mutations which do not prevent the production of FIX but just inhibit its activity. In contrast to what was observed in the liver, the intramuscular (IM) administration of AAV vectors encoding for a foreign transgene product may result in unwanted transgene-specific immune responses which correlated with the MOI used for gene delivery, and varied with the animal species, the serotype, the vector conformation (ss or sc) and the nature of the transgene product [199]–[202].

To conclude, several factors can strongly influence the establishment of immune responses against the transgene product after gene delivery using AAV vectors. It is clearly assumed that the observations made in murine model are unable to predict the immune reactions in humans. Moreover the nature and the intracellular fate of the transgene product, but also the vector features (serotype and genome) highly influence the development of immune responses against the transgene product [183], [185]. These parameters make any prediction of the outcome on gene transfer in humans very difficult and further complicate the design of gene therapy or vaccination strategies.

I.5 Dendritic cells: a pivotal actor of the Immunity

Immune innate responses have two different aims: the first one is to lead to a rapid protective response mediated by several cell effectors and molecules. The second one is “built in”, aiming to allow the transition toward the development of adaptive immune responses. DC are considered as the conductors of the immune orchestra as they are able to efficiently and precisely regulate the immune system at several levels. Able to interact with various cell

effectors of the immunity, they are implicated in both innate and adaptive immune responses. In particular, they also play an important role in the tolerance mechanism limiting self-reactivity of the immune system [203]–[205].

I.5.1 Dendritic cells as the principal professional APC of the immune system

The cells able to present antigens on MHC-II are defined as antigen presenting cells (APC) because they have the property to communicate with T lymphocytes, triggering antigen-specific adaptive immune responses. Several cells express MHC-II molecules such as some epithelial or endothelial cells, but their abilities to efficiently engage T cells appears very variable. B lymphocytes, macrophages and DC are currently considered as the professional APC due to their ability to efficiently present antigens on MHC-II. However, among these three cell types, only DC can present the antigen to the naïve T cells and activate them. In addition, DC present a broad range of interesting features which allow them to play a pivotal role in the immune system.

Initially derived from circulating bone-marrow precursor, DC achieve their differentiation when they take residence in peripheral tissues. The interface between the organism and the environment, composed of epithelia and mucosa present in skin, airway, or intestinal epithelia contains several types of DC. In steady state, the DC present an immature profile characterized by a strong ability to uptake extracellular components. As sentinels, they are seeking out for foreign invaders or danger signals which, when encountered, lead to their maturation. It is important to note that several subtypes of DC have been described *in vivo* which derive from different progenitors and present variable properties, leading to different kinds of immune responses.

I.5.2 Maturation of the dendritic cells

The maturation of DC is a complex mechanism which tightly regulates their function. It can be mediated by the activation of PRR (*e.g.* TLR) or inflammatory cytokines, and trigger a complete modification of DC features. In particular, DC maturation leads to a profound structural and functional reorganization of the cell in order to acquire the capacity to present the antigen (**Figure 13**). Endocytosis of the extra-cellular antigenic environment is initially and

transiently strongly upregulated and then completely inhibited. Mature DC also participate in the innate immune response by secreting IL-12 and IFN-I and by mobilizing natural killer (NK) cells. During this process, DC gain the ability to migrate to secondary lymphoid organs, such as lymph nodes or spleen which are enriched in naïve T cells, where DC activate them by antigen presentation and co-stimulatory signals. Mature DC present a specific morphology with an increase of the membrane surface permitted by the high amount of dendrites, allowing them to simultaneously communicate with many naïve T cells. According to the maturation pathway, the DC can either stimulate adaptive responses, or suppress them (tolerance). Indeed, DC can participate in cytotoxic (mediated by Th1), and humoral immunity (mediated by Th2), and in tolerance mediated by anergy of T cells or expansion of Treg [170].

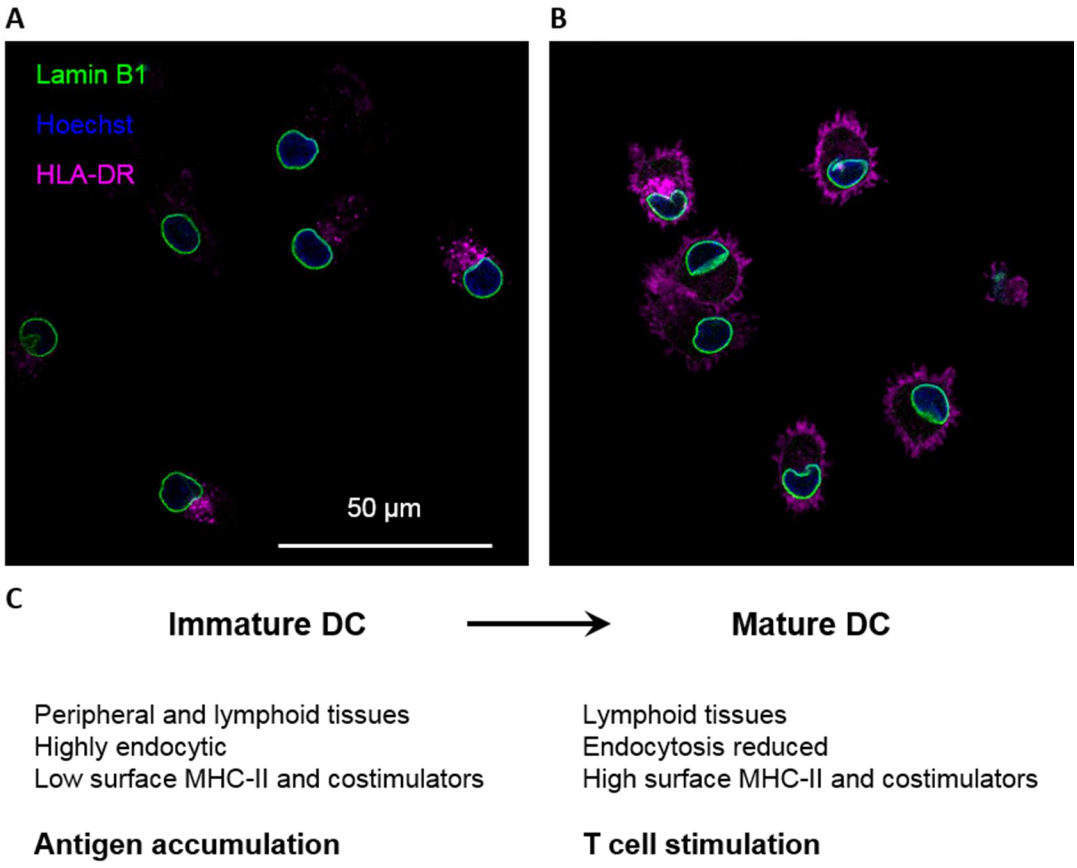


Figure 13. Maturation of DC.
Observation of immature (**A**) DC or mature (**B**) DC by confocal microscopy. Human monocyte-derived DC were maturated by LPS treatment, and analyzed by immune-fluorescence using antibodies recognizing Lamin B1, to label the nuclear membrane, and HLA-DR, to label MHC-II molecules. The DNA was stained with Hoechst. **C.** Main features of DC according to the maturation status (adapted from [170]).

I.5.3 Adeno-associated virus derived and dendritic cells

Due to their pivotal role in the immune system, DC appear as an attractive target for immune regulatory gene transfer strategies aiming to induce active immunization or tolerization [206]. Thus, viral vectors, such as lentiviral vectors have been used to express interesting antigen within DC in order to exploit their ability to present antigens on MHC-I and MHC-II.

The interaction of AAV with DC is also of great interest not only to understand their effect on the immune responses induced after gene therapy but also to potentially develop DC-based immunotherapeutic approaches. Initial studies have shown that conventional ssAAV vectors are unable to efficiently transduce murine or human DC *in vitro* [207], [208]. Later on it was shown that scAAV vectors can transduce DC subtypes differentiated from monocytes or $CD34^+$ hematopoietic progenitors [206]. Then, scAAV vectors derived from serotypes 2, 5 and 6 were described as the most efficient to transduce DC [209], [210]. It was also shown that transduction of the DC progenitors leads to a more efficient expression of the transgene, without important effects on the differentiation process [206], [208]. Different capsid engineering strategies were performed to optimize DC transduction, using AAV2 [211] or AAV6 [212], [213] vectors. These studies succeeded at overcoming different barriers limiting the DC transduction. However, it is important to note that in most of these studies the authors used extremely high doses of AAV vectors. In addition, the maturation state of the DC, prior to rAAV transduction, was rarely examined.

Furthermore, to use AAV vectors in DC-based immunotherapy, the transduction efficiency was not the unique parameter that has to be controlled. Indeed, it was crucial that the transduced DC conserved their immune properties, such as antigen uptake, maturation, antigen presentation and cytokines secretion. Analysis of DC properties after transduction with high doses of AAV vectors reported no effects in terms of maturation or other modifications of the DC phenotype. Interestingly, re-injection in mice of DC transduced *ex-vivo* with wt or engineered AAV vectors was shown to induce antigen-specific humoral and/or cytotoxic immune responses showing the important potential of this strategy for active immunization [210], [211], [213].

Evidences for *in vivo* transduction of DC remain controversial and only one recent study succeed at showing a small percentage of DC transduction after rAAV injection in mice [214]. In this work, the authors showed that a rAAV8 is able to transduce different immune cells in the secondary lymphoid organs, such as B and T cells, and with lower efficiency, DC. Surprisingly, rAAV8 was described as tolerogenic in mice resulting from its very low DC transduction efficiency [215]. However this result was not confirmed in clinical trials using AAV8 vectors. Thus, a comprehensive study is required to better understand the interaction between the AAV vectors and DC, as well as its consequences on transgene expression.

II. Materials and Methods

II.1 Adeno-associated virus derived vector production

Stocks of wild type and recombinant AAV2 particles were generated by calcium phosphate transfection of HEK-293 cells, as previously described, using the pXX6-80 or pDG helper plasmids to provide the AdV helper activities. In contrast to pDG which combined wt AAV and helper genes in the same molecule, use of pXX6-80 required to additionally transfect the cells with the pRC plasmid [18], [216] (**Figure 14**, **Figure 15**). Vector particles were purified on cesium chloride or iodixanol gradients as previously described [217], [218] and the number of vector genomes per milliliter (vg/ml) was determined by quantitative PCR (qPCR).

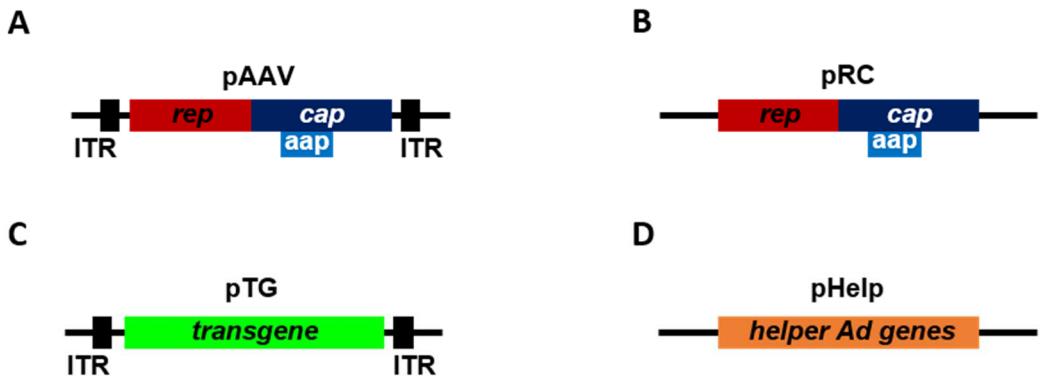


Figure 14. Plasmids for rAAV production.
The plasmids used in this study are: **A.** AAV plasmids (**pAAV**), containing AAV2 genes and ITR. This plasmid is used to produce AAV2 particles. In this study, we used both a plasmid with the wt *cap* gene and plasmids (pLib, and pLG) containing mutations (*i.e.* insertion) in the *cap* gene. **B.** *rep/cap* plasmids (**pRC**), containing the AAV genes without the ITR sequences, which is used to produced rAAV (pRC containing wt AAV2 *rep/cap* gene [219], pRC'99 (*idem*) [220], pRC'99-mut (*idem* with mutation, *i.e.* insertion). **C.** Transgene plasmids (**pTG**) containing a transgene expression cassette flanked with viral ITR is used to produce rAAV (peGFP to produce ssAAV-GFP, pscGFP to produce scAAV-GFP, pcOVA to produce ssAAV-cOVA [221]). The vector can be either ss or sc according to each experiment. **D.** Helper plasmids (**pHelp**), containing helper functions required to produce AAV virions, (pXX6-80 [216] containing helper gene from AdV, pDG, pDG8, pDG9 containing helper gene from AdV and *rep/cap* gene from AAV2, 8, 9 respectively [18]).

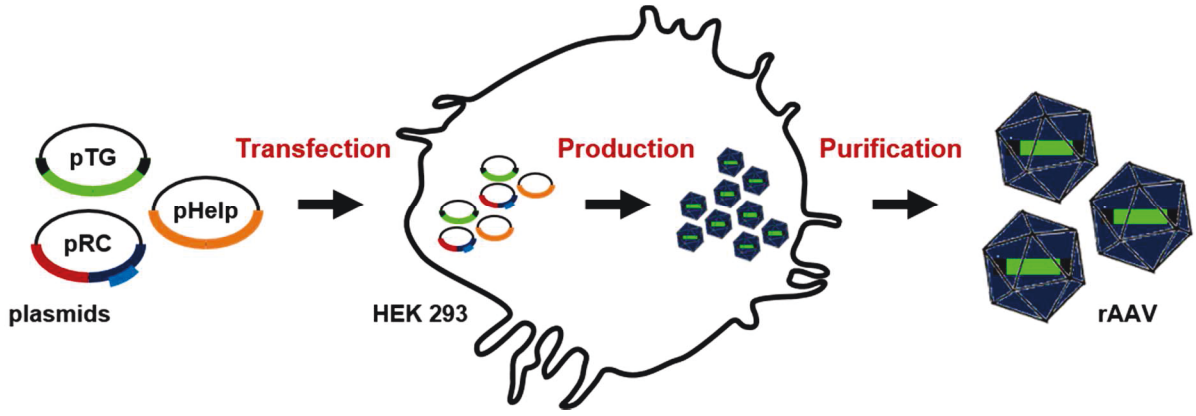


Figure 15. rAAV production.
Plasmids are transfected on HEK 293 cells with $CaCl_2$. 48 h after transfection, cells are lysed and AAV vectors are purified on a CsCl or iodixanol gradient. Different sets of plasmid can be used (*e.g.*pDG8 and pscGFP to produce scAAV8-GFP vectors; pXX6.80, peGFP and pRC to produce ssAAV-GFP vectors *etc.*)

II.2 Cell lines and infection procedures

HeLa, HEK-293, Vero SLAM, H358, U87 and Raw264.7 cells were maintained in Dulbecco's modified Eagle's medium (DMEM; Life Technologies) supplemented with 10% fetal bovine serum (FCS; HyClone) and 1% penicillin-streptomycin (P/S; 5,000 U/ml; Invitrogen), and cultivated at 37°C, 5% of CO_2.

II.2.1 Culture of monocyte-derived dendritic cells (mo-DC)

Monocytes were purified from peripheral blood of healthy donors by two successive density [Ficoll (GE Healthcare Life Sciences; density: 1,077) and Percoll (GE Healthcare Life Sciences; density: 1,131) gradients. Then, they were differentiated or frozen. Differentiation of monocytes into monocyte-derived dendritic cell (mo-DC) was performed by incubating cells for 5 days in DC medium (RPMI with, 10% of FCS, 1% P/S, 10mM HEPES, 2,5mM NEAA; 1mM sodium-pyruvate and 0,05mM β–mercaptoethanol) completed with IL-4 and GM-CSF (renewed every forty-four hours at 100 ng/mL). The differentiated status of mo-DC was verified by FACS analysis, to analyze the level of DC-SIGN, CD14 and CD86 markers (**Figure 16**).

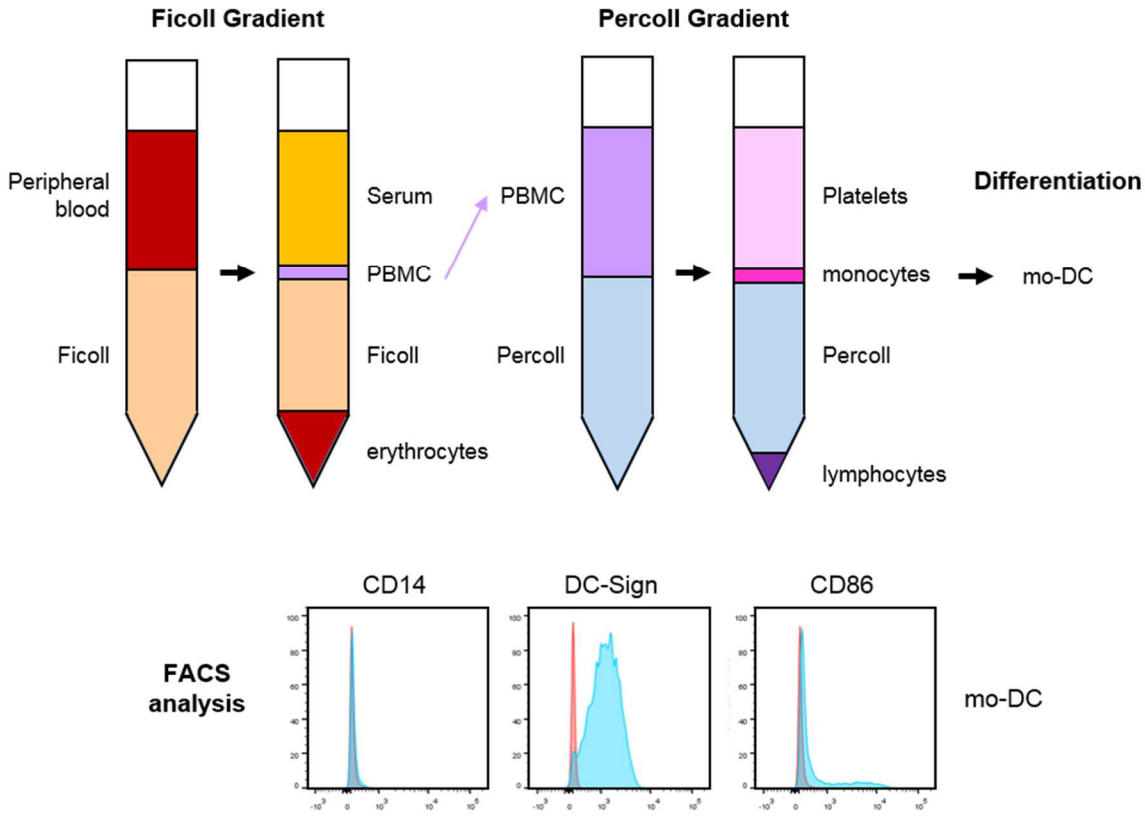


Figure 16. Overview of the mo-DC production and control.
A first Ficoll gradient allowed to isolate peripheral blood mononuclear cells (PBMC) and sera from peripheral blood of healthy donors. A second Percoll gradient permitted to purified monocytes and lymphocytes from PBMC. After the five days differentiation, FACS analysis allowed to control the differentiation process using anti-CD14 (CD14 is a monocyte marker) and anti-DC-Sign antibodies (DC-Sign is a marker of DC). The maturation status of DC was also controlled using anti-CD86 antibody (CD86 is a marker of mature dendritic cell).

II.2.2 Cell Transduction

Cells were plated and then transduced with complete medium containing vector particles diluted at the indicated MOI (vg per cell). At the indicated time point, cell were harvested, trypsinized and washed in PBS. The cell pellets were conserved at -20°C for DNA extraction or -80°C for protein extraction (fractionation assay). When indicated, mo-DC were additionally treated with lipopolysaccharide (LPS; 0.5 - 1 µg/mL), chloroquine (15µM), Dibenziodolium chloride (DPI) (SIGMA: DPI-D2926 10µM) at the indicated time point (**Figure 17**). For the competition assays, the medium containing vector particles was supplemented with heparin (25µg/mL).

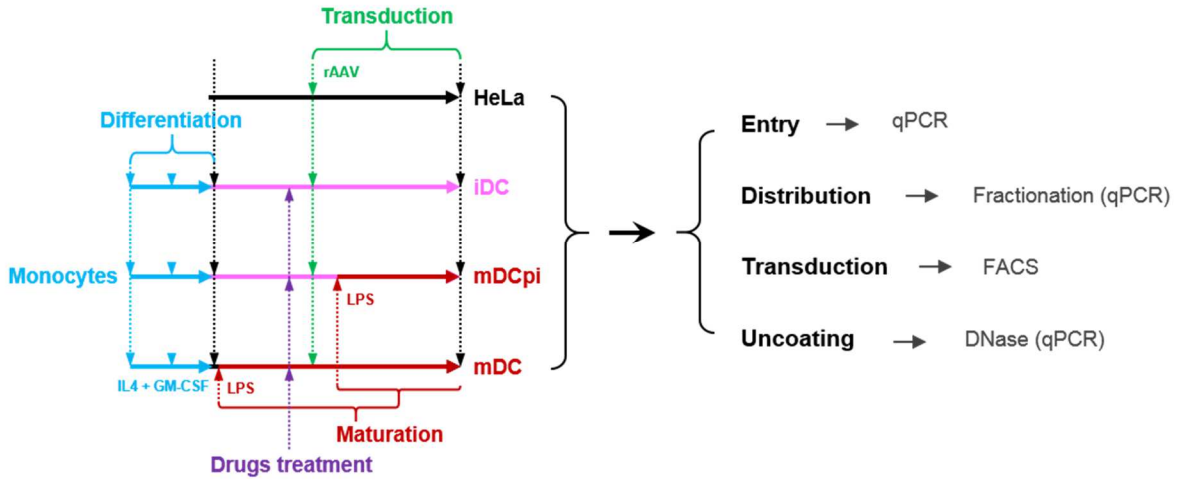


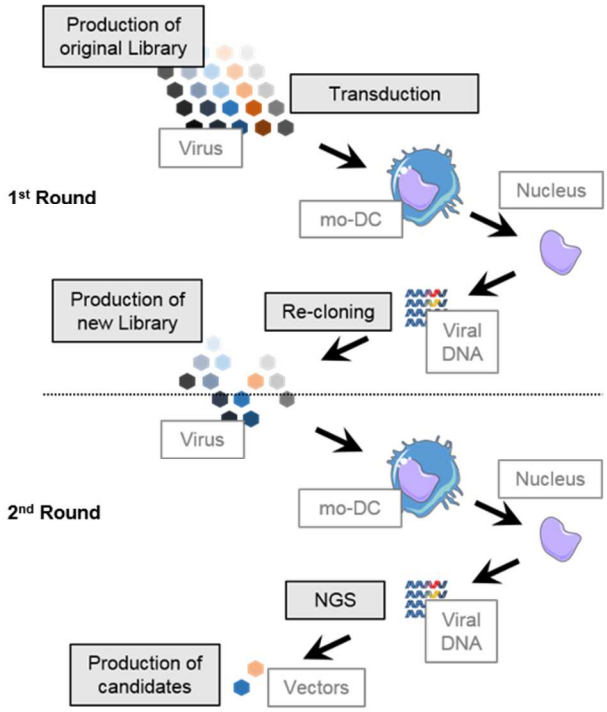
Figure 17. Cell culture, protocol outline.
To differentiate monocytes into mo-DC (*i.e.* immature DC [**iDC**]), cells are cultivated in presence of IL4 and GM-CSF for 5 days, and then plated for the experiment. In order to activate mo-DC, LPS is added to the DC medium 24 h before infection for our mature DC condition (**mDC**), or 2 h post infection for our intermediate condition (**mDCpi**). The transduction with rAAV define the h_0 of the assay, and the medium with AAV particles is not changed until the end of the culture. Drugs (DPI, chloroquine), were added to the cells 15 min before infection. At various times post-infection, cells are harvested and used to analyze rAAV entry (by qPCR), intracellular distribution (by fractionation and qPCR), transduction (by FACS) and uncoating efficiency (by DNase and qPCR).

II.3 *In vitro* directed evolution of AAV particles

II.3.1 Overview of the selection procedure

AAV capsid variants were selected by AAV infection of mo-DC [222]. In this PhD work, three selections were performed with variable selection conditions (**Figure 18**). Each selection was performed in two rounds: briefly mo-DC were transduced with the AAV library (already generated and coupled in H. Büning's laboratory) ; then, at the indicated time point, nuclear viral DNA isolated by fractionation and DNA extraction, was used to generate a new library (re-cloning procedure) (round 1). The new library produced after round 1, was used to transduce mo-DC, and, at the indicated time point, nuclear viral DNA was again extracted and sequenced by next generation sequencing (NGS).

A



B

1st Selection	Donors	MOI	hep	harvest
1st Round	#1	10^3	No	6h pi
2nd Round	#2	10^3	No	6h pi

C

2nd Selection	Donors	MOI	hep	harvest
1st Round	#3	10^5	Yes	4h pi
2nd Round	#4	10^4	Yes	4h pi

D

3rd Selection	Donors	MOI	hep	harvest
1st Round	#3	10^4	Yes	4h pi
2nd Round	#4	10^3	Yes	4h pi

Figure 18. Selection of AAV particles targeting mo-DC by directed evolution.
A. Overview of the procedure. **B.** Experimental conditions for 1st Selection. **C.** Experimental conditions for 2nd Selection. **D.** Experimental conditions for 3rd Selection. To avoid a donor-dependent bias, mo DC used in the 1st and the 2nd round of each selection were purified from two different donors. To increase the selection pressure, the 2nd and the 3rd selections were performed by infecting mo-DC in the presence of heparin (**hep**); in addition, the MOIs used were decreased of 1 log between the 1st and the 2nd round. The incubation time were also decreased (from 6 h to 4 h; pi, post infection).

After identification and cloning of the most representative mutants obtained after the 2nd round of selection, rAAV particles harboring the mutation at the surface of the capsids were generated using standard production procedures.

II.3.2 Construction of AAV sub-libraries

II.3.2.1 Re-cloning procedure

The cloning protocol was optimized by Li-Ang Zhang (PhD thesis of Li-Ang Zhang 2015 H. Büning PhD director) to enhance the selection efficiency and accuracy (**Figure 19A**). After DNA extraction of transduced mo-DC, nuclear viral DNA was amplified by PCR using primers CLO-F (5'- CGT ATC GCC TCC CTC GCG CCA TCA GAC GAG TGC GTT GGA ATC TTT GCC CAG ATG G -3') coupled to biotin, and primer CLO-R (5'- CTA TGC GCC TTG CCA GCC CGC TCA GAC GAG TGC

GTA CAA CCA ATC CCG TGG CTA C -3'). After PCR amplification of viral genome, the PCR product were digested with NotI-HF for 1 h at 37 °C. To enhance the binding between streptavidin and biotin, 20 µl of 10 µl of 1.15 M NaCl were added into the tube together with streptavidin microbeads, and incubated for 20 min at room temperature. The supernatant containing the distal part of the amplicon was removed by centrifugation at 13,000 rpm for 15 min at room temperature. The pellet was then washed with 200 µl of wash buffer (20 mM Tris, 50 mM NaCl). To remove the proximal part of the amplicon, the pellet was suspended and digested with AscI 1 h at 37 °C, followed by centrifugation at 13,000 rpm for 15 min at room temperature. Finally, the supernatant containing the middle part of the amplicon, was transferred into a new 1.5 ml tube and incubated for 20 min at 60 °C. The solution was then slowly cooled down to room temperature. The insert was ligated to 100 ng pLG plasmid between the AscI and NotI sites. The transformation of high competent *Escherichia coli* using the ligation product was performed according to standard procedures.

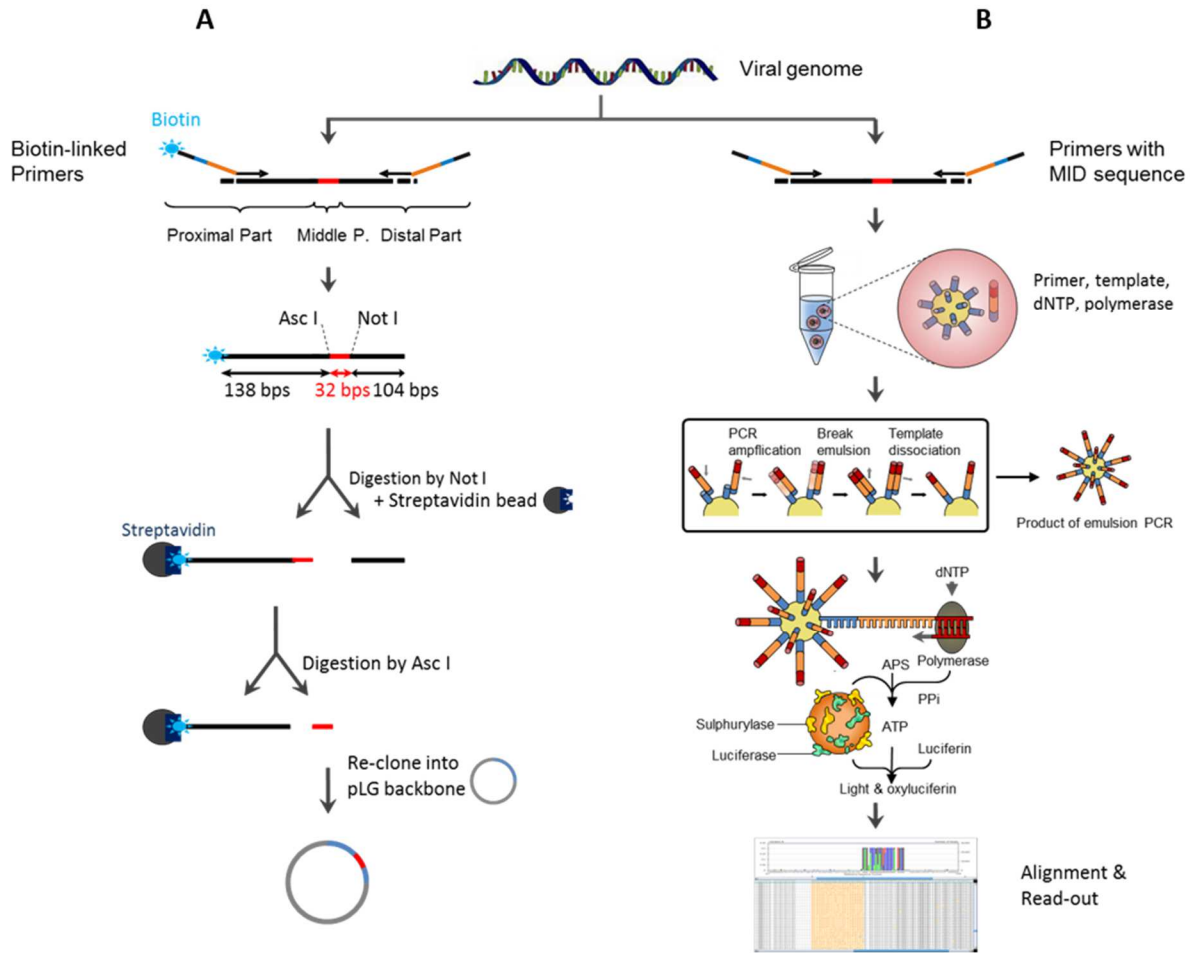


Figure 19. Cloning and sequencing of viral DNA extracted from AAV-transduced mo-DC.
A. Cloning procedure. After the 1st round of selection, the 274 bp DNA amplicons carrying a biotin residue at the 5'-end were purified using streptavidin microbeads-mediated pull-down followed by restriction site-specific release (AscI) of the fragment containing the mutation from the beads. The latter were inserted into pLG plasmid and used to generate the sub-library. **B. NGS-based protocol.** After the 2nd round of selection, NGS were performed and allow to determine the frequency of specific clones within the pool of total clones in order to identify candidates for further characterization; **Abbreviations: Middle P,** Middle Part; **MID,** Multiplex Identifiers; **dNTP,** deoxy-nucleoside triphosphate; **APS,** ammonium persulfate; **PPi,** inorganic pyrophosphate; **ATP,** adenosine triphosphate (taken from PhD thesis of Li-Ang Zhang 2015 H. Büning PhD director).

II.3.2.2 Production of the new library and pheno- and geno-type coupling

After the first round of selection the pool of mutated AAV genomes was used to produce a library of particles for the 2nd round of selection (**Figure 18**). For this, HEK 293 cells were transfected with the rep/cap library plasmid (pLib) and the Helper plasmid (pXX6-80). Viral particles were purified forty-eight hours later on iodixanol gradients. This procedure resulted in the production of library of particles containing the mutations of the *cap* gene selected during the 1st round (**Figure 20A**).

AAV pheno- and geno-type coupling (PCT/EP2008/004366) was then required to ensure that the genome encodes the peptide that is displayed on the capsid [222]. Briefly, A20 antibody (Progen, Heidelberg, Germany) was anchored onto the bottom of a 15 cm2 cell culture plate, followed by incubation with 7.5 x 10^9 genomic viral particles of the uncoupled AAV library at 37 °C for 24 h (**Figure 20B**). The plate was then washed three times with PBS and 7.5 x 10^6 HEK-293 cells in 20 ml of DMEM were then seeded on top of the antibody at 37 °C for twenty-four hours. Transfection was performed using the calcium phosphate method. Briefly, 22.5 µg of pXX6-80 plasmid was used for each 15 cm^2 cell culture plate. After twenty-four hours h incubation at 37 °C / 5% CO2, medium was exchanged for DMEM containing only 2% FBS to reduce cell division. Cells were harvested forty-eight hours later and the AAV library was purified as indicated above.

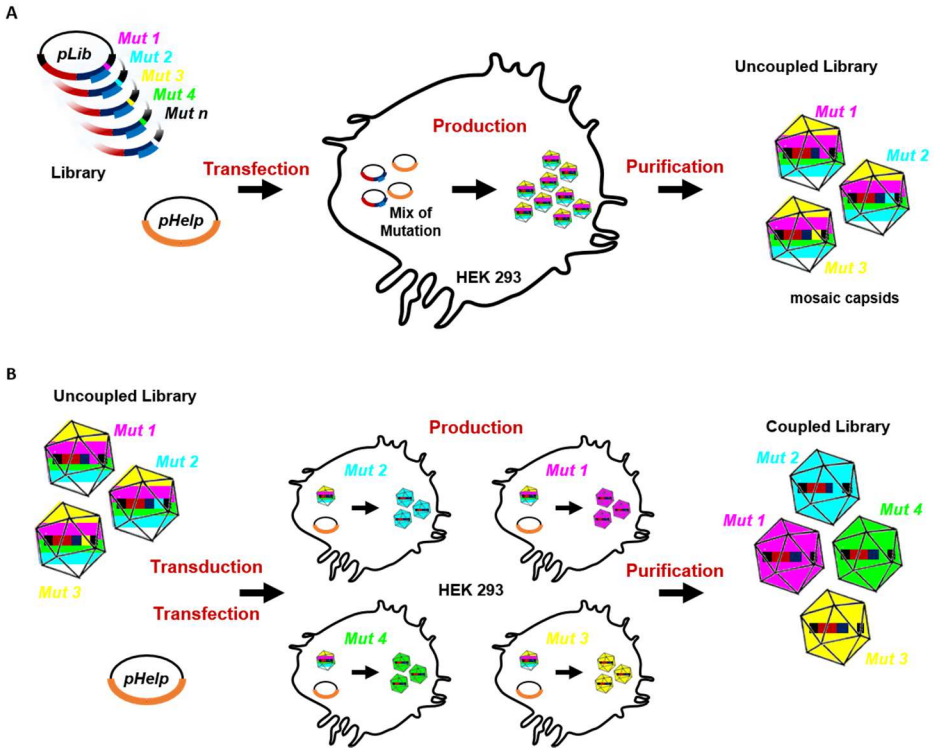


Figure 20. New AAV library production.
A. First step. The pLib library obtained after the re-cloning step, was used to produce an AAV stock containing the mutated viral genomes (uncoupled library). This AAV stock was a library, composed of a heterogenic population of mosaic capsids (rainbow capsid). These mosaic capsids are composed of VP proteins translated from different mutated *cap* genes (obtained by HEK 293 transfection with pLib library). **B. Second step.** The uncoupled AAV library obtained in the first step was used to produce the coupled library. The procedure allowed to infect each HEK 293 with a maximum of one mosaic capsid containing only one mutated *cap* gene (uncoupled AAV library). Thus, after HEK293 transfection with pHelp (pXX6-80), each infected and transfected cell produces a homogenous population of particles derived from a single mutated genome and containing the genome encoding this mutation. The heterogenic cell population allows to produce the coupled library.

II.3.3 Next generation sequencing

Next generation sequencing (NGS) was performed on the 454-pyrosequencing platform (GS Junior, Roche). Before proceeding to the sequencing step, the amplicon library was first purified according to the standard protocol of 454-pyrosequencing (**Figure 19B**). The products of this reaction were again pooled and purified to constitute the library of DNA fragments for the emulsion PCR and subsequent 454-pyrosequencing reactions performed according to the standard protocol of Roche. The data were aligned and analyzed using the GS Amplicon Variant Analyzer software (AVA) (**Figure 21**).

A

Mutations	Copy number (%)
NNPLPQR	518 (8,5)
NAQPPSR	338 (5,5)
ISSSTAR	229 (3,8)
VSSTSPR	160 (2,6)
NQPNPVR	159 (2,6)
VSSSTPR	134 (2,2)
PTRLLP	129 (2,1)
SNSTPLR	95 (1,6)
VSSSLQR	95 (1,6)
...	... (< 1,5)
NSARPNS	47 (0,8)

B

Mutations	Copy number (%)
NNPLPQR	1980 (7,6)
VSSSLQR	1151 (4,4)
LPSRPSL	**887 (3,4)**
NSARPNS	**584 (2,3)**
NQPNPVR	472 (1,8)
ISSSTAR	372 (1,4)
...	... (<1,4)
VSSTSPR	124 (0,5)

C

Mutations	Copy number (%)
LPSRPSL	**1899 (7,9)**
NTPNPLR	525 (2,2)
NSPLAAR	524 (2,2)
NNPLPQR	446 (1,9)
ARTGAVI	**371 (1,5)**
...	... (<1,5)
NSARPNS	289 (1,2)
ISSSTAR	100 (0,4)
VSSTSPR	9 (<0,0)

Figure 21. Selected variants from three independent selections.
A. Result of the 1st selection. **B.** Result of the 2nd selection. **C.** Result of the 3rd selection. Bold sequences were selected to produce rAAV-mut-GFP and tested on mo-DC. Blue R may be implicated in HSPG binding as **R**XXR motif.

II.3.4 Production of rAAV with selected capsid

Oligonucleotides (ordered from Metabion), containing the mutated sequences identified by NGS of viral genomes, and flanked by an Ala-Ser-Ala and an Ala-Ala linker at the 5' and 3' end, respectively, were sticky-end ligated into pRC'99 as described [220]. This resulted the plasmids pRC'99-mut (pRC'99-VSSTSPR or pRC'99-NNPLPQR or pRC'99-ISSSTAR or pRC'99-NSARPNS or pRC'99-ARTGAVI or pRC'99-LPSRPSL). pRC'99-mut sequences were controlled by Sanger sequencing (Cologne Center for Genomics, University of Cologne, Germany) and then used to produce rAAV-mut-GFP vectors.

II.4 Analysis of intracellular AAV distribution

II.4.1 Fractionation assay

Briefly, 10^6 cells infected with rAAV-GFP, were harvested at the indicated time point, washed with PBS, extensively treated with trypsin (to get rid of membrane attached particles) and washed again. Subcellular fractionation was then performed using Subcellular Protein Fraction Kit for Tissue (Thermofisher Scientific) by modifying the protocol provided by the manufacturer (**Figure 22A and B**), in order to improve the purification procedure. The purity of fractions was confirmed by Western blot. Vector genomes were quantified by qPCR after DNA extraction. Importantly, 1 ng of murine TOPO-GAPDH plasmid was added to each fractions as an internal DNA extraction control.

II.4.2 Western blot analysis

After fractionation, an aliquot of each sample was denatured in Laemmli buffer (3X solution: SDS 6%, Glycerol 30%, β–mercaptoethanol 15%, Tris pH 6.8 187,5nM, Bromophenol Blue) at 95°C for 5 min. Then, extracts were loaded on a precast 5-15% SDS polyacrylamide gel and, after SDS-PAGE, transferred to nitrocellulose membrane using the Trans-blot Turbo transfer system (Bio-Rad). After saturation, the membranes were incubated overnight at 4°C with the appropriate antibody diluted in blocking buffer: anti-Rab 5 (Santa Cruz sc 46692; 1:100), anti-tubulin (SIGMA T5198; 1:5000), anti-lamin B1 (Abcam antibody 16048; 1:5000), anti-calreticulin (Affinity BioReagents PA3-900, 1:100). After three washes in PBS/0.1% Tween 20, a horseradish peroxidase-conjugated anti-mouse or anti-rabbit IgG antibody (Sigma) was applied to the membranes at a 1/10,000 dilution for 1 h at room temperature. Finally, the membranes were incubated for 5 min with an enhanced chemiluminescence reagent (West Dura; Pierce) and exposed to an autoradiography film (**Figure 22D**).

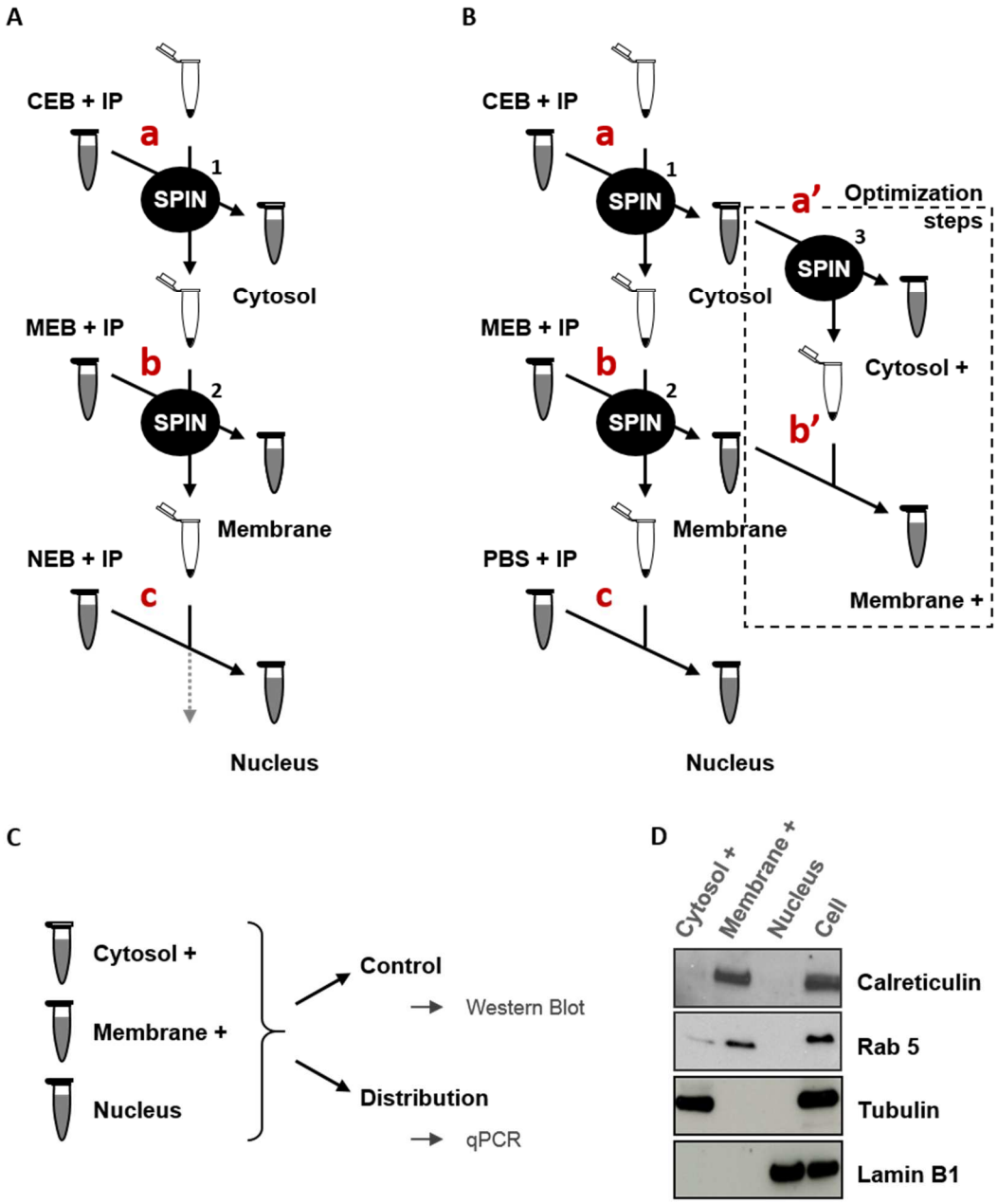


Figure 22. Fractionation procedure.

A. Standard protocol from Thermofisher Scientific. a) 1x10^6 cells were incubated 10 min with cytosol extraction buffer (**CEB**), and then centrifuged 5 min at 500 g; the supernatant (**SPN**) contained the cytosol fraction. **b)** The pellet was then incubated 10 min in membrane extraction buffer (**MEB**), and then centrifuged again 5 min at 3000g; the supernatant contained the membrane fraction. **c)** The pellet was mixed with nuclear extraction buffer (**NEB**), and then conserved as a nuclear fraction. **B. Optimized protocol. a')** the supernatant from **a**) was centrifuged again for 10 min at 17000g, SPN contained the cytosol fraction (cytosol +), **b')** the pellet from **a'** was mixed with SPN from **b** and then conserved as membrane fraction (membrane +). A protease inhibitor was added at all steps (**IP**). All the procedure was performed at 4°C. For the last step, NEB is replaced by PBS**C.** Each fraction was analyzed by Western blot, to detect cellular proteins, and by qPCR to detect AAV vector DNA. **D. Western blot.** The quality of each fraction was confirmed by Western blot, using antibodies recognizing Rab5 (and calreticulin), tubulin and lamin-B1 to label intracytoplasmic membranes, cytosolic and nuclear compartments, respectively.

II.4.3 Quantification of AAV vector DNA by qPCR

Primers used for the qPCRs were as follows: GFP-F (5'-ACG ACG GCA ACT ACA AGA CC-3'), GFP-R (5'-CTC CTT GAA GTC GAT GCC CT-3'), b-Globin-F (5'-CCC TTG GAC CCA GAG GTT CT-3'), b-Globin-R (5'-CGA GCA CTT TCT TGC CAT GA-3'), mGAPDH-F (5'-GCA TGG CTT TCC GTG TTC-3'), mGAPDH-R (5'-TGT CAT CAT ACT TGG CAG GTT TCT-3'), Ova-F (5'-AAG CAG GCA GAG AGG TGG TA-3'), Ova-R (5'-GAA TGG ATG GTC AG CCC TAA-3'). DNA extraction was performed with the Qiagen DNeasy Blood & Tissue Kit according to the manufacturer's instructions. The qPCR reactions were conducted with the FastStart universal SYBR green master reagent (Roche Diagnostics) according to the manufacturer's guidelines. The qPCR was run on the Step One Plus real-time PCR system (Applied Biosystems). All samples were run in duplicate, and the results were analyzed using ABI StepOne software v2.3. For titration, absolute amounts of amplicon were determined using dilutions of vector plasmids used for rAAV production. To measure rAAV genomes in entry, fractionation and uncoating assays the relative amount of each amplicon is expressed as mean ratio of rAAV genome to a housekeeping gene DNA.

II.4.4 Confocal microscopy analysis

After transduction with rAAV, mo-DC were harvested and plated in a 96-Well Optical-Bottom Plates (Fisher Scientific) or in a Labtek, both pre-coated with poly-lysine. Then cells were fixed with 4% paraformaldehyde and permeabilized with 0.2% Triton X100. After three washes with PBS, the cells were saturated with PBS/3%FCS for 1h at room temperature and then incubated with the selected antibodies in PBS/3%FCS overnight at 4°C. After three PBS washes, the cells were incubated with a secondary antibody conjugated to a fluorochrome and then incubated with Hoesch or DAPI, kept in PBS for observation. Images were acquired with a Zeiss LSM 710 laser scanning confocal microscope and analyzed with Image J (http://rsb.info.nih.gov/ij) and IMARIS (Bitplane Inc.) software packages.

II.4.5 *In vitro* uncoating assay

Briefly, 10^5 cells infected with rAAV-GFP, were harvested at the indicated time point, washed with PBS, extensively treated with trypsin and washed again. Then the DNA was extracted (Qiagen kit) and eluted in 100µL. twenty-five µL of DNA were treated with T5 exonuclease (Biolabs, M0363, 30 Unit) at 37°C overnight, then incubated 10 min at 70°C and diluted 2 times. In parallel, 25µL of the same DNA sample were mock treated. The quantification of viral and cellular genes was performed by qPCR (viral genome: GFP; cellular gene: β-globin). The percentage of episomal DNA was calculated from the ratio of T5 resistant GFP DNA on total GFP DNA (**Figure 23**).

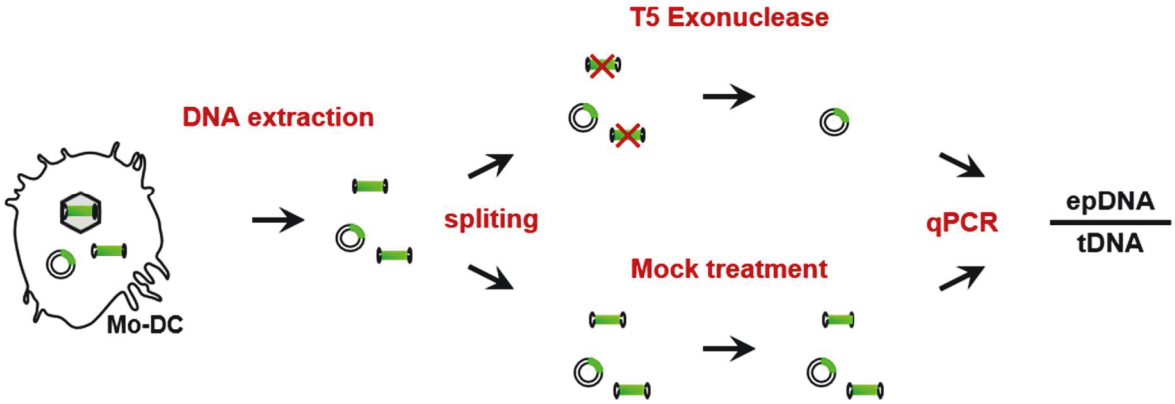


Figure 23. *In vitro* uncoating assay.
The assay is composed by four successive steps, i) the total DNA is extracted (**tDNA**), ii) tDNA is split into two samples, iii) samples are processed either with T5 Exonuclease (elimination of non-double strand circular DNA molecules, *i.e. episomal DNA* [***epDNA***]) or with mock treatment, iv) the amount of viral DNA in each sample is measured by qPCR. The ratio between these two measures allows the indirect calculation of the percentage of uncoated DNA.

II.5 Analysis of capsid stability

AAV capsids were incubated in buffer (citric acid / Na_2HPO_4) at different pH for 15 min at room temperature, then exposed to different temperatures (37, 50, 55, 60, 65, 70, 75, 80, 90 °C) for 15 min. For native dot blot assay, samples were diluted in PBS and transferred to a nitrocellulose membrane using a vacuum blotter. After saturation, the membranes were incubated overnight at 4°C with A20, and B1 antibodies [223] (hybridoma supernatants diluted 1/2 for A20, 1/5 for B1 in blocking solution). After PBS washing steps, a horseradish peroxidase-conjugated anti-mouse or an anti-rabbit IgG antibody (Sigma) was applied to the membranes at a 1/10,000 dilution for 1 h at room temperature. Finally, the membranes were

incubated for 5 min with an enhanced chemiluminescence reagent (West Dura; Pierce) and exposed to an autoradiography film. For the AFM imaging, samples are deposited on mica surface.

II.6 *In vivo* experiments in mice

Seven week old C57BL/6J mice were bred in "Université de Rouen" animal facility, housed under specific pathogen-free conditions and handled in accordance with French and European directives. For intramuscular injection, mice were anesthetized and injected into the two gastrocnemius muscles with rAAV-cOVA at the dose of $3.5.10^9$ vg/mouse. Viral stock are diluted on PBS [221], [224].

II.6.1 Quantification of rAAV mRNA in transduced muscles

For quantification of OVA mRNA, 100 ng of total RNA were reverse transcribed using iScript DNA Synthesis Kit (Biorad, Marnes-la-Coquette, France). Then, 2 µL of cDNA were subjected to real-time PCR amplification using Ova-F (5'-AAG CAG GCA GAG AGG TGG TA-3'), Ova-R (5'-GAA TGG ATG GTC AG CCC TAA-3'), Eef2-F (5'- AAG CTG ATC GAG AAG CTG GA -3'), and Eef2-R (5'- CCC CTC GTA TAG CAG CTC AC -3') primers. For all reaction mixtures, 10 µL of Fast Start Universal SYBR green mastermix (Roche, Boulogne-Billancourt, France) was used in a final volume of 20 µL. OVA primers were used at 500 nmol/L and β-actin primers at 400 nmol/L. The absolute amount of OVA mRNA for each sample was then normalized against the β-actin mRNA amount (arbitrary units) and determined using serial dilutions of pAAV–CMV–OVA plasmid and β-actin purified PCR product.

II.6.2 IFNγ-ELISPOT assay

Multiscreen nitrocellulose microplates (Millipore, Molsheim, France) were coated with anti-IFNγ mouse antibody (clone R4-6A2). Freshly isolated splenocytes (1.10^6/well and serial dilutions) were cultured in complete RPMI 1640 medium supplemented with 10% fetal calf serum (FCS) with or without 1 µmol/L of indicated peptides, *i.e.* OT-I (SIINFEKL), OT-II (ISQAVHAAHEINEAGR), PL-8 (PQYGYLTL). For each assay, Concanavalin A was added (5µg/ml) as a positive control. After 20 hours, plates were incubated 2 hours with biotinylated mouse

anti-IFNγ antibody (clone XMG1.2) and 15 hours with alkaline phosphatase-conjugated streptavidin (Roche, Mannheim, Germany). Spots were developed by adding peroxidase substrates, 5-bromo-4.3-indolyl phosphate and nitroblue tetrazolium (Promega, Madison, WI) and counted using an AID reader (Autoimmun Diagnostika). Spot forming units (SFU) are represented after subtraction of background values obtained from unpulsed splenocytes (always below 10 spots/well).

II.6.3 Anti-OVA IgG ELISA

ELISA microtiter plates (Nunc.) were coated overnight with 50 µl per well of a 10 µg/ml dilution of OVA protein (Sigma-Aldrich) in carbonate buffer pH 9.5. Plates were then extensively washed and blocked for 2 hours with PBS/1% BSA/5% milk. Serial dilutions of experimental sera as well as of a reference serum from an OVA protein-immunized mice, were diluted in PBS/BSA 1% and incubated for 2 hours at room temperature. Bound anti-OVA IgG were detected with HRP-conjugated goat anti-mouse IgG (Vector Laboratories, Eurobio, Les Ulis, France) and revealed with TMB substrate reagent set (BD Biosciences). The reaction was stopped after 3–5 minutes with 2 mol/L H_2SO_4 and the absorbance at 450 nm was determined. All sera were tested in duplicate and antibodies levels are represented as a ratio of the reference serum (arbitrary units).

II.6.4 Fluorescence-activated cell sorting analysis

All reagents used for flow cytometry were purchased from BD-Biosciences (Le Pont de Claix, France). For peripheral blood lymphocyte (PBL) staining, erythrocytes were eliminated by hypotonic shock with PharMLysis buffer. Cell suspensions were first incubated with anti-FcγRIII/II (2.4G2) antibodies for 15 minutes at 4 °C and then stained for 30 minutes at 4 °C in PBS/0.1%BSA with saturating amounts of the following antibodies: FITC anti-CD4, PE anti-CD69, Pacific Blue anti-CD8, and APC-Cy7 anti-CD45.2. Dead cells were excluded using 7-actinomycine D (Sigma-Aldrich, Lyon, France) or LIVE/DEAD Fixable Near-IR Dead Cell assay.

Flow cytometric analysis was performed on a BD FACS calibur or FACS Canto II flow cytometer (BD Biosciences). Data were analyzed using FlowJo (Tree Star) software.

II.7 Experiments on brain sections

The *ex vivo* mice brain culture method was developed and optimize by J.Welsch, a protocol paper is in preparation. Briefly, SLAMxIFNAR KO new born mice were anesthetized and beheaded. Then the different sub-localization of brain such as cerebellum and hippocampus were separated and sliced according to the transversal axis. Slices are then plated on cell culture insert membrane (Millipore) and maintained in OBC medium (MEM Glutamax, 25% of horse serum, 5g/L of D-Glucose, 0,1mg/mL of Human insulin). OBC transduction was performed by adding a drop of vector mix containing particles diluted in PBS at the indicate MOI (vg/slice). Transduction analysis was performed by fluorescence microscopy.

II.8 Statistical analysis

Non-parametric test was performed for statistical comparison between groups using one-way analysis of variance (Kruskal-Wallis test), this test was performed on Stata (vs13) software. Two different groups of observation were considered as “significantly” different if the p value calculated by the test was smaller than 0.05. Thus, statistics are summarize on figure by four different symbols (*i.e.* [**ns**] (no significant difference): p value > 0.05; [*****]: p value < 0.05, [******] p value < 0.01, [*******] p value < 0.001).

III. Results

III.1 Presentation of the project and its objectives

Development and optimization of safe and efficient medical applications of gene transfer require a deep knowledge of the interaction between the vector and the immune system. DC, the professional antigen presenting cells, function at the interface between the innate and adaptive immune responses. Indeed, these cells are able to prime immune responses positively, to lead to the clearance of antigen-expressing cells, or negatively, to induce a tolerant state. The interaction between AAV vectors and DC is still poorly understood. Indeed, even though AAV vectors are unable to efficiently transduce DC, they do interact. The consequences of this interaction, however, remained unclear. Moreover, AAV capsid engineering, which is commonly used to modify the transduction efficiency of wt AAV capsid, can also have an important impact on their immunogenicity.

My PhD project was focused on the analysis of the interaction between AAV vectors and DC, and on its impact on gene transfer. The first goal of this project was to identify the intracellular barriers limiting the transduction of human DC by AAV vectors derived from natural AAV serotypes and to select a new AAV capsid variant able to efficiently transduce the DC using an *in vitro* directed evolution procedure. The second aim, was to characterize the consequences of AAV-mediated DC transduction on *in vivo* gene transfer.

III.2 Deciphering the interaction between AAV particles and human DC

Because DC have a key role in the initiation and regulation of the host immune response, a better knowledge of their interaction with rAAV is crucial to optimize the medical applications of these vectors. DC are known to have a low permissiveness to AAV. Indeed, despite applying high AAV multiplicity of infection (MOI) low transduction rates are achieved in this particular cell type. This holds true for a portfolio of AAV serotypes and has independently been reported by different laboratories [206], [209]. The first part of my project aimed to identifying barriers that block AAV-mediated DC transduction.

III.2.1 rAAV particles enter DC but remain unable to transduce them

To further investigate the interaction of rAAV with human DC, we firstly examined the transduction efficiency of AAV2 vectors in human immature monocyte derived DC (iDC). A self-complementary (sc) AAV2 vector coding for GFP was first used to evaluate the level of iDC transduction. Immature DC were incubated for twenty-four or forty-eight hours with scAAV2-GFP and the GFP expression was measured by FACS analysis. For comparison, cell transduction was performed in parallel, on the highly permissive HeLa cell line (**Figure 24A**). The transduction efficiency of scAAV2-GFP on human DC – measured at twenty-four hours – was less than 1%. In contrast, transduction of HeLa cells with the same MOI resulted in more than 95% of GFP expressing cells. Increasing the incubation time from twenty-four to forty-eight hours did not modify this result. In addition, use of ssAAV-GFP vectors derived from other serotypes (AAV1, AAV8 and AAV9) resulted in transduction efficiencies even lower than those observed with ss or scAAV2-GFP (data not shown).

To investigate the ability of iDC to internalize various AAV serotypes, we then quantified the amount of ssAAV genomes inside the transduced cells by qPCR using GFP primers (**Figure 24B**). Interestingly, despite the lack of GFP expression, all the AAV serotypes tested were internalized into iDC, although with different efficiencies. Therefore, internalization constitutes the first barrier faced by AAV (**Figure 24B**).

We used scAAV vector in most of the following sections to overcome the single-to-double strand conversion step, which is rate-limiting during the AAV transduction process.

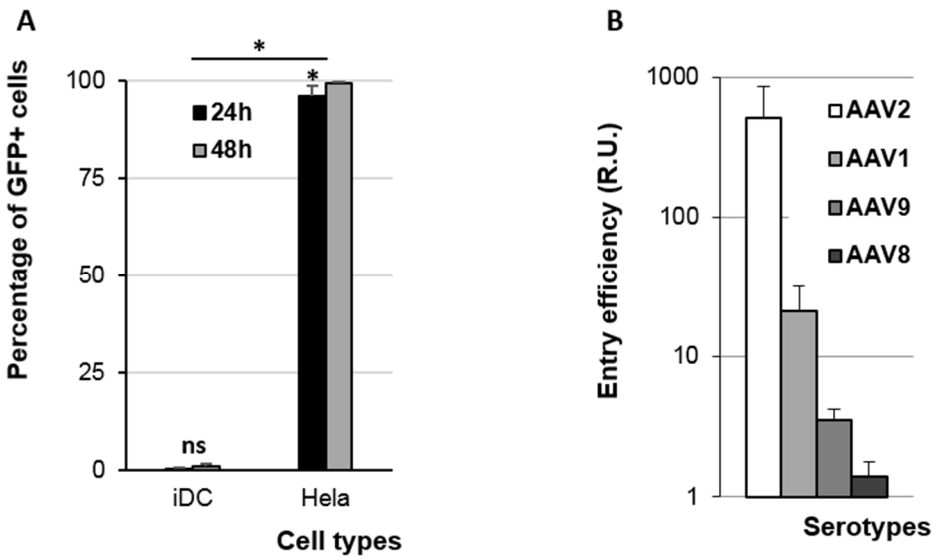


Figure 24. AAV vectors are unable to transduce iDC despite their entry.
A. Transduction of iDC or HeLa cells by scAAV2-GFP. Cells were infected with 10^4 vg per cell and analyzed by FACS 24 or 48 h later. **B.** Entry efficiency into iDC of ssAAV-GFP vectors derived from different AAV serotypes. AAV vectors were delivered to iDC at an MOI of 10^4 vg per cell. 48 h after vectors delivery, cells were treated with trypsin, washed, and DNA was extracted. Results are presented as the mean GFP to β-globin ratio (R.U.). Error bars represent standard deviation (n=3).

III.2.2 rAAV2 particles can reach the nucleus of DC

Because of their APC properties, the intracellular trafficking in iDC is dramatically different from that observed in other cell types such as HeLa cells. Indeed, iDC can capture the antigen via several mechanisms used for the internalization of extracellular particles such as endocytosis, phagocytosis or micropinocytosis [225]. Moreover, their intra-vesicular system presents some interesting characteristics, such as a lower acidification capacity and a reduced protease activity [226]. As previously described, the intracellular processing of AAV in the intracellular environment has a key role in the transduction process and several dead end pathways were reported [72], [91]. To analyze the intracellular fate of AAV particles within iDC, we performed a confocal microscopy analysis of iDC transduced with scAAV2-GFP (**Figure 25**). Immature DC were incubated with scAAV2-GFP particles during seven hours, then fixed with paraformaldehyde, and analyzed by immunofluorescence using an anti-AAV2 capsid antibody (A20). Importantly, this antibody recognizes only intact capsids [223]. The nucleus was stained with DAPI and the nuclear membrane with an anti-lamin B1 antibody. The result confirmed that rAAV enter DC (**Figure 24**). The majority of the intact AAV particles were

localized in the cytoplasm as discrete foci, probably associated with vesicular system. However, few discrete A20 signals were also detected in the nucleus (see arrows in **Figure *25***).

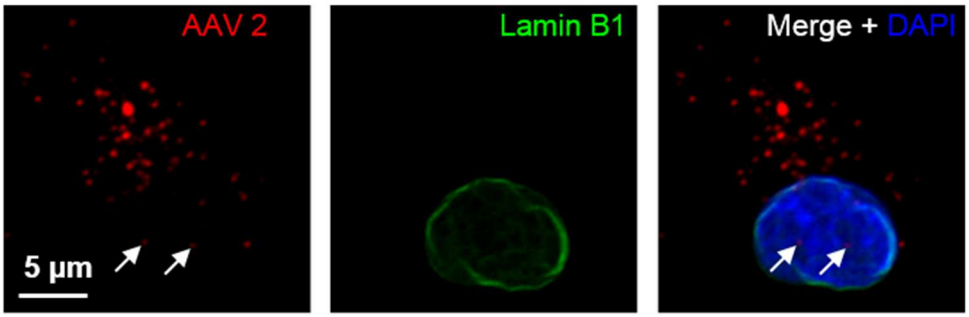


Figure 25. Immunofluorescence analysis of scAAV2-GFP particles localization within iDC.
AAV2 was delivered to iDC, at a MOI of 10^4 vg per cell. 7 h after vectors delivery, cells were washed, AAV2 capsids were labeled with A20 antibody and the nuclear membrane was visualized using an anti-lamin B1 antibody. The observation was performed by confocal microscopy. The arrows indicate A20 signals in the nucleus.

To further analyze the intracellular localization of rAAV particles in more details, we performed a fractionation assay (see **Figure 22** for details on the procedure) to isolate three different cell compartments: the intracellular membranes, the cytosol and the nuclei. The quality of the fractionation procedure was confirmed by Western blot, using antibodies recognizing Rab5, tubulin and lamin-B1 proteins indicative of intracytoplasmic membranes, cytosolic, and nuclear compartments, respectively (**Figure 26A**). DNA was then extracted from each fraction and quantified by qPCR to detect the presence of AAV vector genomes. These assay showed that rAAV genomes were found not only in the membrane/endosomal compartment, but also in the cytosol and the nucleus, confirming that a least a fraction of AAV particles was able to reach the nuclear area (**Figure 26B**). However, the majority of AAV particles remained sequestered in the intracytoplasmic membrane fraction. For comparison, we performed the same assay on HeLa cells, and obtained comparable results. These results indicated that most of the AAV particles were sequestered within the membrane compartment independently on the cell type (HeLa or DC). However, despite a strong retention of rAAV2 virions in endosomal system of HeLa cell, a strong transduction was observed in these cells as opposed to iDC in which no GFP expression was observed. Thus, a similar intracellular distribution of rAAV particles can lead to different transduction

efficiencies. Moreover, these results indicate that nuclear entry of rAAV particles in iDC is not sufficient to ensure cell transduction.

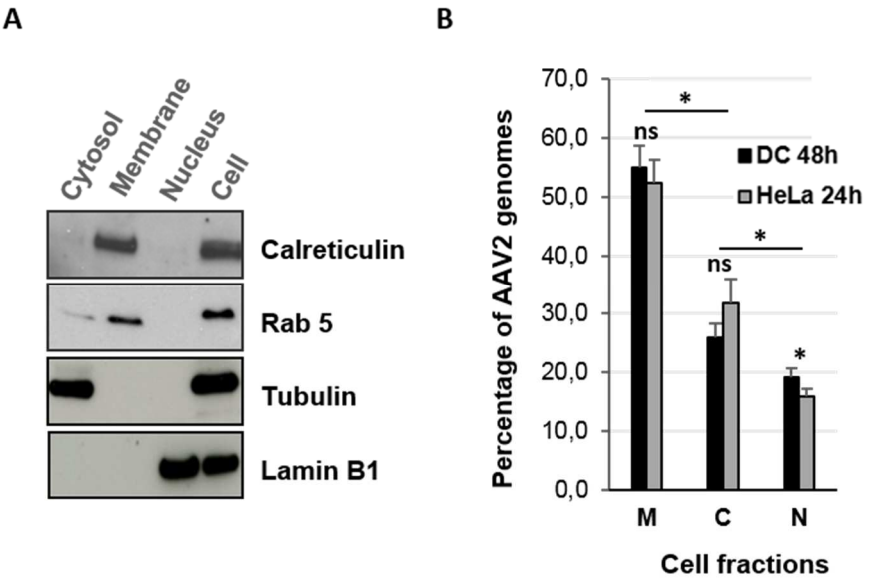


Figure 26. Intracellular fate of rAAV2 vector particles.
A. Analysis of subcellular fractions from AAV-transduced iDC by Western blot. **B.** Quantification of rAAV2 genomes in subcellular fractions (**M,** membrane; **C,** Cytosol; **N,** nucleus) from iDC (scAAV2-GFP) and HeLa cells (ssAAV2-GFP). AAV2 was delivered to iDC or HeLa cells at a MOI of 10^3 vg per cell. 24h (Hela cells) or 48h (iDC) after vectors delivery, cells were trypsinized, washed, and fractioned. The AAV-GFP DNA extracted from each compartment was quantified by qPCR. Error bars represent standard deviation.

III.2.3 Selection of AAV capsid variants able to transduce DC

We next aimed to select a new AAV capsid variant able to efficiently transduce iDC. Such a genetically modified particle may serve as a tool to identify barriers against natural AAV serotypes in DC. In addition, the selection of an AAV capsid able to transduce DC would represent an interesting tool to determine the consequences of this phenomenon on immune response and gene transfer, with several potential medical applications. To reach this aim, we used an *in vitro* evolution procedure to select AAV variants from a library of capsid mutants already developed in Büning's laboratory.

III.2.3.1 Design of an optimized in vitro evolution process

For non-enveloped viruses, especially for AAV, the viral capsid determines most early steps of the interactions with the host cell. It protects not only the viral DNA from the external

environment, but determines the tropism, the entry route and the intracellular processing of the particle. As described previously, the most variable capsid domains are in the loop regions at the three-fold axis of symmetry of the capsid. For our selection procedure, we focused on this region and used an AAV library that consists of mutants displaying a library of 7mer random peptides inserted at position 587 of the *cap* ORF [222] (**Figure 27**). This region participates in the binding of AAV particles to the cell.

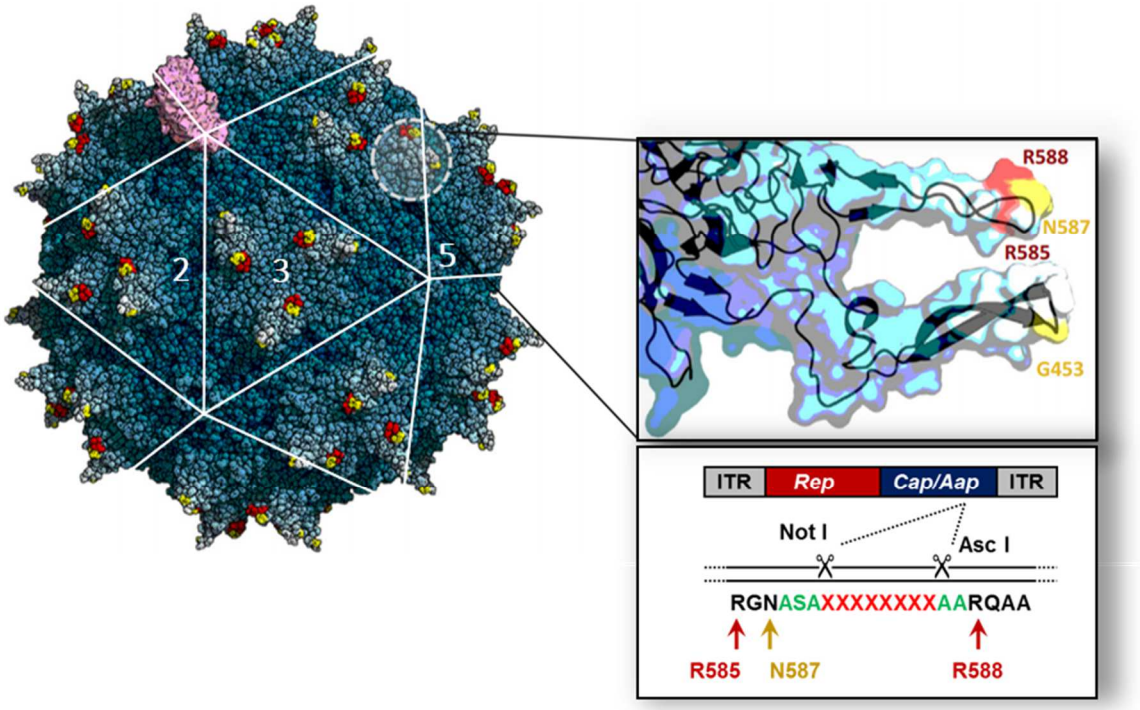


Figure 27. Mutagenesis of AAV capsid.
Illustration of the precise location of the insertion of the oligonucleotide library of 7mer peptide on the AAV2 capsid and on the AAV2 *cap* gene. The symmetry axis were labelled 2, 3 and 5 for the two-, the three- and the five-fold axis respectively. AAV2 structures created using Pymol and PDB files adapted from [135]. Origin AAV *cap* gene sequence (black), linker (green), and 7mer peptide inserted sequence (red).

In order to select an AAV capsid variant able to efficiently transduce iDC, we incubated target cells with the AAV library at a MOI of 10^3 vg per cell. DC were harvested six hours post infection and the cell nuclei were isolated (see **Figure 18** for details on the procedure). Viral genomes found in the nuclei, the final destination of AAV virions, were used to generate a new library of AAV particles. This sub-library was then used in a new round of selection. We performed two rounds of selections on iDC purified from two different blood donors to avoid to select for donor-specific variants. This enrichment process was performed to increase the

chance of selecting AAV particles that – due to peptide insertion – could efficiently reach the nucleus of iDC. After two rounds of selection, AAV genomes isolated from the nuclei of DC were sequenced to identify the most frequent mutations recovered after this two rounds selection procedure (**Figure 28A**). The most frequently selected peptides presented some obvious consensus sequences as shown by the alignment of the 7mer peptide sequences using a maximum likelihood method, resulting in two separate groups (**Figure 28B**). In order to evaluate the potential of these selected AAV capsid variants, we focused our attention on three mutations: NNPLPQR representative of the first group, and VSSTSPR and ISSSTAR as representatives of the second group. To simplify the nomenclature, we will further refer to these mutated AAV vectors using the sequence of the peptide inserted into the capsid (*e.g.* VSSTSPR: AAV with VSSTSPR insertion in the 587 position of the *cap* ORF).

A

Mutations	Copy number (%)
NNPLPQR	518 (8,5)
NAQPPSR	338 (5,5)
ISSSTAR	229 (3,8)
VSSTSPR	160 (2,6)
NQPNPVR	159 (2,6)
VSSSTPR	134 (2,2)
PTRLLP	129 (2,1)
SNSTPLR	95 (1,6)
VSSSLQR	95 (1,6)
...	... (< 1,5)

B

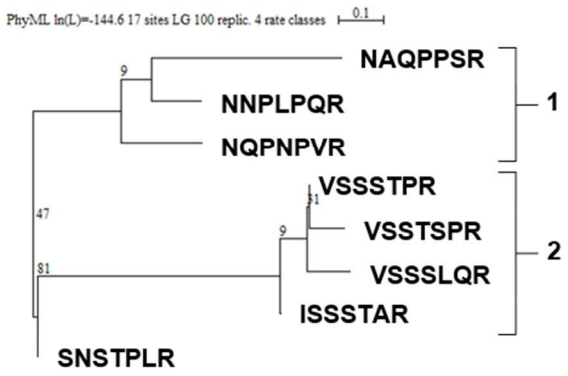


Figure 28. Mutations selected on iDC.
A. Mutations obtained after two selection rounds on iDC. **B.** The amino acid sequences of the mutated region were aligned using the flanking linker sequences as common regions. Then, a phylogenic tree was constructed using the maximum likelihood method resulting in two separate groups (1 & 2).

III.2.3.2 Characterization of selected variants on human DC

In order to characterize the potential of the selected variants to efficiently transduce human iDC, we produced rAAV vectors encoding for GFP under the control of CMV promoter and exhibiting on their capsids the mutation selected by the *in vitro* evolution process. In particular, for these studies, we used scAAV vectors. During the transduction assay, we also modulated the maturation status of the human DC. Indeed, iDC can be activated by TLR agonists such as LPS. As described before, this activation has several consequences for the cell

homeostasis: it triggers a decrease of endocytic efficiency and modifies the intracellular environment [225]. Therefore, the analysis of AAV-infected DC in different maturation status, is an indirect way to understand which barriers are limiting their transduction. Human DC were incubated with scAAV-GFP (derived from either AAV2 or the selected mutants) in three different conditions defining three maturation status: i) iDC were incubated with the vector in the absence of LPS (iDC); ii) iDC were activated two hours after AAV transduction by adding LPS mimicking an intermediate maturation status (mDCpi); and iii) iDC were activated by LPS twenty-four hours prior to infection (mDC) (see **Figure 17** for more details on the procedure). Forty-eight hours after infection, the percentage of GFP positive cells was determined by FACS analysis (**Figure 29A**). Our results showed a very low transduction efficiency of iDC and mDC, with both wt AAV2 capsids and the capsid variants even though the latter resulted in slightly improved percentages of transduced cells [*i.e.* from 0.2% of GFP^+ cells (rAAV2) to 2.1% (VSSTSPR) or to 2.9% (ISSSTAR) (**Figure 29 inset**)]. However, in our intermediate model consisting in iDC stimulated with LPS two hours post-infection (mDCpi), the rAAV transduction efficiency was strongly increased for both the wt and two out of three tested variants (*i.e.* from 0.2% to 2.9% for rAAV2, from 2.1% to 25.7% for VSSTSPR, and from 2.9 to 23.1% for ISSSTAR). Thus, the VSSTSPR and ISSSTAR variants exhibited a better transduction efficiency in comparison to rAAV2 in both iDC and mDCpi (approximately tenfold). The results with the VSSTSPR variant were also confirmed by fluorescence microscopy (**Figure 29B**). Interestingly, the NNPLPQR variant, although being the candidate that had been selected with the highest frequency, did not display an increased transduction efficiency as compared to rAAV2. Moreover, the VSSTSPR and ISSSTAR variants, which belonged to the same cluster (**Figure 28B**), shared similar transduction efficiencies on DC independently of the maturation status. The maturation status seems to influence the transduction efficiency: indeed, independently of the capsid (wt or mutated), the transduction is approximately tenfold in mDCpi as compared iDC and mDC which are poorly permissive for AAV.

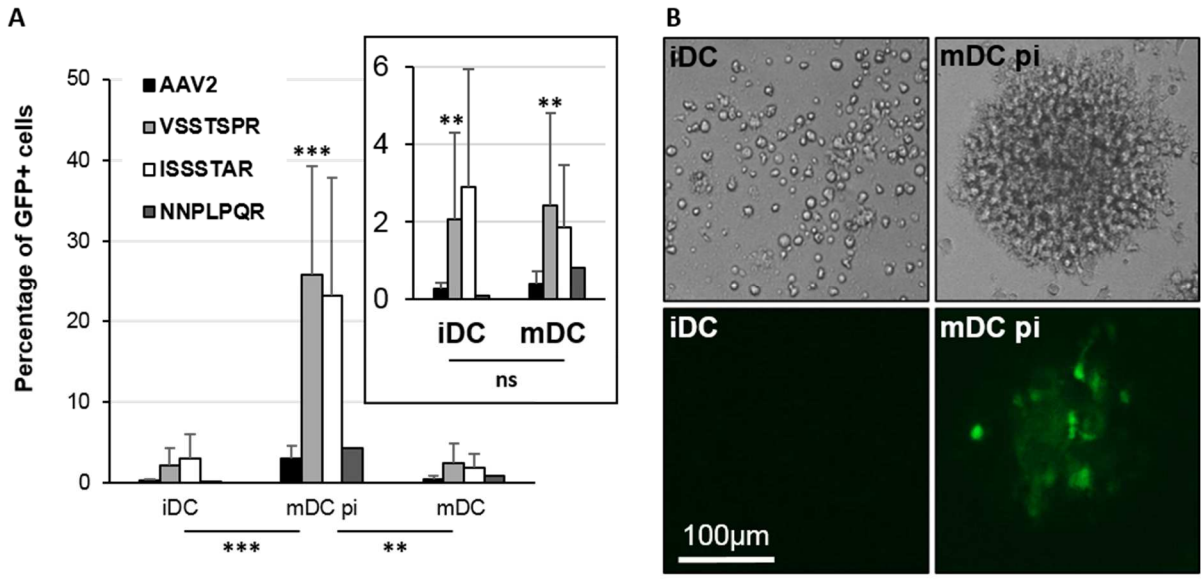


Figure 29. Transduction efficiencies of rAAV on human DC according to their maturation status.
A. Transduction efficiencies of human DC by natural and mutated AAV capsids. scAAV2-GFP, scVSSTSPR-GFP, scISSSTAR-GFP, scNNPLPQR-GFP vectors were used to infect immature dendritic cells (iDC), mature dendritic cells (mDC: maturated with LPS 24h before vector delivery) or mature dendritic cell post infection (mDCpi: maturated with LPS 2 h after vector delivery). The MOI used was of 10^4 vg per cell; 48 h after vector delivery, cell were trypsinized, washed, and the percentage of GFP^+ cell was determined by FACS. Inset: results with an adapted y axis to focus on iDC and mDC. **B.** Direct observation by fluorescence microscopy of human DC transduced with the scVSSTSPR-GFP capsid variant (10^4vg per cell), 48 h after gene delivery. Error bars represent standard deviation from at least three independent experiments performed using DC derived from different donors except for NNPLPQR (n=2).

III.2.4 Identification of the rate-limiting steps for rAAV transduction of human DC

III.2.4.1 Binding to HSPG is required to transduce human DC with AAV vectors

Interestingly, the three capsid variants selected by our evolution procedure exhibited an RXXR motif, which is also present on the wt AAV2 capsid (**Figure 21**). This $R_{585}GNR_{588}$ motif is involved in binding of AAV2 to HSPG [56]. In our *in vitro* evolution process we performed a heparin chromatography on the AAV library after the first selection round, to remove AAV capsid mutants that displayed peptides responsible for binding to HSPG (HSPG AAV binders). Despite this pre-selection, our prime candidates show a RXXR motif arguing that the ability to bind to HSPG is a strong pre-requisite for entering DC. To further evaluate the importance of HSPG binding for DC transduction, we performed a heparin competition assay. To this end, the transduction efficiency of mDCpi by rAAV was analyzed in the absence or in the presence of heparin using the same conditions as described above (**Figure 30**).

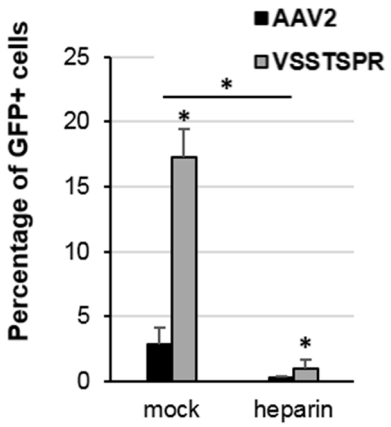


Figure 30. HSPG binding is required for efficient transduction of mDCpi with rAAV.
Heparin competition assay. scAAV2-GFP or scVSSTSPR-GFP were delivered to mDCpi at a MOI of 10^4 vg per cell. The infection mix contained heparin or not (mock), at the concentration of 25 µg per mL. 48h after vector delivery, cells were harvested and the percentage of GFP^+ cell was determined by FACS. Error bars represent standard deviation (n=4).

The presence of soluble heparin in the incubation mix strongly inhibited the transduction of mDCpi by the VSSTSPR variant. We observed the same inhibition with the AAV2 vector. These results strongly suggest that, as the parental AAV2, the AAV variant VSSTSPR uses HSPG to bind DC. We also performed two additional *in vitro* selections in which we increased the stringency of the selection procedure by adding heparin to the medium during infection of DC with the AAV library (**Figure 18**). After two rounds of selection, the AAV genomes were sequenced as described before (**Figure 21**). Surprisingly, in these newly performed selections, the two groups of mutants described before were still present as top candidates. Moreover, the NNPLPQR variant was again selected. In addition, several heparin non-binder variants selected in this latter screen (*i.e.* LPSPRPSL, NSARPNS, ARTGAVI; these mutant did not have the RXXR motif) were tested on DC and presented a transduction efficiency on DC lower than that observed for the mutants selected in the initial screen (data not shown). All together these results strongly suggest that rAAV has to keep its HSPG binding properties to efficiently enter and transduce the DC.

III.2.4.2 Mutation of AAV capsids does not alter their intracellular distribution

As described before, the entry of the rAAV particles into the target cell is rate-limiting. It appeared therefore important, at this step, to compare the entry efficiency of rAAV2 to that of the VSSTSPR variant. Moreover, because uptake of external particles by DC is significantly influenced by their level of maturation, we also compared the entry efficiencies of these two kinds of particles in iDC to those measured in mDCpi, and mDC. For this, DC were incubated with scAAV-GFP during twenty-four hours, then harvested and trypsinized to get rid of

externally bound rAAV particles. Total DNA was extracted and the vector genomes were quantified by qPCR and normalized to a housekeeping gene (β-globin DNA) (**Figure 31A**). In all three conditions of DC maturation, the amount of vector genomes measured with the capsid variant VSSTSPR did not differ significantly from that of rAAV2. As expected, the quantity of vector DNA measured was lower in mDC than in iDC or mDCpi. Indeed, when DC are mature, their internalization machinery is inhibited [225]. Interestingly, despite the stronger transduction efficiency observed for mDCpi in comparison to iDC (**Figure 29**), the amount of vector DNA found within the cell was similar (**Figure 31A**). These results suggest that the improvement in cell transduction measured with the VSSTSPR mutated capsid in DC compared to rAAV2, was not due to a more efficient cell entry of the selected variant.

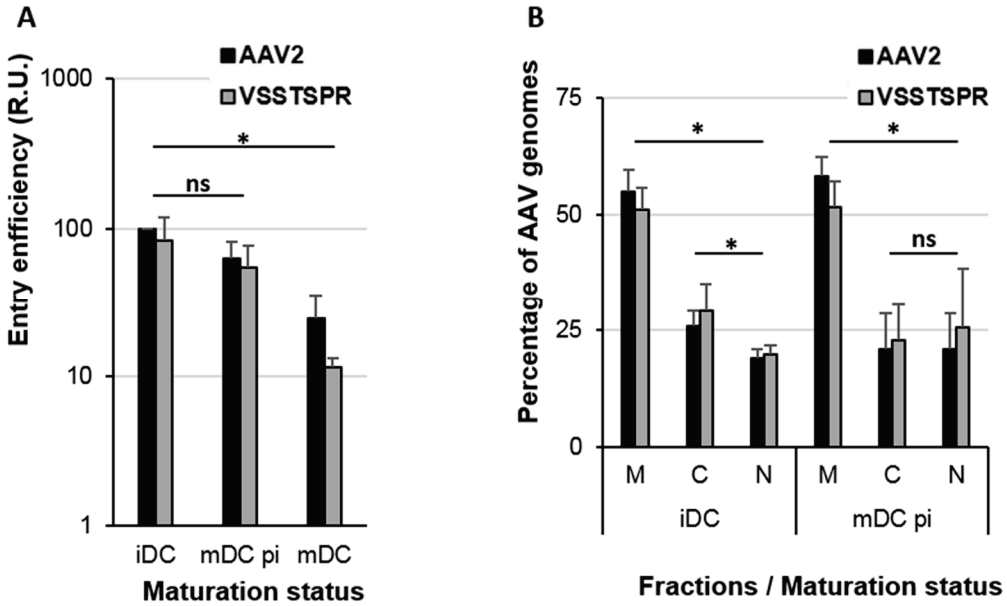


Figure 31. Intracellular distribution of AAV particles within mo-DC.
A. Entry efficiency into iDC, mDCpi or mDC of scAAV2-GFP and scVSSTSPR-GFP vectors. rAAV2 or VSSTSPR were used at a MOI of 10^4 vg per cell. 24 h after vectors delivery, cells were washed, DNA was extracted, and analyzed by qPCR using gfp or β-globin primers. The results were normalized by the entry efficiency of AAV2 into iDC. **B.** Fractionation assay on iDC and mDCpi. scAAV2-GFP or scVSSTSPR-GFP vectors were delivered to iDC or mDCpi at a MOI of 10^3 vg per cell. 48 h after vectors delivery, cells were washed and fractioned. The DNA from each compartment (**M,** membrane; **C,** Cytosol; **N,** nucleus) was extracted and rAAV genomes were quantified by qPCR. Error bars represent standard deviation (A, n=4; B, n=3).

The previous analysis of the intracellular distribution of rAAV2 on iDC identified vesicular retention as an important barrier (**Figure 26B**). In addition, our transduction assays indicated an improved transduction rate of both rAAV2 and VSSTSPR in mDCpi (**Figure 29**). Therefore,

we next analyzed the intracellular distribution of rAAV particles according to the DC maturation status (**Figure 31B**). Our results indicated that the intracellular distribution of rAAV particles was not altered by the capsid mutation or by the maturation status of the DC. Indeed, in these different conditions, the majority of the rAAV particles are still blocked in the intracellular vesicular compartment (M). Moreover, similar amounts of rAAV particles are found in the cytosol and the nucleus of transduced iDC and mDCpi, as compared to iDC. Altogether, these results suggest that the increased transduction efficiency measured with the selected capsid variants was not due to an improved intra-cellular trafficking (at least quantitatively). However, the intracellular environment, which is completely modified during DC maturation, may qualitatively influence the AAV capsid trafficking.

III.2.4.3 Acidification of the endosomal system is required during the DC transduction process

The AAV capsids are sensitive to the intra-endosomal micro-environment. Specifically, it is required for inducing/mediating an AAV capsid conformational change that is required for cell transduction. It is a consequence of vesicular maturation and correlates with a decrease in the intra-luminal pH and in an increase in the activity of endosomal proteases such as cathepsins. Interestingly, compared to other somatic cells, iDC exhibit some differences in their intra-vesicular environment. In particular, a decrease in the intraluminal pH and an improvement of the protease activity is induced by activation of DC with TLR ligands or other stimulatory molecules [170], [227], [228]. To analyze the influence of the pH in transduction by rAAV of mDCpi, we performed a transduction assay with cells pretreated with chloroquine, a drug known to block the acidification of endosomes. The DC pretreated with chloroquine were first incubated with scAAV-GFP and two hours later activated with LPS. The percentage of GFP positive cells was measured by FACS analysis forty-eight hours later (**Figure 32A**). Interestingly, in mDCpi the percentage of GFP positive cells was strongly reduced by chloroquine pretreatment and infection with rAAV2 or the VSSTSPR variant. These results strongly suggested that, as for other cell types, endosomal acidification was critical for the transduction of mDCpi. To know if the acidification observed during the maturation is sufficient to explain the difference of the transduction efficiency between iDC and mDCpi, we tried to artificially decrease the intra-endosomal pH of iDC and mDCpi by using dibenziodolium chloride (DPI), a drug described as able to decrease the intraluminal pH of one unit approximately [229], [230]

(**Figure 32B**). However, treatment with DPI did not improve the transduction efficiency of either iDC or mDCpi with VSSTSPR or rAAV2. All together these results suggest that the acidification of the endosomal system is required but not sufficient for the DC transduction with AAV vectors.

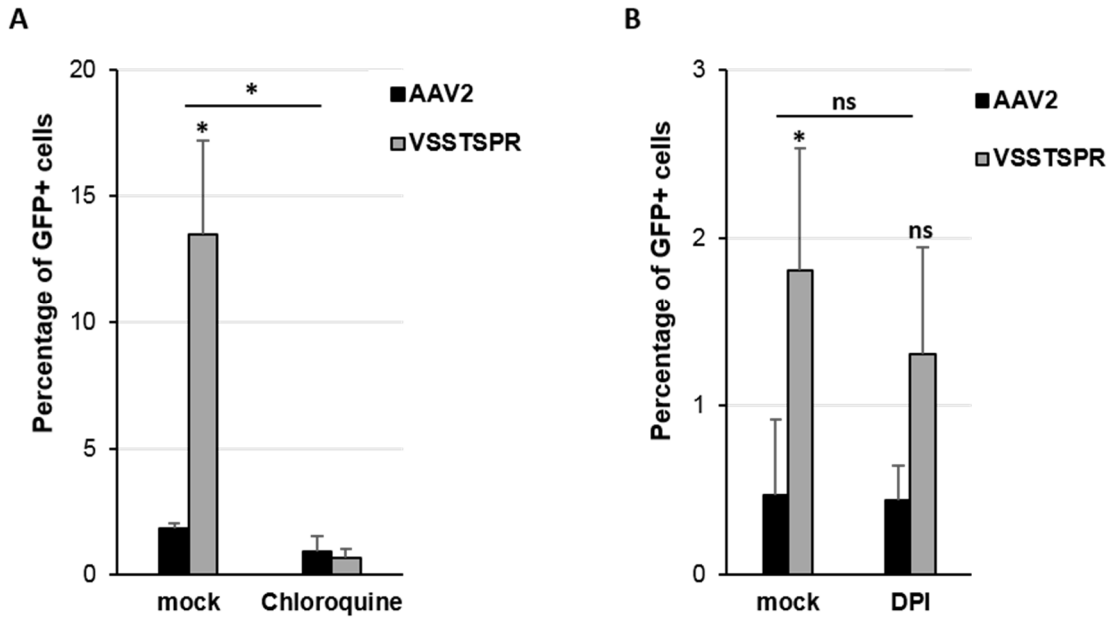


Figure 32. Effect of intra-vesicular acidification on AAV transduction of human DC.
A. Effect of the chloroquine on AAV transduction efficiencies in mDCpi. scAAV2-GFP, scVSSTSPR-GFP vectors were used to infect mDCpi (pretreated with chloroquine 15 min before infection) at a MOI of 10^4 vg per cell; 48 h after vector delivery, cell were washed and the percentage of GFP^+ cell was determined by FACS. **B.** Effect of the DPI on AAV transduction efficiencies in iDC. scAAV2-GFP, scVSSTSPR-GFP vectors were used to infect iDC (pretreated with DPI 15 min before infection) at a MOI of 10^4 vg per cell; 48 h after vector delivery, cell were washed and the percentage of GFP^+ cell was determined by FACS Error bars represent standard deviation (n=3).

III.2.4.4 The selected mutations modify the physical properties of the AAV capsids

AAV capsids are known to be very stable, however strong differences of stability were observed between several AAV serotypes [71]. To evaluate the impact of the selected mutations on AAV capsid stability we performed an *in vitro* destabilization assay. AAV particles were incubated in a buffer at different pH, and heated at increasing temperatures for 15 min. Then, the capsids were dot blotted on a nitrocellulose membrane under native conditions and their integrity probed with specific antibodies. Intact capsids were probed with A20 antibody that recognizes a conformational epitope on assembled capsids, and denatured capsids were

probed with B1 antibody, which recognizes an epitope in the C-terminal domain of VP3 localized inside of the capsid and thus accessible only when capsid are disassembled [223] (**Figure 33**). This assay indicated that the AAV2 capsids are more resistant to the increase in temperature than mutated capsid, and this independently of the pH. At the physiological pH of 7.2 units, most of the AAV2 particles seemed intact at 65°C, whereas at the same temperature and pH, the mutated capsids were completely denatured. A similar difference in stability was observed at the acidic pH of 5.2 units but interestingly, under this acidic condition, both mutated and wt capsid were more resistant to the heat denaturation. Indeed, intact AAV2 or VSSTSPR capsids could still be detected until 75°C and 70°C, respectively. These results suggest that the VSSTSPR mutation decreases the stability of the AAV capsid.

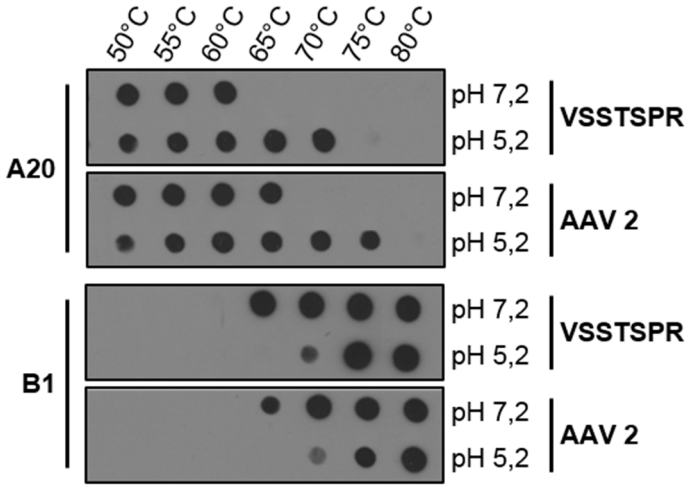


Figure 33. The VSSTSPR mutation decreases the stability of the capsid.
Capsids destabilization assay on AAV2 and VSSTSPR. A native dot blot was performed on AAV capsid which were submitted to a temperature gradient at two different pH conditions. Denatured capsids were detected with B1 antibody, intact capsids were detected with A20 antibody.

III.2.4.5 Uncoating of the AAV vector genome is inefficient in human DC

The stability of the capsid may have an impact on the uncoating efficiency of the vector genome. Indeed, the energetic barrier that has to be overcome to induce the release of the genome may be lower for a more fragile capsid. The AAV uncoating mechanism remains unclear, but it was recognized to be inefficient and rate-limiting [118], [119]. To evaluate the uncoating efficiency, we performed an assay based on the ability of AAV vectors to form ds

circular molecules in the nucleus of the infected cell. Indeed, when ssAAV particles succeed at reaching the nucleus, the genome is released and can be converted to a ds molecule which is then circularized to form monomeric or multimeric episomes [21]. Similarly, scAAV genomes, which can bypass the ss to ds conversion step are also rapidly circularized in the nucleus. Alternatively, AAV vector genomes can also randomly integrate but this event remains extremely inefficient, in particular in resting cells. The circular episomal form of the AAV DNA is very stable and cannot be digested by exonucleases like the Plasmid Safe nuclease (PS) [231]. Therefore, the detection of circular ds AAV genomes can be used to indirectly measure the level of genome uncoating.

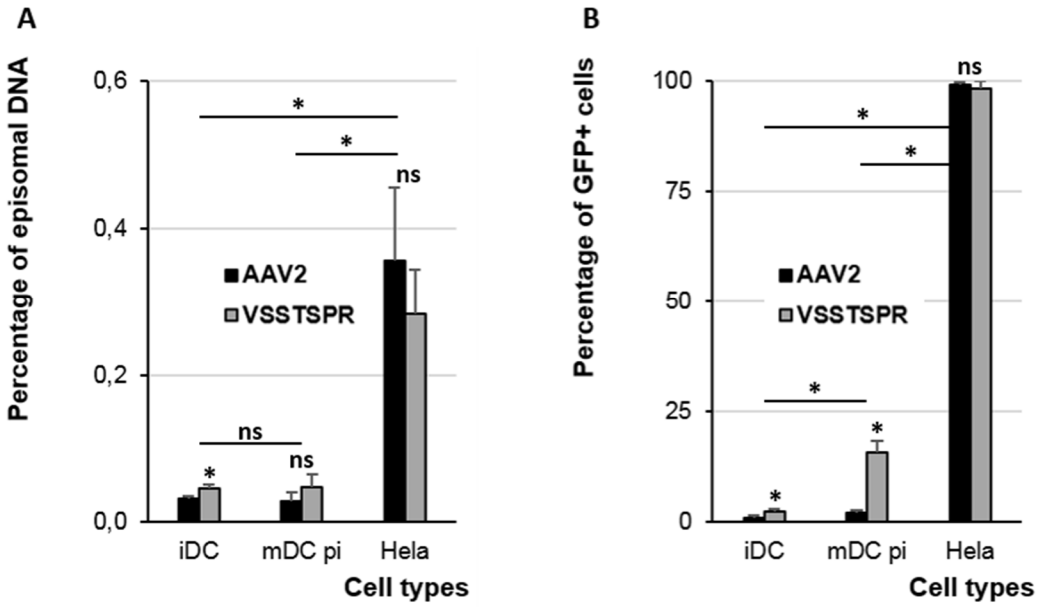


Figure 34. The uncoating is inefficient in hDC in comparison to HeLa cells.
A. Uncoating assay on iDC, mDCpi or HeLa cells. AAV2 or VSSTSPR were delivered to cells with a MOI of 10^4 vg per cell. 9 h after vectors delivery, cells were washed and DNA extracted, treated or not with T5 exonuclease, and then quantified by qPCR using gfp or β-globin primers. **B.** Transduction efficiency of iDC, mDCpi, or HeLa cells transduced with scAAV2-GFP or scVSSTSPR-GFP vectors. AAV2 or VSSTSPR were used at a MOI of 10^4 vg per cell. 48 h after vector delivery, cells were harvested and the percentage of GFP^+ cell was determined by FACS. Error bars represent standard deviation (n=3).

For this study we used T5 exonuclease, a nuclease characterized by its strong ability to degrade ss and strands linear DNA molecules, and which is currently described as more active than PS. To compare the uncoating efficiency of scAAV2-GFP and scVSSTSPR-GFP vectors, we incubated DC (under several maturation conditions) and HeLa cells with the vectors at a MOI

of 10^4 vg /cell; nine hours after infection the cells were harvested and total DNA was extracted. One fraction of the DNA was treated with the T5 exonuclease, and another was left untreated, then the amount of rAAV genome was quantified by qPCR in each condition. These quantifications allowed calculating the percentage of rAAV episomal DNA which is resistant to T5 (**Figure 34A**). The efficiency of the T5 treatment was evaluated by the quantification of an endogenous cellular gene in treated and untreated samples (data not shown). In parallel, parts of the cells were kept in culture forty-eight hours after infection to measure transgene expression by FACS analysis (**Figure 34B**).

The results indicated that percentage of episomal DNA was at least tenfold higher in HeLa cells infected with scAAV2-GFP or scVSSTSPR-GFP particles, than in iDC. This observation correlates with the difference in the transduction efficiency observed in both cell types, thus confirming the non-permissive state of iDC. In addition, in HeLa cells and in mDCpi, the VSSTSPR mutant did not display any significant difference in the level of episomal as compared to AAV2 vectors. Interestingly, however, a slight difference was measured in iDC. These results confirmed the inefficiency of the rAAV uncoating in DC and clearly suggest that this step is an important barrier for the transduction of DC.

III.2.4.6 The selected mutation increases the uncoating efficiency in human DC

Importantly, in the previous uncoating assay (**Figure 34**), the percentage of episomal DNA measured by qPCR nine hours after addition of the vector was extremely low, for both cell types, and in particular in DC. Thus, this measure appears poorly informative to highlight potential slight differences. In order to improve the detection of episomal DNA, we changed the experimental conditions by increasing the incubation period of AAV vectors with the target cells (Hela or DC) (from 9 to a minimum of 15 hours) to allow more time for the formation of episomal DNA. At the same time, we decreased the AAV vector MOI (one log) to reduce the time required for all the particles to enter the cell. The entry and uncoating efficiency of VSSTSPR and rAAV2 were first compared again in HeLa cells. As previously observed in DC, twenty-four and forty-eight hours after transduction, we did not observe any difference between the VSSTSPR and AAV2 capsids in terms of entry efficiency (**Figure 35A**). The percentage of episomal DNA measured twenty-four hours after transduction was

approximately 2.5 % for both vectors (**Figure 35B**). These results strongly suggest that the selected mutation does not present any advantage for uncoating in Hela cells.

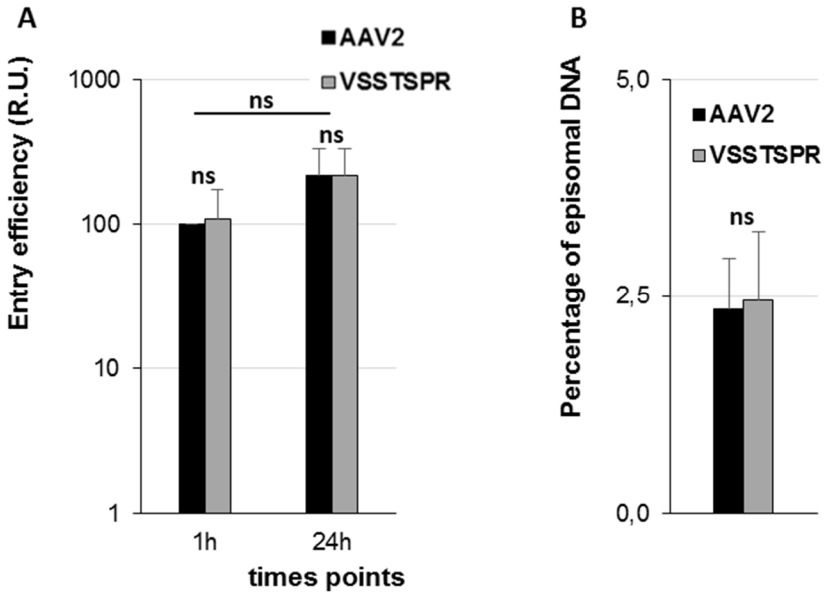


Figure 35. The uncoating is not influenced by the VSSTSPR mutation into HeLa cells.
A. Entry efficiency of scAAV2-GFP or scVSSTSPR-GFP vectors into HeLa cells of. rAAV2 or VSSTSPR was added to HeLa cells at a MOI of 10^3 vg per cell. 1 or 24 h after vectors delivery, cells were trypsinized, washed and DNA was extracted. rAAV genomes levels were measured by qPCR. The result was normalized to the entry efficiency of rAAV2 into Hela cells 1h after infection (R.U). **B.** Uncoating assay on HeLa cells. scAAV2-GFP or scVSSTSPR-GFP vectors were used at a MOI of 10^3 vg per cell. 24 h after vectors delivery, cells were trypsinized, washed, and DNA extracted. The DNA was treated or not with T5 exonuclease, and quantified by qPCR using gfp or β-globin primers. Error bars represent standard deviation (n=4).

We then performed this optimized uncoating assay on DC. Transduction, entry and uncoating efficiency (episomal DNA) for scAAV2-GFP and scVSSTSPR-GFP vectors were analyzed twenty-four (**Figure 36A, B, and C**) and forty-eight hours (**Figure 36D, E, and F**) post transduction. As observed previously, a tenfold lower transduction efficiency was measured on DC transduced with either vector, as compared to HeLa cells (data not shown). In addition, we confirmed that the VSSTSPR mutant capsid displayed a higher transduction efficiency in mDCpi, as compared to the AAV2 capsid, despite similar levels of internalization (**Figure 36A, B, D, and E**). Most interestingly, the measure of episomal DNA in DC suggested that the VSSTSPR mutation greatly increased the uncoating efficiency of the vector which was further stimulated by treatment of cells with LPS two hours post-infection (mDCpi) (**Figure 36C, and F**). Interestingly, the DC maturation exclusively improved the uncoating efficiency of the VSSTSPR

variant and not that of rAAV2. Altogether, these results suggest a different mechanism for rAAV uncoating dependent on the cell type. In addition, they strongly suggest an advantage in uncoating for the VSSTSPR variant as compared to the parental AAV2 capsid in DC.

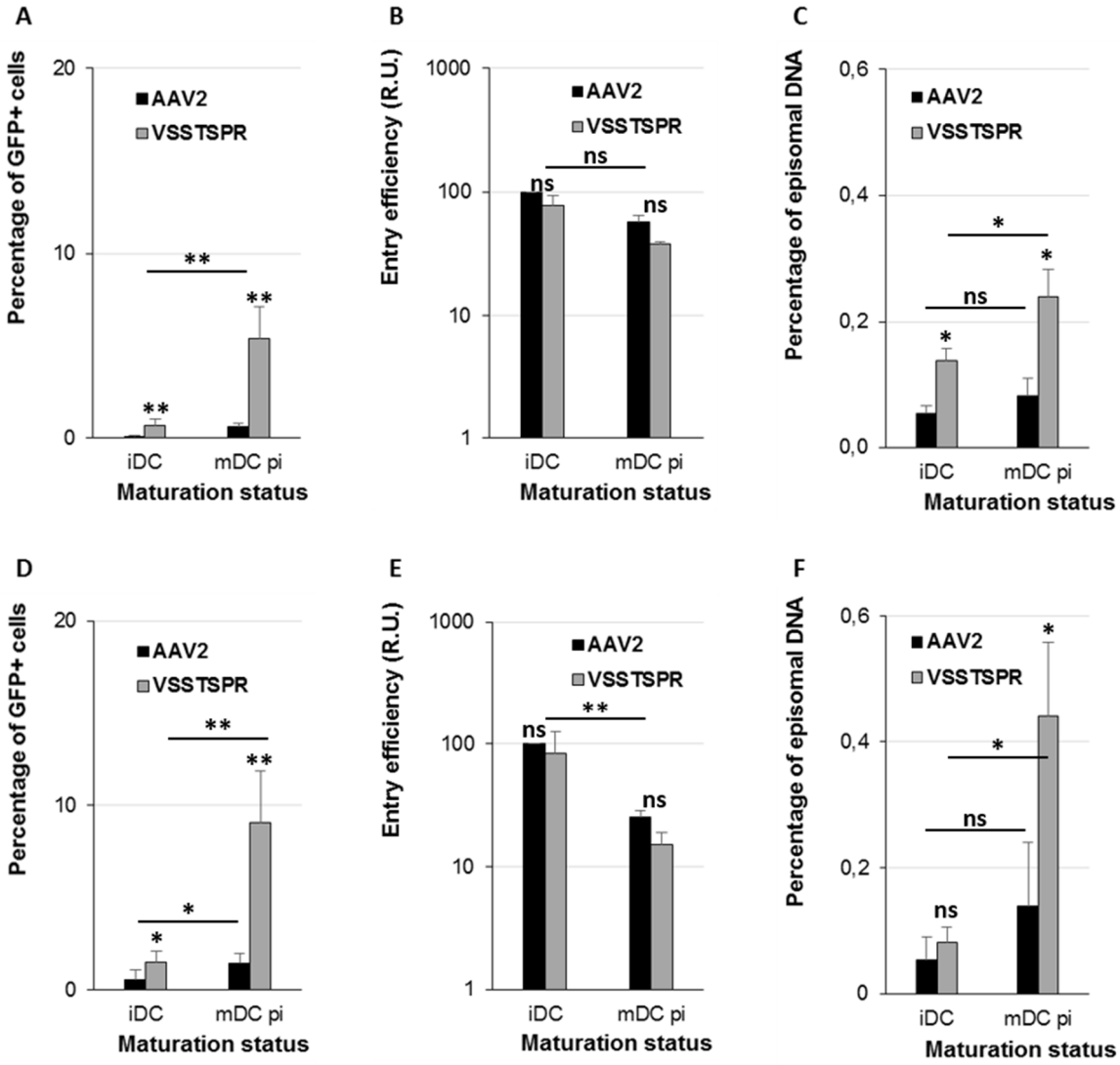


Figure 36. VSSTSPR and DC maturation of DC enhance the uncoating efficiency.
A, D. Transduction efficiencies of iDC or mDCpi transduced with scAAV2-GFP or scVSSTSPR-GFP vectors. rAAV particles were used at a MOI of 10^3 v/cell. (**A, B, C**) 24 h or (**D, E, F**) 48 h after vector delivery, cell were trypsinized, washed, and either analyzed by FACS (**A**, and **D**), or used to extract total DNA which was then analyzed by qPCR using gfp or β-globin primers to measure the entry efficiency (**B**, and **E**). The percentage of episomal DNA (**C**, and **F**), indirectly reflecting the level of genome uncoating was measured by qPCR after mock or T5 endonuclease treatment of the DNA. Error bars indicate standard deviation (A, n=6; B, n=4; C, n=4; D, n=6; E, n=6; F, n=5).

III.2.5 Analysis of the cell tropism of the selected AAV variants

As previously shown by the uncoating assay, the VSSTSPR variant is able to transduce HeLa cells with a similar efficiency as rAAV2. More interestingly, a similar selection procedure from the same original library was performed by a collaborator (PhD thesis of Li-Ang Zhang 2015 H. Büning PhD director), on endothelial cell (EC, *i.e.* Human umbilical vein endothelial cell [HUVEC]). Four rounds of selection allowed to isolate the NNPLPQR, VSSTSPR and VSSSTPR capsid variants which exhibited an advantage for the transduction of EC, in comparison to rAAV2 (data not shown). Therefore, our selection process did not allow to select a capsid variant specific of the DC. However, the VSSTSPR variant presents an advantage for transducing low permissive cells (DC or EC). Moreover, the variant possesses several features of the parental AAV2 such as a wide tropism may due to the ability to bind HSPG.

III.3 Immune responses induced by the VSSTSPR variant *in vivo*

Due to the interesting biological features of the VSSTSPR capsid variant, we decided to further explore its potential for *in vivo* gene transfer application. A collaboration was established with Dr. S. Adriouch from the University of Rouen (INSERM U905), who is studying immune responses developed by AAV vectors and who is developing strategies to reduce such responses in order to optimize the efficiency the gene delivery. The results presented in this chapter were obtained by L. Dupaty, the PhD student working with Dr. Adriouch.

III.3.1 VSSTSPR presents interesting features *in vivo*

Intramuscular gene delivery using rAAV may trigger to a strong immune responses leading the emergence of T $CD8^+$ cytotoxic cells directed against transduced cells and antibodies against the transgene product. In order to investigate the impact of the VSSTSPR capsid variant on such responses, a comparative study with AAV2 capsid was performed. For these analyses we used ssAAV vectors encoding for the intracellular form of ovalbumin (cOVA), a model antigen allowing to easily monitor rAAV-induced immune responses [221], [224].

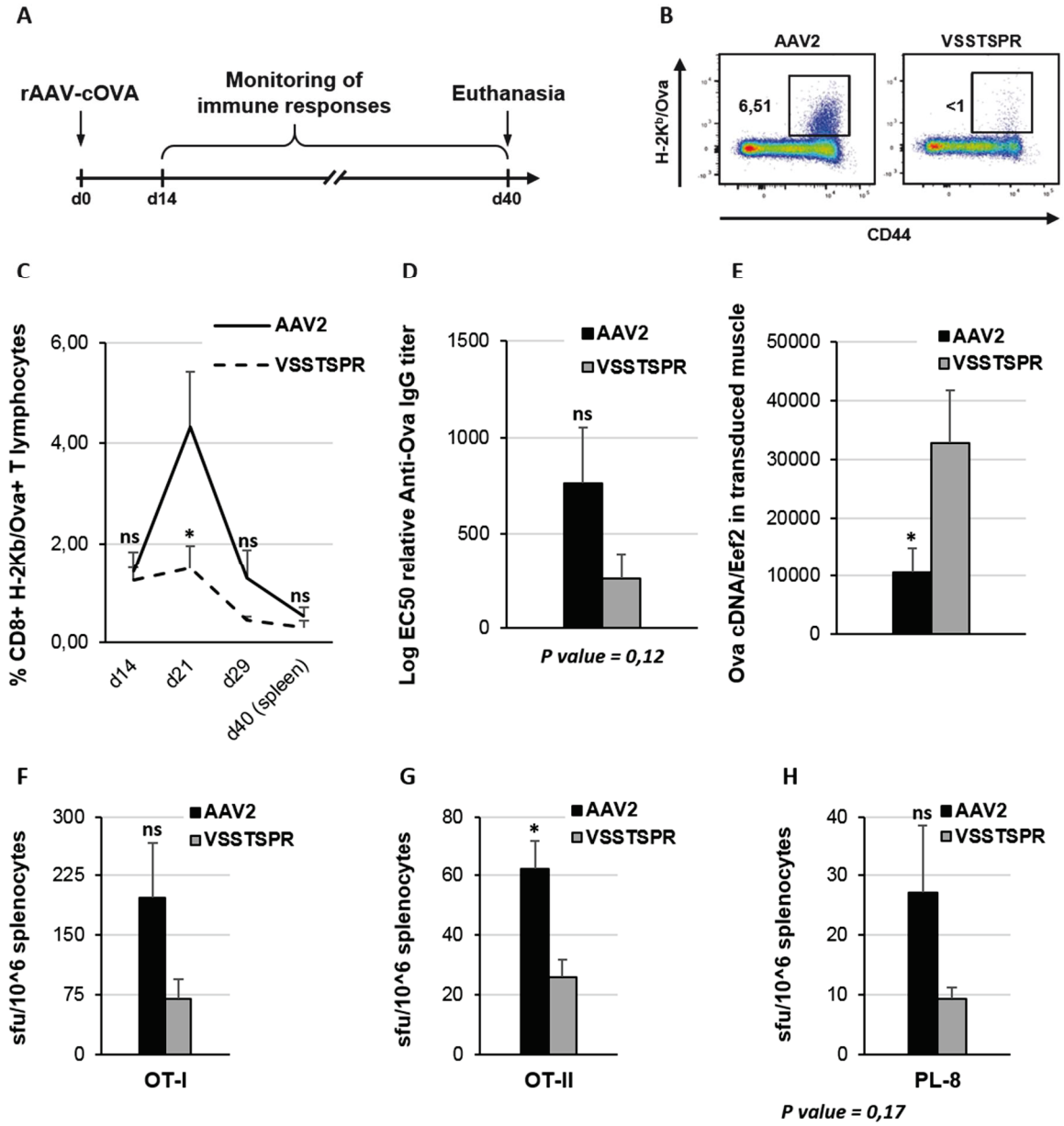


Figure 37. Analyses of VSSTSPR induced immune responses *in vivo*.

A. Protocol outline. B6 mice were injected with ssAAV2-cOVA or ssVSSTSPR-cOVA at a dose of 3.5 x 10^9 vg per mouse, in both gastrocnemius muscles (n = 7 per vector). Immune responses were monitored between day 14 and 40 after injection. **B.** Blood samples were collected 21 days post transduction and percentage of OVA-specific $CD8^+$ T-cells was determined using H-$2K^b$/$OVA_{257/264}$ dextramers staining and flow cytometry. The representative flow cytometric panels indicate the percentage of OVA-specific $CD8^+$ T-cells in the gated $CD8^+$ population. **C.** Percentage of OVA-specific $CD8^+$ T-cells in blood were determined at the indicated times points post AAV injection, and in spleen at d40. **D.** At days 40 post injection, sera were collected and the anti-OVA IgG titers were determined by ELISA. Results were expressed as the last dilution yielding 50% of the optical density obtained with a positive control serum. **E.** At day 40, mice were sacrificed, gastrocnemius muscles were collected and used to measure transgene persistence and expression by quantification of OVA mRNA by RT-qPCR. Data are normalized against the level of Eef2 mRNA (relative units). **F, G, H.** Splenocytes were tested by IFN-γ ELISPOT assay for their ability to secrete IFNγ after stimulation with OT-I peptide (F: CD8-OVA response), OT-II (G: CD4 anti-OVA response), PL-8 peptide (H: AAV2 anti capsid response). Error bars represent S.E.M.

At day 0, three groups of B6 mice were intramuscularly (IM) injected with ssAAV vectors coding for cOVA. Immune response were then monitored overtime from day 14 to day 40 post-injection (**Figure 37A**). For the selected variant, the percentage of the circulating T-CD8^{+} cells able to recognize OVA were significantly lower at day 21 in comparison to those measured in rAAV2-injected mice (**Figure 37B and C**). At day forty mice were sacrificed, and the level anti-OVA IgG antibodies was measured by ELISA. The results indicated that the VSSTSPR capsid variant induced a lower production of anti-cOVA antibodies than rAAV2 injection (**Figure 37D**). Moreover, the persistence of the transgene product in the muscle was analyzed by RT-qPCR and showed that the amount of cOVA mRNA, at day 40, was three fold higher with the variant as compared to rAAV2 (**Figure 37E**).

OVA-specific or capsid-specific immune responses were also measured at day 40, by ELISpot assay. This assay allowed to measure the IFNγ secretion after stimulation of splenocytes with OVA- or capsid-specific peptides (**Figure 37F, G and F**). These assays revealed that IM injection of the selected variant induced a weaker immune response against both the transgene product and the capsid in comparison with the AAV2 vector. In contrast, the mutant capsid resulted in a level of expression of the transgene, higher to that observed for rAAV2. Altogether, these results suggest our selected variant might be able to induce a tolerization state in mice.

III.4 Analysis of AAV virions features by Atomic Force Microscopy

In the two previous parts, we analyzed the effect of capsid modification on the biology of the vector both *in vitro* and *in vivo*. To further evaluate the physical properties of the AAV capsid, a collaboration with Cendrine Moskalenko (Laboratoire de physique, ENS, Lyon) was initiated.

The aim of this interdisciplinary project was to use a physical approach to compare the morphological and mechanical properties of various AAV capsids derived from natural serotypes and then to translate/adapt these methods for the analysis of the engineered capsids generated by my work. The studies presented in this part were performed by Julien Bernaud (PhD student) and Anny Fiss (Master student), who were in charge of performing the

AFM imaging and data analyses. I contributed to these studies by producing the vector stocks, performing some *in vitro* experiments (dot blot), and by participating to the analysis of the data in particular to correlate these results with some biological features of the vectors.

III.4.1 Atomic Force Microscopy

Briefly, the atomic force microscopy (AFM) is a microscopy method based on the use of a local probe, more precisely a tip with a diameter of some nanometers (nanoscale tip) (**Figure 38**). This probe is localized at the extremity of a cantilever characterized by its own stiffness and allows for contacting the analyzed object with the tip. The object is deposited on a stiff surface as mica or glass which is movable in three dimensions due to a piezoelectric crystal which can move according to an x, y, and z axis. According to the stiffness properties of the cantilever, and the nanoscale dimension of the probe, the interaction between the tip and the object deforms the cantilever. In order to collect information from the deformation of the cantilever, this one is lit with a laser which is reflected and strikes a photodiode composed of four quadrants. The computational analysis of the data obtained by the photodiode and the position of the support, allows to extract information about the analyzed sample. In particular, this method allows to evaluate the morphology and the stiffness of the object. A complete scan of the object, via the movement of the support, allows to re-create its morphology. In order to measure the stiffness of the object, the probe is approached to it along the z axis. This leads to a deformation of the cantilever and the sample according to their mechanical properties. The analysis of these deformations allows to evaluate the stiffness of the object.

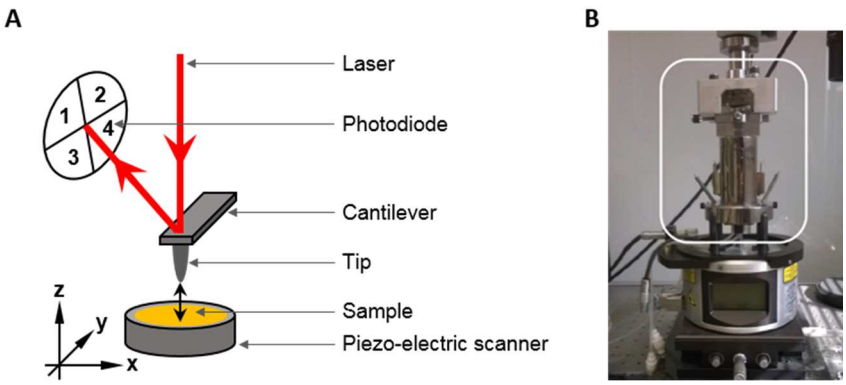


Figure 38. Atomic Force Microscope.
A. Main elements of AFM. The interaction between the probe and the sample allows to make images by measurement of the deviation of the laser on the photodiode. **B.** Picture of the AFM used for this study.

This technology which is used to study the morphology and the stiffness of various materials by physicists, currently gains in popularity to evaluate the mechanical properties of biological objects as tissues, cells or viruses [232]. Importantly, AFM can be used to obtain information from a unique virion in contrast to other methods as cryo-electron microscopy which permits to obtain the tridimensional structure of particles by the average of several observations. The high potential of AFM to observe the tridimensional morphology of AAV virions is illustrated by the **Figure 39A**, which represents a high resolution AFM image of the AAV2 capsid, obtained by J. Rodriguez-Ramos a post-doctoral fellow in C. Moskalenko's team. The imaging of AAV2 allows to clearly visualize the five-fold (**Figure 39B and D**) and three-fold (**Figure 39C and E**) symmetry axes.

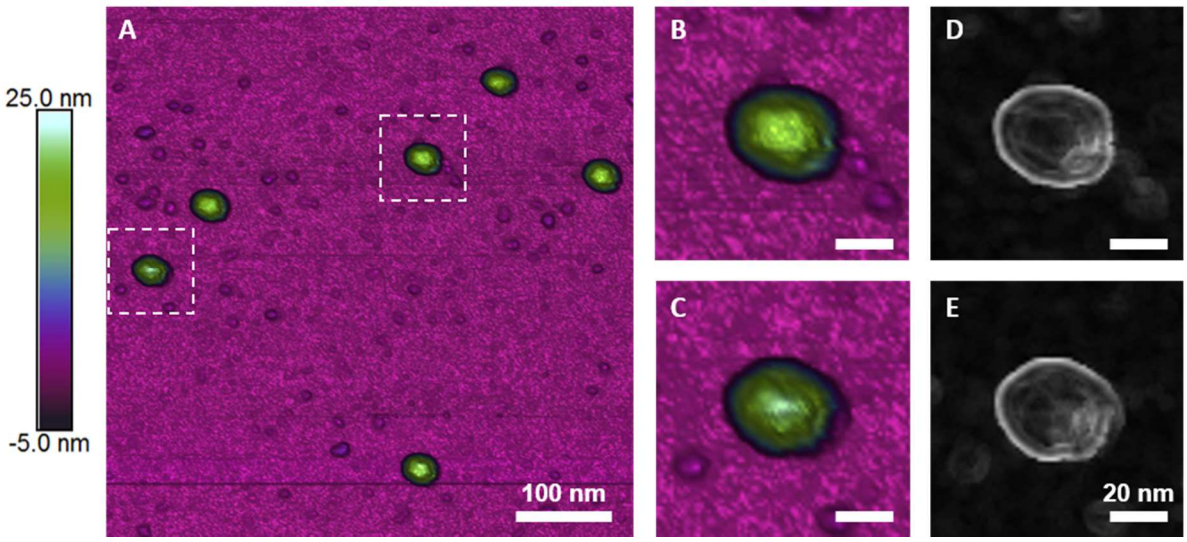


Figure 39. Super resolution image of AAV2 full capsids obtained from AFM.
scAAV2 particles were deposited on functionalized mica in the presence of $NiCl_2$. Imaging was performed in air under low force (280pN). **A.** Overview of the sample. **B. D.** Zoom at a five-fold axis of symmetry. **C. E.** Zoom at a three-fold axis of symmetry. For D and E, the color scale was adapted to highlight the symmetry axis (slope scale).

III.4.2 Quantitative analysis of the virions destabilization

When this work was initiated, the mutated capsid previously presented in the first chapter of this experimental work had not been selected yet. Thus, a comparative study was performed on two interesting serotypes, AAV8 which gains in interest in gene therapy due to its high tropism for the liver, and AAV9, known to be an atypical AAV serotype relatively distant

to AAV8 (83% of amino acid homology sequence), which exhibits several interesting properties for gene therapy, as its delayed blood clearance compared to other serotypes as AAV8 when delivered intravenously, and its ability to efficiently cross the blood-brain barrier [233]–[236]. We first used the same native dot blot assay described before in order to analyze the thermal stability of these two serotypes (**Figure 40**). Our experiment revealed that AAV9 is more stable when submitted to a temperature gradient in comparison to AAV8. At the physiological pH of 7.2 units, denatured AAV8 capsids are detectable at a temperature greater than or equal to 70°C, whereas they are detectable at a temperature greater than or equal to 75°C for AAV9. Interestingly, the increased resistance of the AAV capsids in an acidic environment, previously observed for the AAV2 and VSSTSPR (**Figure 33**) is also observed for AAV8 and 9, which both required an additional 5°C to be denatured at pH of 5.2 units. It is important to note that in this experiment, both AAV8 and 9 contain one ss AAV genome whereas our previous analysis was performed with scAAV vectors.

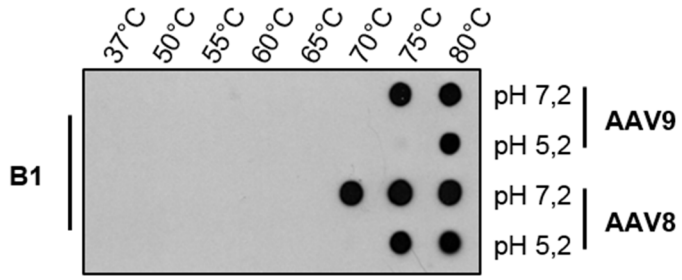


Figure 40. Analysis of AAV8 and AAV9 thermal stability by native dot blot.
Capsid destabilization assay on AAV9 and AAV8. A native dot blot was performed on AAV capsids which were heated at different temperatures in two different pH conditions. The denatured capsids were detected with B1 antibody.

To further explore the stability of AAV capsids, J. Bernaud used AFM to image ssAAV8-GFP particles submitted at different temperatures (**Figure 41**). As expected, the amount of intact capsids decreased upon heating, resulting in the release of DNA molecules clearly visible on the mica surface with a 5 nm color scale (**Figure 41, left panel**).

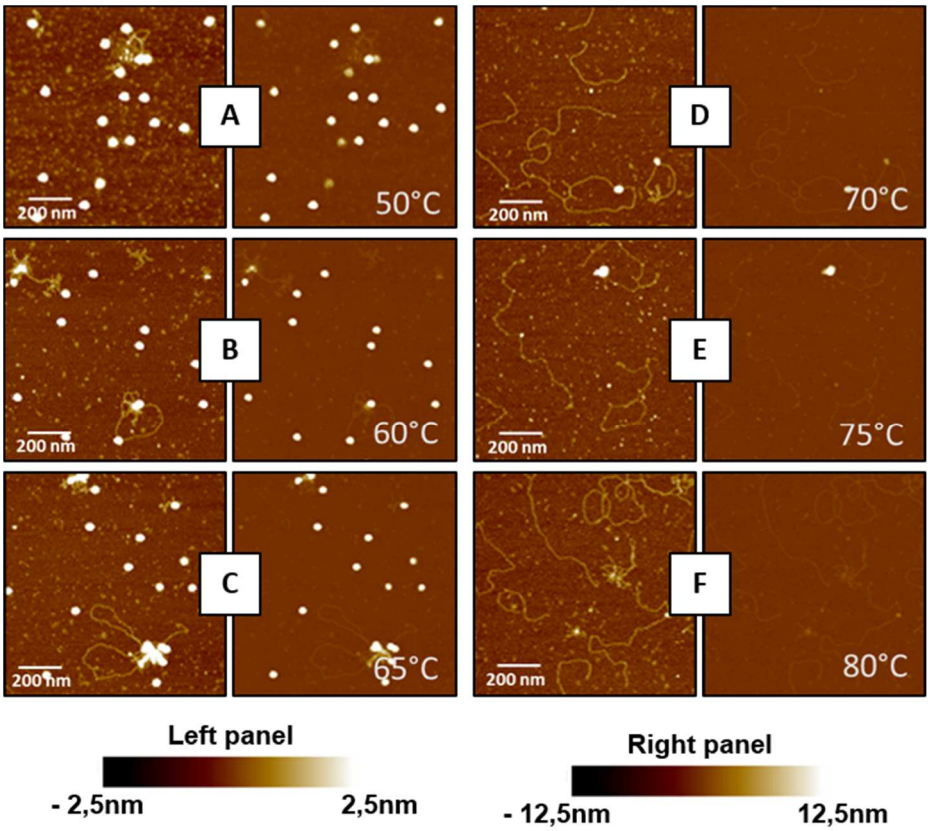


Figure 41. AFM images of ssAAV particles submitted to increasing temperatures.
Each image is shown twice: on the right panel a color scale of 25 nm is used to see the viral capsids. On the left panel, a 5 nm color scale is used to explore the surface (the ssDNA width is below 1 nm). At a temperature below 50°C (**A**) mainly intact capsids are observed. By increasing the temperature some DNA filaments can be seen around the capsids (**B**) and (**C**). At higher temperatures (**D**), (**E**), both free DNA and DNA linked to capsids exist. At 80°C only free DNA is detected on the surface (**F**).

Based on this observation, a quantitative destabilization assay was performed to compare the stability between the AAV8 and 9 (**Figure 42**). Three different objects can be visualized and quantified on the AFM images: intact capsids, capsids linked with DNA and free filaments of DNA (**Figure 42A**). The quantification of these three objects at different temperatures confirmed the result obtained with the biochemical assay: AAV9 is less thermosensitive than AAV8. Indeed, 80% of the AAV8 capsid have released (at least partially) their genome at 70°C (**Figure 42B**), whereas only 20% of AAV9 started to uncoat at the same temperature (**Figure 42C**). This result is consistent with that obtained by dot blot (**Figure 40**). Moreover, the single molecule quantification by AFM provided information concerning the distribution of different populations (intact capsid, capsid linked with DNA, and free filaments of DNA) for each condition. The analysis of the heterogeneity of the subpopulation suggests that the AAV9 genome is released more progressively from the capsids than AAV8. Furthermore, the

biochemical assay also indicated differences in capsid thermal stability according to the pH. The AFM analysis of ssAAV8 under pH treatment was consistent with the dot blot (data not shown).

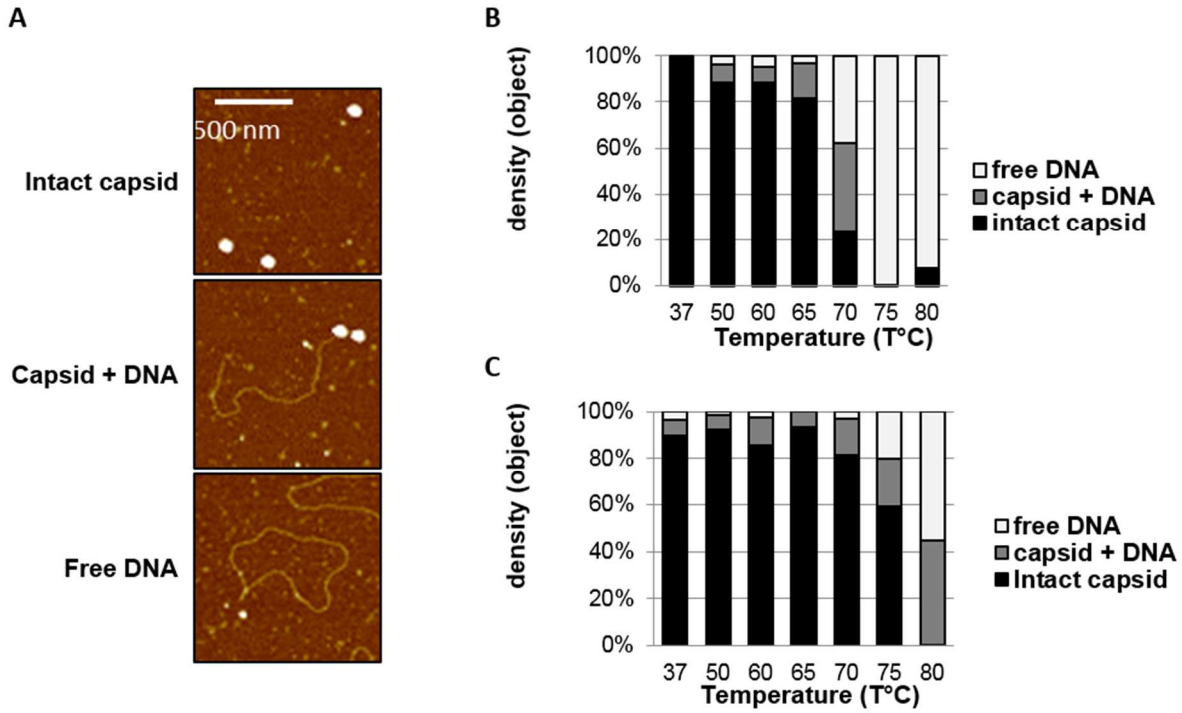


Figure 42. Destabilization behavior of AAV8 and AAV9 at different temperatures.
A. AFM imaging of the three main populations observed after thermal destabilization of ssAAV8 particles at pH=7.2). **B. and C.** Histograms representing the amount of each population at different temperatures for ssAAV8 (B), and ssAAV9 (C). The temperature required to observe more than 50% of the capsid uncoated is 70°C for ssAAV8 and 80°C for ssAAV9. (Data obtain in collaboration with Physics laboratory).

III.4.3 Genome releasing

In addition to providing a quantitative method to analyze the destabilization of the virions, AFM imaging of heated virions by AFM allows to directly visualize the secondary structure of the released DNA molecule. After ejection, the DNA molecule (free or associated with a capsid) can appear in two forms: either linearized or "compacted" (**Figure 44A**). Furthermore, computational analysis of the images allows to measure with a nanometric accuracy the length of the ejected DNA. Julien Bernaud quantified the DNA molecules, obtained after heating ssAAV8 at various temperature, according to their length (**Figure 44B**). This experiment indicated the presence of two major populations of DNA molecules: one characterized by a

length of 0.1 µm (small DNA filament or “compacted” molecule), and one by a length of 1.2 µm (linearized complete genome). Interestingly, however, one intermediate DNA population with a specific length of 0.5 µm (approximately corresponding to a linearized molecule of 1.5 kb) was over represented at all tested temperatures. In this experiment the temperature is used as a sensor to evaluate the energetic threshold necessary for capsid disassembly. In addition, the conformation of the DNA might provide information about the mode of disassembly. It is important, however, to keep in mind the importance of several parameters such as the temperature, the secondary structure of the DNA, or the interaction between the DNA molecule and the substrate (mica). These physical considerations are not detailed here (PhD thesis of Julien Bernaud, C. Moskalenko PhD director).

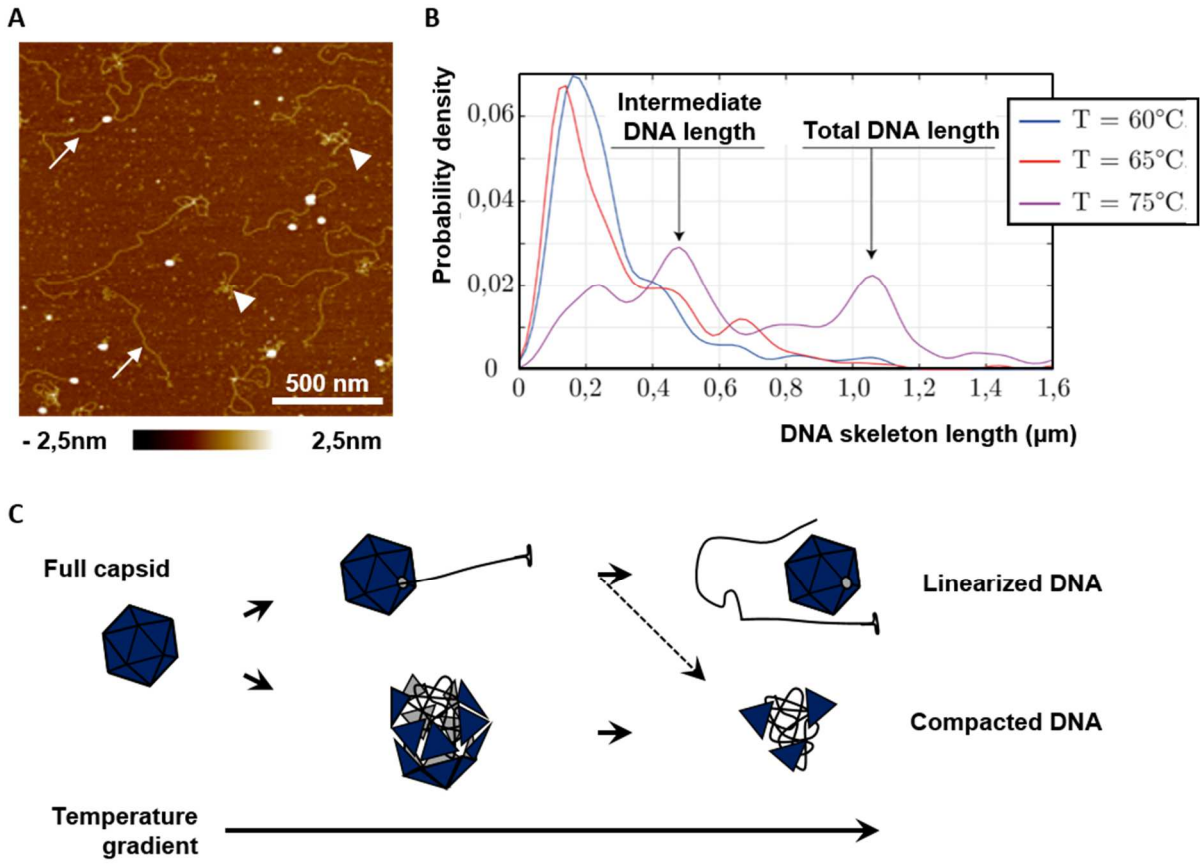


Figure 43. AAV8 genome release upon heating.
A. Imaging of ssAAV8 particles after heating allows to observe two subpopulation of DNA molecules, the linearized DNA molecule (arrow) and “compacted” DNA molecule (arrow head). **B.** The probability density of the different DNA molecules was calculated at the three temperatures. **C.** Proposed models for AAV genome release (Data obtain in collaboration with Physics laboratory).

These results allowed J. Bernaud to propose a bimodal ejection model of the viral genome characterized by two different pathways for the genome releasing (**Figure 43C**): i) the genome is ejected through a small hole in a capsid which may be the pore of the five-fold axis of symmetry; this pathway requires to overcome two energetic barriers to be completed, indeed an intermediate state can be observed; ii) the uncoating of the genome occurs by the complete disassembly of the more fragile capsids leaving the DNA as a compacted DNA molecule. The frontier between these two pathways seems blurry, moreover, additional studies will be required to evaluate the biological relevance of these pathways inside the target cell and the influence of AAV serotypes.

These results indicated important biophysical differences between ssAAV8 and ssAAV9 particles which may account for the greater stability observed for AAV9 when delivered intravenously. To confirm and improve the biological relevance of these biophysical methods, a comparative analysis of rAAV2 particles with the capsid variant previously described (VSSTSPR) using this method is ongoing. Indeed this variant has interesting biological and physical features such as a more efficient genome uncoating within DC and a weaker thermal stability than rAAV2.

III.5 VSSTSPR, a powerful tool for research in brain

AAV vectors were described as one of the most promising tools for gene delivery in medical applications, but they are also a powerful tool to answer at several biological questions. During my PhD project, I had the chance to be contacted by J. Welsch who is interested in infection of the brain with Measles (MeV) and Nipah (NiV) viruses. During his PhD project, he developed an organotypic brain culture (OBC). He aims to use this model to investigate in real time, the tropism of MeV in the central nervous system (CNS) and, more challenging, the consequences of the infection on the organization of this complex tissue in term of cell migration and interaction. For these studies, it was necessary to first label, by gene transfer, specific cell types in OBC. After different fruitless test in his model with lentiviral vectors, J.Welsch contacted me to know if I had in my toolbox AAV vectors able to overcome the several constraints of his project.

III.5.1 Organotypic brain culture as an elegant model to study MeV infection

OBC allows observations of the brain cells within a preserved tridimensional tissue architecture and cellular composition that includes neurons, microglial cells and astrocytes [89-92]. The OBC developed by J. Welsch during his PhD provides several interesting properties to further explore the consequences of viral invasion into the brain. Indeed, the maintenance of the organization of the CNS tissue with a heterogenic cell population better reflects the *in vivo* conditions than conventional cell lines. However, this model derived from isolated sub-structural parts of the brain, such as hippocampus or cerebellum, restricts the possibility to observe viral dissemination throughout the whole organ. Indeed, potential neuronal or cerebrospinal fluid (CSF) streams cannot be maintained in OBC. Moreover, brain isolation from the rest of the organism considerably restricts the analysis of the interactions of the virus with circulating host immune cells.

J. Welsch aims to use this brain model to further analyze the MeV infection into the brain. Indeed, this encephalic virus infect neuronal cells, cause lethal encephalitis and/or persistent brain infections that can lead to disease relapses from several months to years after primary infection. However, the underlying cellular and molecular mechanisms involved in virus infection and dissemination within the CNS remain poorly understood. Thus, in order to follow the MeV invasion in the early phases of the infection, it is crucial to be able to discriminate the various cell types present in the brain. One strategy it is to pre-infect the tissue with vectors able to efficiently transduce the wide range of cell types present in the tissue to express fluorescent protein under the control of cell specific promoters. The vector used have to exhibit several properties such as an efficient transduction, a low impact on immune responses and no interaction with the studied virus. Due to their features, AAV vectors seemed to be an interesting choice to be used in this study.

III.5.2 Preliminary results

The analysis of the MeV infection using OBC and AAV vectors to label various cell populations, requires an efficient transduction of the different cell types present in the brain by rAAV. Due to the capacity of the VSSTSPR variant to transduce a larger range of cell types in comparison to rAAV2, we decided to first analyze the transduction efficiency of both these

vectors in various human and murine cell lines. Indeed, the variant was selected in human primary cell, whereas the OBC is derived from the murine brain. This preliminary study was performed to evaluate the potential of our AAV vectors in brain cells. Thus, scAAV2-GFP or scVSSTSPR-GFP vectors were used to transduce U87 (derived from human glioblastoma), Raw 264.7 (mouse macrophage model) and SH-5YSY (derived from human neuroblastoma) cells. For this experiment a gradient of MOI was used in order to evaluate the performance of these vectors and the cell transduction was evaluated twenty-four hours after vectors incubation. Initially analyzed by fluorescence microscopy (**Figure 44A**), the transduction efficiency of U87 cells by rAAV2 and VSSTSPR vectors appeared similar. Both vectors were able to efficiently transduce U87 cell line at a MOI of more than 100 vg per cell. Then, the transduction efficiency was quantified by FACS and two different parameters were measured, the percentage of GFP positive cells and the fluorescence intensity (**Figure 44B and C**). While the percentage of GFP positive cells appeared similar (more than 95% of GFP^+ cells at a MOI of 10^3 vg per cell) between rAAV2 and VSSTSPR, the measure of the mean fluorescence intensity revealed an important difference between the two capsids at a high MOI. The same measures were performed after transduction of Raw 264.7 cells (**Figure 44D and E**), for which the transduction efficiency appears lower than in U87 cell line (less than 1,5% of GFP^+ cells MOI of 10^3 vg per cell). However, the mean fluorescence intensity was higher for VSSTSPR at a high MOI. The transduction on SH-5YSY cells indicated a good and similar transduction profile for both AAV vectors (data not shown). All together these results confirmed the capacity of VSSTSPR to transduce a wide variety of cell types at a level superior than rAAV2. They also suggested that AAV vectors could be tested on the OBC.

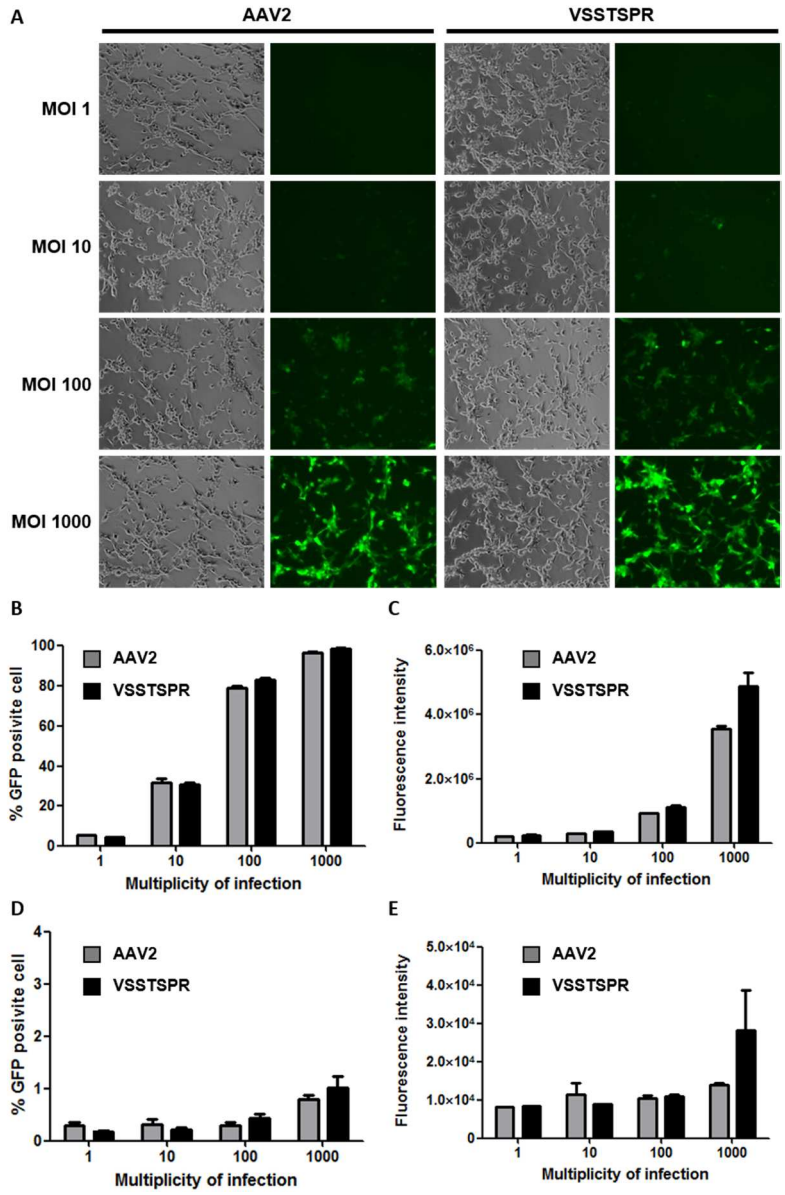


Figure 44. Comparative analysis of the transduction efficiency of rAAV2 vs VSSTSPR.
A. Direct observation of U87 cells 24 h after transduction with scAAV2-GFP or scVSSTSPR-GFP at several MOI (10^0, 10^1, 10^2, 10^3 vg per cell). **B, C, D, E.** FACS analysis of GFP expression by U87 (B and C) and Raw 264.7 (D and E) cells transduced with scAAV2-GFP or scVSSTSPR -GFP at several MOI (10^0, 10^1, 10^2, 10^3 vg per cell). Error bars represent standard deviation (data obtained in collaboration with J. Welsch).

III.5.3 VSSTSPR in action in OBC

The study of the transduction efficiency of AAV vectors was initiated on OBC. The mouse hippocampus and cerebellum were incubated with scAAV-GFP vectors, and a comparative analysis between the rAAV2 and the mutated VSSTSPR capsid was performed. The transduction efficiency was controlled by fluorescence microscopy seventy-two hours after transduction (**Figure 45**). In contrast to the results obtained in the transduction assay on cell

lines *in vitro*, the *ex vivo* assay strongly suggests that VSSTSPR vectors transduced the mouse brain with a better efficiency in comparison to rAAV2. It is important to note that, due to the complexity of this culture method the evaluation of the vector doses used in this assay was more difficult to estimate as compared to the *in vitro* assays. Thus, the experiment was reproduced with different vector preparations (at least n=3 for each preparations) and the transduction efficiency was also evaluate twenty-four hours post transduction. The transduction efficiency of the VSSTSPR was always higher than that measured for rAAV2; even if the measure was made in the early phase of the infections (twenty-four hours post infection: data not shown). These data provide a strong and unexpected argument for the utilization of VSSTSPR in the OBC model.

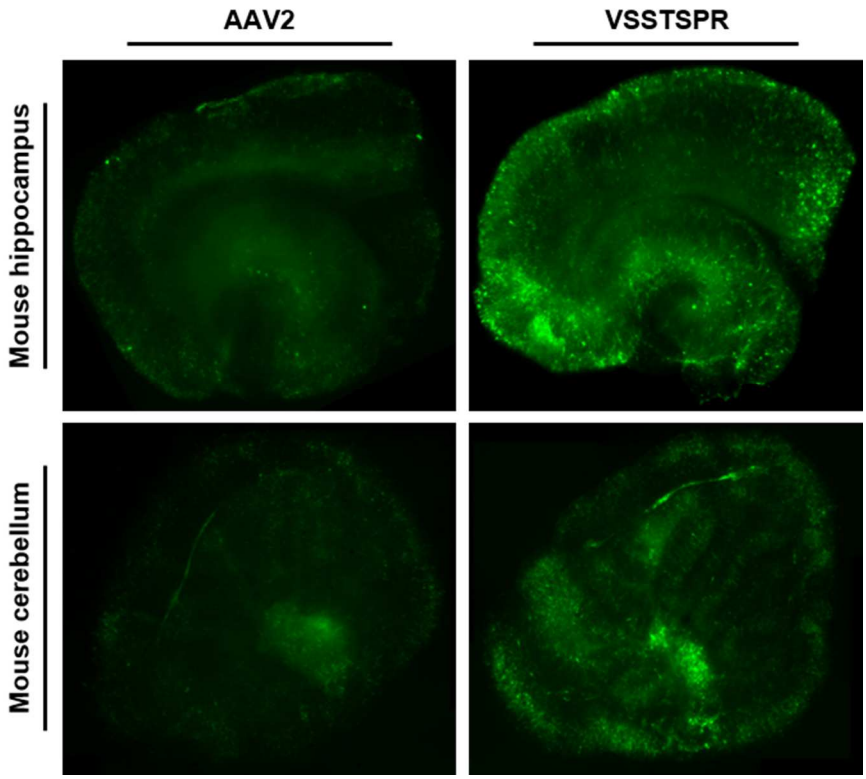


Figure 45. VSSTSPR is a better candidate than rAAV2 to transduce cells within OBC.
Direct observation of mouse hippocampus or cerebellum slices after transduction with scAAV2-GFP or scVSSTSPR-GFP vectors at a MOI of 4.10^8 vg per slice. Observations were performed 72h after vectors incubation (data obtained in collaboration with J. Welsch).

The final aim of this work is to discriminate the different cell populations present into the brain tissue. Thus, it was therefore important to know if the VSSTSPR variant was able to transduce all the cell types residing in the brain. In order to evaluate this point, cells of the hippocampus incubated with scAAV2-GFP and scVSSTSPR-GFP vectors were analyzed by

immunofluorescence (**Figure 46**). Twenty hours after rAAV transduction, the slice of hippocampus were fixed with paraformaldehyde and incubated with antibodies specific of astrocytes (anti-GFAP antibodies) and microglia cells (anti-Iba1 antibodies) markers. The majority of the GFAP positive cells expressed GFP protein (**Figure 46A**); however only a few amount of Iba1 positive cells expressing GFP were found on the slice (**Figure 46B**). This preliminary result suggests a high potential of VSSTSPR to efficiently transduce the astrocytes in OBC; this capsid also allows to transduce microglia cells although with a lower efficiency. Further analyses have to be performed to confirm these observations and improve the transduction of microglia. It is important to note that in this assay, the GFP expression was regulated by the CMV promoter. The use of specific promoters for these different cell populations may improve the efficiency of transduction.

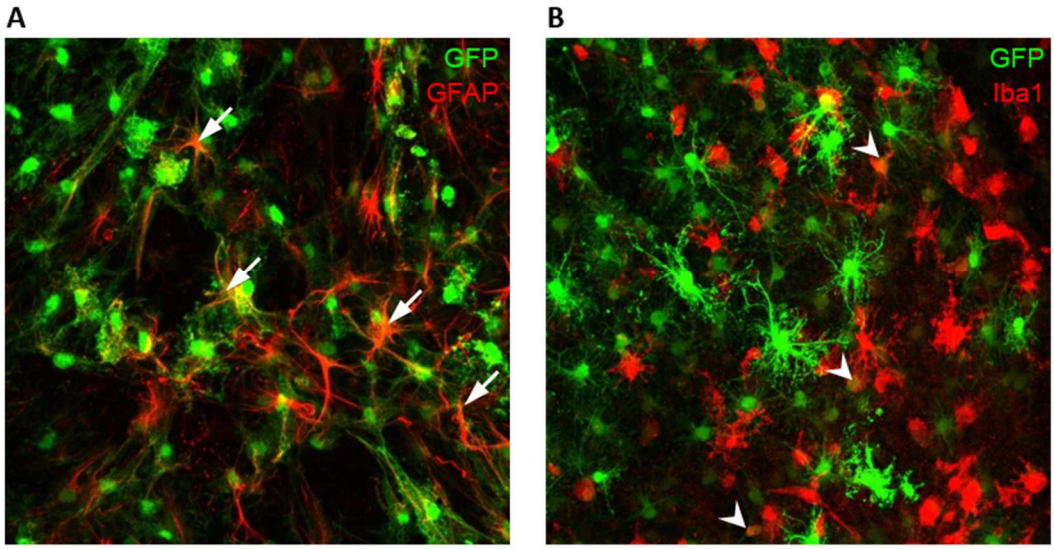


Figure 46. Transduction efficiency of OBC cell types by VSSTSPR.
Direct observation by confocal microscopy of mice hippocampus slices transduced with scVSSTSPR-GFP at a MOI of 6.10^8 vg per slice. 20 h after infection, slices were fixed and astrocytes were labeled with anti-GFAP antibodies (**A**) or microglia cells were labeled with anti-Iba1 antibodies (**B**). Arrows indicate some astrocytes efficiently transduced with rAAV; arrow heads indicate some microglial cells efficiently transduced by rAAV (data obtained in collaboration with J. Welsch).

III.5.4 VSSTSPR has no effect on MeV replication *in vitro*

Using AAV vectors in OBC to further explore the MeV invasion in CNS requires that the impact of rAAV on MeV biology is as low as possible. To evaluate the impact of the scVSSTSPR-GFP vector on MeV replication, a replication assay was performed on Vero SLAM cell line

which is an interferon deficient (IFN) cell line. Cells were co-infected with MeV which is tagged with Tomato protein in the H2 hemagglutinin (tagging performed by J.Welsch using a classical protocol [241]) (MOI 10^{-2} pfu per cell) and scAAV-GFP (MOI 10^{3} vg per cell). Then, replication of MeV was evaluated qualitatively by fluorescence microscopy over time. The presence of the AAV vectors did not seem to have any impact on the replication of MeV (**Figure 47A**). The titer of the MeV was further measured over time in presence or absence of rAAV. This quantification did not show any influence of AAV on the amount of produced MeV virions (**Figure 47B**).

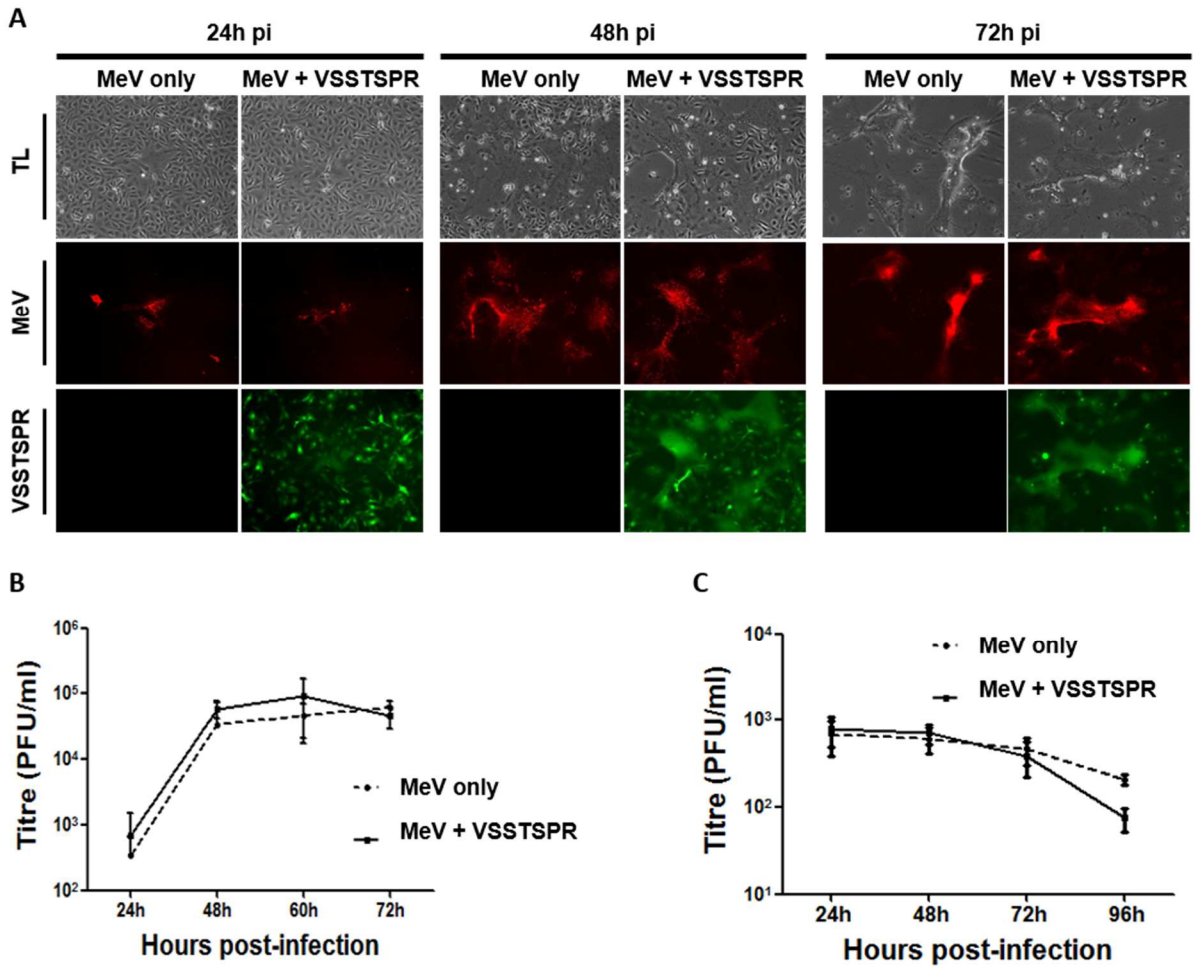


Figure 47. Analysis of VSSTSPR impact on MeV replication *in vitro*.
A. Vero cells were infected with MeV IC323 L Td Tomato at a MOI of 10^{-2} pfu per cell and co-infected or not with scVSSTSPR-GFP vector at a MOI of 10^{3} vg per cell. GFP and Tomato expressing cells were visualized under a fluorescence microscope. **B. and C.** Measure of the MeV titers over time in Vero SLAM (**A**) or H358 (**B**) cell lines infected with MeV IC323 L Td Tomato at a MOI of 10^{-2} pfu per cell and superinfected or not with scVSSTSPR-GFP vector at a MOI of 10^{3} vg per cell. Error bars represent standard deviation (data obtained in collaboration with J. Welsch).

In order to evaluate the impact of rAAV on MeV replication in condition closer to the *ex vivo* conditions, a same assay was performed on H358 cell line which is IFN competent. The result from this assay confirmed that rAAV does not modulate the replication of MeV (**Figure 47C**). These results show how our selected AAV capsid variant was a promising candidate to complete the study of J.Welsch and better understand the dissemination of MeV and its consequences on the brain. All together these results show the high potential of our selected capsid variant which can be used as a powerful tool to developed elegant strategy to answers several biological questions using complex culture models.

III.6 Conclusion

To conclude this work, after an *in vitro* directed evolution procedure performed on monocyte-derived dendritic cells, we selected an AAV capsid variant (VSSTSPR) which exhibits some interesting properties. Despite sharing several common features with rAAV2, such as HSPG binding and a similar intracellular distribution, the selected variant exhibits an important advantage in term of transduction of DC. This property can be explained by a more efficient uncoating of the genome from the mutated capsids which also displays a lower stability than the parental AAV2 capsid. Because of the importance of the DC in the establishment of the immune responses, the impact on gene delivery mediated by this vector was evaluated in mice. Our results suggest that the VSSTSPR vector induces less immune responses against the transgene product and the capsid in comparison to an AAV2 vector. This interesting property has to be further explored. Moreover, our analyses of AAV by AFM, suggest that the stability of the capsid is a major property that may distinguish different AAV serotypes and variants, and which could be linked to their capacity to differentially uncoat the vector genome. Interestingly, the higher efficiency of VSSTSPR to transduce human DC, as compared to AAV2, is also observed on other transformed and primary cells.

IV. Discussion

As described above, gene therapy using AAV vectors is already under way, but it is still limited by several key obstacles which need to be overcome to improve the efficiency and the safety of these treatments. My PhD project was focused on the study of the intracellular fate of AAV virions in DC and its impact on gene transfer. Indeed, DC are an interesting target for both gene therapy and genetic vaccination due to their property of APC. However, these cells cannot be transduced by AAV vectors and the limiting barriers are still unclear. To understand this phenomenon and to try to overcome the intracellular barriers we used an *in vitro* selection procedure which was previously developed in several studies to improve the transduction efficiency of AAV vectors on various targets cells. After its optimization, this process allowed us to select an interesting AAV capsid variant, called VSSTSPR which is able to transduce DC with a greater efficiency as compared to the parental AAV2 capsid. We performed a detailed study of the intracellular fate and properties of this variant, as compared to rAAV2, in DC and other target cell types. In addition, we performed an *in vivo* analysis to investigate the consequences of this mutation on the immune responses induced against the transgene product encoded by the AAV vector.

IV.1 Intracellular fate of AAV particles in human DC

Our results showed that the majority of AAV particles derived from rAAV2 are retained into the host vesicular system. Interestingly, this intracellular distribution was identical between permissive (HeLa cells) and non-permissive (DC) cells. However, a fraction of particles can reach the nucleus of the cells. This observation was confirmed by other studies in different cells types [23]. Indeed, it was clearly demonstrated by different studies that a pool of rAAV virions succeed at escaping from the vesicular system to reach the cytosol and then the nucleus. This escape requires the maturation of the AAV capsid allowed by the acidification and the protease activity of the vesicular machinery.

Previous studies indicated that the endosomal system of immature dendritic cells is characterized by a higher intraluminal pH and a lower protease activity, as compared to most the other cell types. These properties which are intimately linked to their main function of DC

in antigen presentation, are dramatically changed during their maturation [170], [227], [228]. Therefore, we can postulate that AAV particles trafficking through the DC endosomal system are not properly matured as in other permissive cell types. Our studies on DC showed that treatment of cells with DPI, a drug lowering the pH of one unit [229], [230] was not sufficient to increase the transduction efficiency of AAV vectors in these cells. Conversely, an inhibition of the acidification of the endosomal system negatively impacted on the AAV transduction. The absence of improvement in the presence of DPI may be explained by the need to further decrease the pH in order to favor AAV capsid maturation. In addition, it is possible that pH lowering is not sufficient and that an increase in endosomal proteases activity is also required. Indeed, *in vitro* studies indicated that incubation of purified capsids in an acidic buffer was not sufficient to induce full capsid maturation, including externalization of the VP1 N-terminal domain [96]. Interestingly however, we observed an important improvement of the transduction efficiency when the DC are activated with LPS, an agonist of the TLR4. This improvement, which occurred for both parental and variant AAV vectors, may be explained by the increase of the acidification and of the protease activities taking place into the intravascular system of activated DC [170], [227], [228].

Despite being massively arrested within the intra-vesicular system, it was surprising to find that a significant percentage of rAAV particles were also found in the cytosol, and in the nuclear compartment as shown by cell fractionation followed by rAAV genome detection by qPCR, as well as by immuno-fluorescence analysis to detect assembled capsids (**Figure 25**, **Figure 26**). The presence of capsids within the cytosol strongly suggests that despite the absence of maturation within the endosomes some of them succeed at escaping from the vesicles. In addition, even though we cannot exclude that AAV capsids remain blocked at the nuclear membrane, the presence of rAAV genomes with the nuclear compartment suggests that some AAV particles entered the nucleus. Unfortunately, the detection of matured AAV capsids (*i.e.* with externalized VP1 domain) in this compartments failed because our fractionation process partially denatured the AAV capsid. Nevertheless, it may be hypothesized that despite being immature AAV particles could use alternative pathways to traffic through the cytoplasm and enter the nucleus. Alternatively, it may be envisioned that some particles in the initial population were more prone to maturate even in these non-favorable conditions. Both these hypotheses may explain why the intracellular distribution of

AAV particles was not quantitatively different in immature DC and HeLa cells, and when DC were infected during maturation (mDCpi) (**Figure 31**).

Despite the presence of AAV particle in the nucleus of DC, at a level similar to that observed in HeLa cells, AAV2 vector cannot transduce these cells (**Figure 24**). This observation suggests that capsids uncoating constitutes an important barrier in this, and probably other non-permissive cell types. Interestingly, the VSSTSPR variant shares with the parental AAV2 the same intracellular distribution, despite a better transduction efficiency of both immature and mature DC (**Figure 31**). We explain this different phenotype by an improved uncoating of the variant. Indeed, the VSSTSPR resulted in a higher level of episomal DNA within DC, either immature or undergoing maturation, compared to rAAV2. This latter result which indirectly measures the efficiency of genome uncoating, strongly suggests that mutant AAV particles were more prone to disassembly once in the nucleus of DC, as compared to AAV2 capsids (**Figure 34**, **Figure 36**).

The cellular factors influencing the AAV uncoating are still poorly documented, but during their intra-vesicular transport, AAV particles are known to be partially digested by protease activities, which may prime the particles for uncoating in the nucleus [97]. Interestingly, the intra-vesicular machinery of DC are deficient for several protease activities as compared to HeLa cells which might explain the difference observed in these two cell types. Attractively, VSSTSPR presents a lower thermal-stability than the parental AAV2, a property which correlates with its higher uncoating capacity (**Figure 33**).

Our *in vitro* analysis of the thermal stability of the AAV capsids (AAV2, 8, 9, and VSSTSPR): indicated that the acidification of the environment increased capsids stability. This property, which was also confirmed by other authors [67], suggests that AAV particles may have evolved to protect their genome during their passage in the late endosomes.

IV.2 VSSTSPR: a bipolar candidate for gene transfer?

As noted above, one of the most important challenge for *in vivo* gene transfer applications is the control of the immune responses directed against the vector and the transgenic protein. Indeed, the outcome of the gene transfer strategy is closely linked to the interaction between the vectors and the host immune system. Each specific application requires a different control

of the immune responses. Thus, in most gene therapy applications, the transgenic protein needs to be continuously expressed and to be accepted by the immune system to reach a therapeutic effect. This is the case for the treatment of monogenic disorder such as Hemophilia B or LCA. In contrary, in gene vaccination the transgenic protein has to be detected by the host immune system to lead to the immunization of the host. This is the case for the treatment of infectious diseases or cancer (**Figure 9**).

We aimed to select a capsid variant able to transduce human DC because this particular cell type plays a pivotal role in the establishment of the immune response. Indeed, this APC is the only one able to activate the naïve T-cells leading to a positive or a negative orientation of the immune responses. The interaction between the AAV vectors and the DC *in vivo* remains obscure, and the consequences of the transduction of the DC by AAV vectors are unknown. Our selected variant VSSTSPR able to transduce human DC is a promising tool to understand this interaction and its consequences on immune responses.

In order to shed light on this issue, we decided to evaluate the consequences of the *in vivo* gene transfer mediated by our selected variant in a mouse model, to follow the fate of the transgenic protein and the induction of the immune responses. For comparison, we used the parental AAV2 capsid (**Figure 37**). To evaluate the immune responses, vectors were injected in the muscle. Indeed, rAAV injection in this tissue is known to induce a humoral and cellular immune responses against the transgene product, in particular when the vectors is expressing an immunogenic transgenic protein such as OVA. For this assay, the persistence of the transgene was measured in the muscle after the euthanasia of the mice 40 days after injection, and the humoral and cellular immune responses were monitored from the 14^{th} to the 40^{th} day after injection. Interestingly, transgene expression was higher in the case of gene transfer mediated by our selected variant as compared with the control AAV2 vector. This higher level of OVA correlated with lower cellular and humoral immune responses directed against OVA. In addition, a reduced level of T-cell responses against the capsid was also measured. Importantly, some recent analyses performed at earlier time points (7 and 14 days post-injection) indicated that, despite being internalized at a similar/slightly lower level than rAAV2, the VSSTSPR mutant was more efficient to express the transgene even at these earlier time points (data not shown). In addition, the detection of OVA-specific CD8+ T-cell responses

showed that after an initial increase (at day 7), T-cell responses against the transgene product, raised by the VSSTSPR variant, rapidly decreased to levels inferior to those found with rAAV2 (at day 14) (data not shown).

Altogether, these results suggest that our selected variant, which displays a lower stability and a higher uncoating capacity *in vitro*, was less prone to induce effective immune responses against both the transgene product and the capsid, compared to rAAV2. This resulted in a higher level of expression of the transgene both at early and late times post-transduction probably resulting from a combined effect of the mutant capsid on genome uncoating (at early times) and T-cell responses (at late times). Importantly, the initial raise in T-cell responses at day 7 followed a rapid decline also strongly suggests that the mutant induced a tolerization state against the transgene product and the capsid, likely due to transduction of murine DC without inducing a concomitant stimulating signal. Indeed, it is known that the presentation of the antigen without maturation of the DC induced by PRR activation, leads to active tolerization. In order to confirm this hypothesis we plan to measure the Treg expansion and the DC transduction *in vivo.* In addition, future experiments will be also performed to compare VSSTSPR to other AAV serotypes, notably AAV1 and AAV8 (encoding for OVA). We expect that VSSTSPR will be able to induce a lower level of immune responses than the other serotypes. Preliminary results do indicate that it is case when compared to AAV1 vectors (data not shown).

Our *in vitro* analyses have shown that activation of TLR4 by LPS increases the transduction efficiency of human DC with rAAV (both rAAV2 and VSSTSPR) (**Figure 29**). Therefore, it will be very interesting to test the consequences of the *in vivo* injection of AAV vectors in presence of LPS as an adjuvant. We expect that, in these “inflammatory” conditions, the higher level of expression of the transgene induced by the VSSTSPR in DC, will be able to induce a level of adaptive immune responses, quantitatively and qualitatively superior to those obtained with conventional AAV serotypes. This important experiment will indicate if, under particular conditions, the here developed capsid-engineered vector can be “switched on” in terms of immune reactions. If so, the VSSTSPR capsid could also represent a very interesting vector for genetic vaccination. Thus, further work are required to confirm the potential of VSSTSPR to

induce an active tolerization, and its potential as an efficient vaccine vectors in the case of injection with an adjuvant such LPS.

If the data obtained in the next few months confirm these results, then it will be necessary to move into larger animal models. Indeed, past experience from several laboratories working on AAV vectors has shown that responses observed in mice are not always directly translatable to other animal species.

Nevertheless, it should be noted that our selection procedure has been performed using human DC to be able to develop a capsid-engineered vector that could be finally applied in patients. Therefore, the fact that it behaves as expected in mice strongly suggest that this feature can be translated cross-species, a benefit for pre-clinical establishment of strategies with the option of directly translating results into human clinical trials.

Finally, this study is the first one to demonstrate the feasibility of this concept of modifying AAV immune properties by destabilizing its capsid in order to facilitate expression of the transgene in immune cells such as DC. Therefore, even if future studies indicate that the properties of this precise AAV mutant are restricted to mice, other “destabilized” mutants could be further selected using the same procedure.

IV.3 New criteria for future selections

The design of new AAV particles with interesting features is required for a broad range of medical applications. In this work, we were focused on the transduction efficiency of a particular target cell. We used an optimized *in vitro* directed evolution process which allowed to select a variant able to transduce our target cells more efficiently than the parental AAV2 derived vector. Surprisingly, the selected variant presents an improved capacity to uncoat its genome may due to a lower stability of the capsid. This interesting features may overcome a limiting step which consist in the priming event(s) during the intracellular trafficking of the capsid toward the nucleus. This interesting feature also results in a better ability for our selected variant to transduce different primary cell types which are refractory for rAAV transduction, such as EC or astrocytes in a murine OBC model (**Figure 46**).

An important modification introduced in the directed evolution method consisted in the isolation of AAV sequences from the nuclei of DC and not, as routinely performed, from the

whole cell, to selectively retrieve only the particles which could arrive in their final cell compartment (**Figure 18**) [222]. Even if we have not verified that it is the case, we believe that this modification in the protocol was key for the success of the procedure. Starting from this initial work, additional conditions for selection of new improved capsids ca be envisioned. In particular, it will be very interesting to be able to select AAV variants on their capacity to release the DNA and express it in the nucleus of the target cells. For this, it could envisioned to extract the viral mRNA after each round of selection in order to identify the mutant capsids which have been able to uncoat and express their genome, thus rendering the selection more stringent by focusing on the last step of the intracellular fate of AAV particles in the nucleus. Since the directed evolution procedure is performed using wt (carrying only the mutations in the cap gene) and not recombinant AAV genomes, this would imply to be able to detect the longer mRNA produced from the AAV p5 promoter. In theory, a helper virus such as AdV is required to express the wt AAV genes. However, we and others have noticed that a transient low level of expression of the *rep* gene can be detected at early times after transduction of cells with wt AAV (data not shown). Therefore, a more stringent selection of new candidates should be feasible using selective amplification procedures able to detect the low level of AAV mRNA. In addition, this selection procedure which was based on the Li-Ang Zhang PhD work, demonstrated the feasibility to monitor the procedure by NGS. Thus, further improved selections methods could be developed by sequencing the AAV variants obtained at each step, and not only at the end of the procedure, and by comparing different conditions such as, DC infected in the presence of LPS or immature DC or DC versus other cell types. This would notably allow to select variants specific of the state of DC or of any other cell type. An additional selection layer could consist in comparing the variants found in the nucleus to those found in endosomes, to exclude those retained in the vesicular system. Other more powerful comparative selections could also be performed by using a library of AAV in which the mutations can target the whole cap gene and not only a specific position in VP3.

Finally, it would be important for future selections to couple the biological analyses with physical measures. Our collaboration with the laboratory of C. Moskalenko allowed us to better understand the physical properties of AAV capsids. In particular, this study highlighted the different behavior of AAV8 and AAV9 in terms of thermal stability (**Figure 40**, **Figure 42**). This parameter likely correlates with the physical properties of the capsids. Indeed, some

ongoing indentation experiments by AFM, which measure capsid stability, do indicate that AAV9 is more resistant than AAV8 to an external pressure (data not shown). Interestingly, some studies have indicated that AAV9 has a higher stability than AAV8 when delivered intravenously [236]. These data strongly suggest a correlation between the physical properties of the capsids, measured *in vitro*, with their biological properties. It will be interesting in the future to establish how these physical features such (*e.g.* capsid stiffness) can correlates with the maturation and/or the uncoating capacity of the capsid, in the target cells (**Figure *43***). In collaboration with C. Moskalenko we have undertaken the study of the physical properties of the VSSTSPR mutant, in comparison with AAV2. Unfortunately, so far, the visualization of AAV2 and derived capsids by AFM has been hampered by problems linked with aggregation of the particles once deposited on the mica surface.

IV.4 Going beyond…

Besides showing individual differences, our *in vitro* analysis of AAV capsids revealed a common property, shared by at least AAV2, 8, 9, and VSSTSPR: the thermal stability of AAV capsids increases in an acid environment. This property, which was also demonstrated by others for AAV2 [67], could have been selected to protect the viral genome from a premature release within the endosomes, in particular to avoid recognition by the innate immunity sensors. Alternatively and not exclusively, this property may allow to the capsid to persist in the cytoplasm until the cell is co-infected with a helper virus. Viral helper activities were largely documented for the nuclear steps of the AAV life-cycle. Indeed, many helper viruses (*e.g.* AdV, HSV, *etc.*) were described to participate in AAV replication. However, different studies also indicated that AdV is able to help the AAV to escape from the endosomal system and to enter the nucleus [109]. Therefore, we can postulate that AAV has co-evolved with AdV to persist in the endosomal system or outside in the cytosol waiting for AdV to infect the cell. This would lead to consider the cytosol and/or the endosomal system as another main retention site of AAV particles, similar to that described in the case of the nucleolus. These speculations suggest that the optimization of the efficiency of the AAV vectors may also requires a better knowledge of influence of the helper virus on the early phases of AAV life-cycle.

V. Popularization project on gene therapy using viral vectors

V.1 Project description

V.1.1 Project and members

The aim of the project is to popularize gene therapy using viral vectors. It arose after a meeting with Rémy Mattei a comic illustrator, publisher, and creator of "Le collectif mauvaise foi" – a working group of artists, illustrators, and printers recently rewarded at the famous comic festival in Angouleme, for an alternative comic project produced with more than 20 independent illustrators. Our project is to create a comic allowing the readers to explore a metaphoric world and learn more about several biological and molecular concepts. In this project we aim to provide an entertaining scenario, and we are focused on the truthfulness of the biological concepts.

V.1.2 A useful and challenging project

Explaining gene therapy using viral vectors requires to be able to transmit several biological concepts. A better knowledge of these scientific notions by lay persons, in particular the patients and their relatives, would allow to better communicate about new therapies and new technologies, which – when not understood – are causing fears and fantasies. It is therefore useful to explain these biological concepts. The first barriers to understand these concepts is the specialized vocabulary. To overcome this language barrier, the project aims to explain various biological concepts using metaphors illustrated by drawings and with only few words.

V.1.3 Concepts of biology

The project aims to explain various biological concepts to understand the broad field of gene therapy using viral vectors. We plan to have two chapters, the first one talking about the viral infection in order to explain how a cell works in our body and how it reacts against viruses. The second one, dealing with inherited diseases, gene mutations and how to restore a function with viral vectors. The format of the project allows to illustrate several biological and

molecular concepts such as DNA transcription into RNA, RNA translation into proteins, protein transport, protein functions, protein degradation, protein recycling, DNA mutation, protein function, and so on.

V.1.4 Method

The metaphor is useful to answer difficult questions, indeed it provides guidance with visual insights and helps to understand new concepts. In this project, the comic shows the cell as a big city with several citizens, trains, neighborhoods, and buildings. The main building is the nucleus, inside various citizens (the proteins) read, organize and repair several books in a big library. This library is the DNA, containing the genetic information. With this metaphor it is easier to explain, for example, the synthesis of RNA from DNA: some of these citizens write small letters copied from books and post them to another neighborhood. The first chapter is focused on viral infection: during their travel, the virions have to cross the whole organism and overcome several barriers using cell machinery. The illustration of the travel of the virions in the organism can be helpful to progressively describe various biological concepts. At the end of the first chapter the lectors have to understand the interplay between a virus and a cell during a natural infection. In the second chapter, using the same metaphor we will illustrate the interaction between a viral vector and a diseased cell. For the cell, we have focused on an inherited disease. The genetic mutation is illustrated by a mistake in the book inducing the production of a nonfunctional protein, with several consequences on the organism. For the virus, we will describe the artificial modification of a virus into a vector and its implications for gene therapy.

V.1.5 Format

The project is a comic of 100 pages. To focus the lector on the mechanisms and overcome the language barrier, biological concepts are illustrated with colored pictures without any words. It is crucial that the comic has an educative interest. Therefore, the biological context will be clearly presented to the readers at the beginning by a small written introduction. In addition, some really important elements are introduced with some text that explain the illustrated images. For example, the part VI.3 contain 3 pages from the comic explaining the

cell/virus attachment step. The virus and the cell have been introduced. On the scene, several individuals land on the cell surface, the floor is unstable, they use the cables on the surface to avoid to fall (**Figure 48**). However some of them are blocked, and sequestered by the cables (**Figure 49**). Interestingly, lot of locks are present on the cell and the characters use their keys in order to go inside. One individual cannot enter into the cell because the key is misfolded (**Figure 50**).

V.1.6 Target lectors

We can divide targets in two classes, the first is composed of non-scientific persons who are curious and interested in biology. It represents a wide variety of persons of various ages. Therefore, we will adapt the pictures and make them as clear as possible, and we will focus on the scenario. The second class, is composed of members of the scientific community (students, teachers, experts, physicians…) requiring efficient tools to explain various biological concepts on a number of occasions. Indeed, we will focus our attention on the truth of the provided biological knowledge, and we will make sure that the comic can be used as an efficient educative support.

V.2 Resources

V.2.1 Estimated budget

Total budget:	**30 000€**
Graphic production: 100 original pages	20 000€
Editing and publishing: for 500 copies	6 000€
Communication: educating events, publicity	4 000€

V.2.2 Collaborators

To complete the project we are helped by many collaborators who have very interesting abilities and interests intricately linked to the project:

Names	Contacts	Activity
Mauvaise foi	rem.matteil@gmail.com	Illustration, Editing, Publishing
CIRI	axel.rossi@ens-lyon.fr	Research on infectious diseases
CRCL	anna.salvetti@inserm.fr	Research in oncology
CIRI'PAMP	vincent.grass@ens-lyon.fr	Scientific, educating, social events
LudoViro	ludoviro.new@gmail.com	Scientific popularization

V.2.3 Financial support (prospection in progress)

After a selective procedure, the "Rhône-Alpes" region has decided to support this project and offered a 5000€ grant. This money allowed us to start working on the production of approximately 25 pages. To obtain more financial supports several negotiations with scientific societies, companies and university have been initiated. We also plan to create a crowd funding project.

V.3 Extract of the comic



Figure 48. Illustration of the binding step (p1).
Virions approach the target cell, the surface is unstable and virions face the risk of falling off.

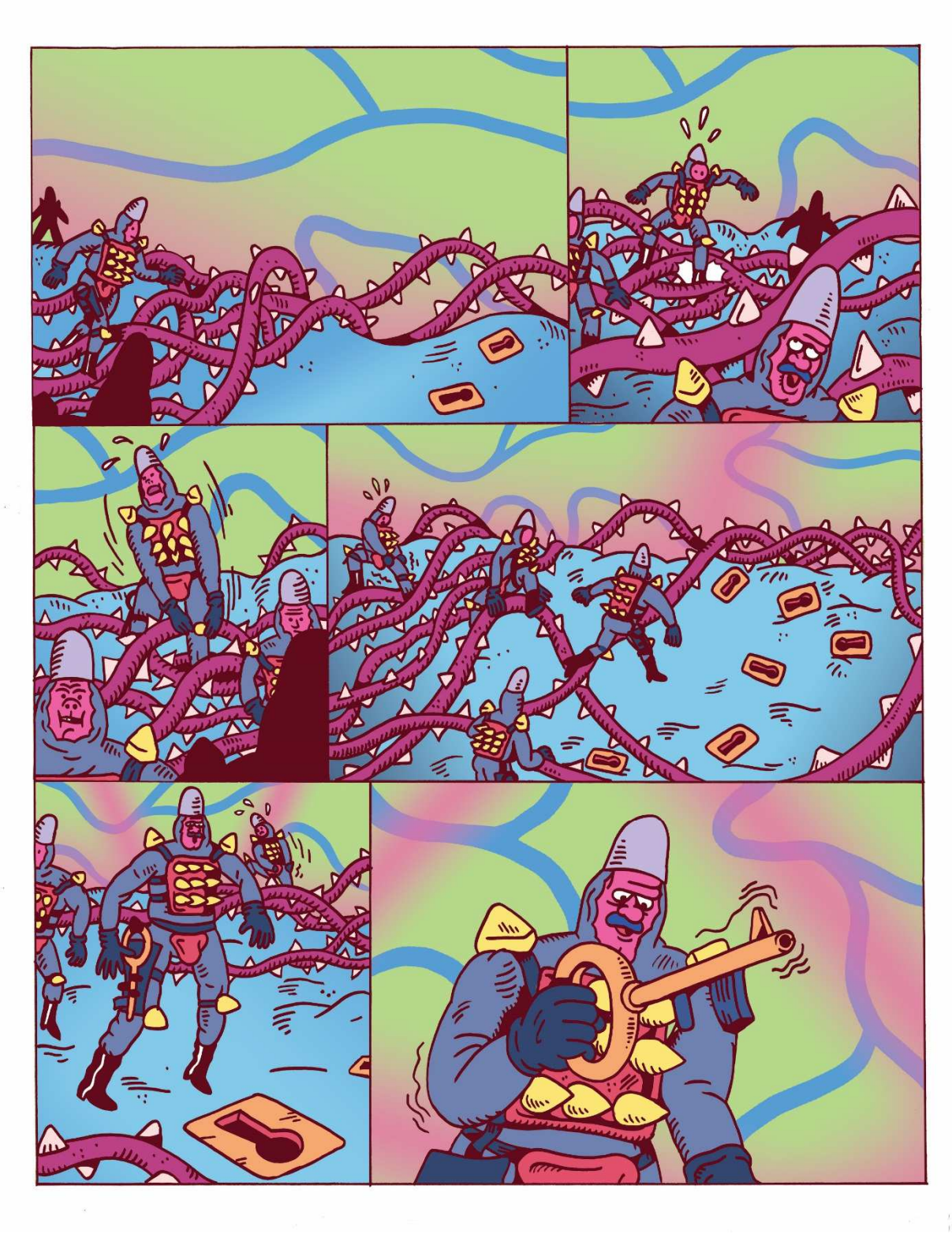


Figure 49. Illustration of the binding step (p2).
Virions scan the cell surface to find the lock that enables for entry. Some particles never find the correct pathway and remain sequestered at the surface. Infectious virions have the key to go inside.



Figure 50. Illustration of the binding step (p3).
The activation of the lock with the key triggers the entry of virions. One of them has a damaged key and is therefore unable to activate the entry mechanism.

VI. References

[1] N. Muzyczka and K. I. Berns, “AAV’s Golden Jubilee,” *Mol. Ther.*, vol. 23, no. 5, pp. 807–808, May 2015.

[2] E. Hastie and R. J. Samulski, “Adeno-Associated Virus at 50: A Golden Anniversary of Discovery, Research, and Gene Therapy Success—A Personal Perspective,” *Hum. Gene Ther.*, vol. 26, no. 5, pp. 257–265, May 2015.

[3] H. Büning, “Gene therapy enters the pharma market: The short story of a long journey: Gene therapy enters market,” *EMBO Mol. Med.*, vol. 5, no. 1, pp. 1–3, Jan. 2013.

[4] N. Miller, “Glybera and the future of gene therapy in the European Union,” *Nat. Rev. Drug Discov.*, vol. 11, no. 5, p. 419, May 2012.

[5] S. Ylä-Herttuala, “Endgame: Glybera Finally Recommended for Approval as the First Gene Therapy Drug in the European Union,” *Mol. Ther.*, vol. 20, no. 10, pp. 1831–1832, Oct. 2012.

[6] K. E. Brown, “The expanding range of parvoviruses which infect humans,” *Rev. Med. Virol.*, vol. 20, no. 4, pp. 231–244, May 2010.

[7] R. W. Atchison, B. C. Casto, and W. M. Hammon, “Adenovirus-Associated Defective Virus Particles,” *Science*, vol. 149, no. 3685, pp. 754–755, Aug. 1965.

[8] M. D. Hoggan, N. R. Blacklow, and W. P. Rowe, “Studies of small DNA viruses found in various adenovirus preparations: physical, biological, and immunological characteristics,” *Proc. Natl. Acad. Sci. U. S. A.*, vol. 55, no. 6, pp. 1467–1474, Jun. 1966.

[9] J. L. Melnick, H. D. Mayor, K. O. Smith, and F. Rapp, “Association of 20-Millimicron Particles with Adenoviruses,” *J. Bacteriol.*, vol. 90, no. 1, pp. 271–274, Jul. 1965.

[10] R. M. Buller, J. E. Janik, E. D. Sebring, and J. A. Rose, “Herpes simplex virus types 1 and 2 completely help adenovirus-associated virus replication,” *J. Virol.*, vol. 40, no. 1, pp. 241–247, Oct. 1981.

[11] B. J. Thomson, F. W. Weindler, D. Gray, V. Schwaab, and R. Heilbronn, “Human herpesvirus 6 (HHV-6) is a helper virus for adeno-associated virus type 2 (AAV-2) and the AAV-2 rep gene homologue in HHV-6 can mediate AAV-2 DNA replication and regulate gene expression,” *Virology*, vol. 204, no. 1, pp. 304–311, Oct. 1994.

[12] J. R. Schlehofer, M. Ehrbar, and H. zur Hausen, “Vaccinia virus, herpes simplex virus, and carcinogens induce DNA amplification in a human cell line and support replication of a helpervirus dependent parvovirus,” *Virology*, vol. 152, no. 1, pp. 110–117, Jul. 1986.

[13] C. Walz, A. Deprez, T. Dupressoir, M. Dürst, M. Rabreau, and J. R. Schlehofer, “Interaction of human papillomavirus type 16 and adeno-associated virus type 2 co-infecting human cervical epithelium,” *J. Gen. Virol.*, vol. 78 (Pt 6), pp. 1441–1452, Jun. 1997.

[14] R. Calcedo, L. H. Vandenberghe, G. Gao, J. Lin, and J. M. Wilson, “Worldwide Epidemiology of Neutralizing Antibodies to Adeno-Associated Viruses,” *J. Infect. Dis.*, vol. 199, no. 3, pp. 381–390, Feb. 2009.

[15] C. L. Halbert, A. D. Miller, S. Mcnamara, J. Emerson, R. L. Gibson, B. Ramsey, and M. L. Aitken, “Prevalence of Neutralizing Antibodies Against Adeno-Associated Virus (AAV) Types 2, 5, and 6 in Cystic Fibrosis and Normal Populations: Implications for Gene Therapy Using AAV Vectors,” *Hum. Gene Ther.*, vol. 17, no. 4, pp. 440–447, Apr. 2006.

[16] T. R. Flotte and B. J. Carter, “Adeno-associated virus vectors for gene therapy,” *Gene Ther.*, vol. 2, no. 6, pp. 357–362, Aug. 1995.

[17] R. J. Chandler, M. C. LaFave, G. K. Varshney, N. S. Trivedi, N. Carrillo-Carrasco, J. S. Senac, W. Wu, V. Hoffmann, A. G. Elkahloun, S. M. Burgess, and C. P. Venditti, “Vector design influences hepatic genotoxicity after adeno-associated virus gene therapy,” *J. Clin. Invest.*, vol. 125, no. 2, pp. 870–880, Feb. 2015.

[18] D. Grimm, A. Kern, K. Rittner, and J. A. Kleinschmidt, “Novel Tools for Production and Purification of Recombinant Adenoassociated Virus Vectors,” *Hum. Gene Ther.*, vol. 9, no. 18, pp. 2745–2760, Dec. 1998.
[19] G. Gao, L. H. Vandenberghe, M. R. Alvira, Y. Lu, R. Calcedo, X. Zhou, and J. M. Wilson, “Clades of Adeno-Associated Viruses Are Widely Disseminated in Human Tissues,” *J. Virol.*, vol. 78, no. 12, pp. 6381–6388, Jun. 2004.
[20] Z. Wu, A. Asokan, and R. Samulski, “Adeno-associated Virus Serotypes: Vector Toolkit for Human Gene Therapy,” *Mol. Ther.*, vol. 14, no. 3, pp. 316–327, Sep. 2006.
[21] S. Daya and K. I. Berns, “Gene Therapy Using Adeno-Associated Virus Vectors,” *Clin. Microbiol. Rev.*, vol. 21, no. 4, pp. 583–593, Oct. 2008.
[22] L. Lisowski, S. S. Tay, and I. E. Alexander, “Adeno-associated virus serotypes for gene therapeutics,” *Curr. Opin. Pharmacol.*, vol. 24, pp. 59–67, Oct. 2015.
[23] M. Nonnenmacher and T. Weber, “Intracellular transport of recombinant adeno-associated virus vectors,” *Gene Ther.*, vol. 19, no. 6, pp. 649–658, Jun. 2012.
[24] S. Pillay, N. L. Meyer, A. S. Puschnik, O. Davulcu, J. Diep, Y. Ishikawa, L. T. Jae, J. E. Wosen, C. M. Nagamine, M. S. Chapman, and J. E. Carette, “An essential receptor for adeno-associated virus infection,” *Nature*, vol. 530, no. 7588, pp. 108–112, Jan. 2016.
[25] H. Azuma, N. Paulk, A. Ranade, C. Dorrell, M. Al-Dhalimy, E. Ellis, S. Strom, M. A. Kay, M. Finegold, and M. Grompe, “Robust expansion of human hepatocytes in Fah-/-/Rag2-/-/Il2rg-/- mice,” *Nat. Biotechnol.*, vol. 25, no. 8, pp. 903–910, Aug. 2007.
[26] K. Jakab, C. Norotte, F. Marga, K. Murphy, G. Vunjak-Novakovic, and G. Forgacs, “Tissue engineering by self-assembly and bio-printing of living cells,” *Biofabrication*, vol. 2, no. 2, p. 022001, Jun. 2010.
[27] E. Masat, G. Pavani, and F. Mingozzi, “Humoral immunity to AAV vectors in gene therapy: challenges and potential solutions,” *Discov. Med.*, vol. 15, no. 85, pp. 379–389, Jun. 2013.
[28] R. Calcedo and J. M. Wilson, “Humoral Immune Response to AAV,” *Front. Immunol.*, vol. 4, 2013.
[29] L. V. Tse, S. Moller-Tank, and A. Asokan, “Strategies to circumvent humoral immunity to adeno-associated viral vectors,” *Expert Opin. Biol. Ther.*, vol. 15, no. 6, pp. 845–855, Jun. 2015.
[30] D. S. Im and N. Muzyczka, “The AAV origin binding protein Rep68 is an ATP-dependent site-specific endonuclease with DNA helicase activity,” *Cell*, vol. 61, no. 3, pp. 447–457, May 1990.
[31] D. M. McCarty, D. J. Pereira, I. Zolotukhin, X. Zhou, J. H. Ryan, and N. Muzyczka, “Identification of linear DNA sequences that specifically bind the adeno-associated virus Rep protein,” *J. Virol.*, vol. 68, no. 8, pp. 4988–4997, Aug. 1994.
[32] R. O. Snyder, D. S. Im, T. Ni, X. Xiao, R. J. Samulski, and N. Muzyczka, “Features of the adeno-associated virus origin involved in substrate recognition by the viral Rep protein,” *J. Virol.*, vol. 67, no. 10, pp. 6096–6104, Oct. 1993.
[33] R. O. Snyder, R. J. Samulski, and N. Muzyczka, “In vitro resolution of covalently joined AAV chromosome ends,” *Cell*, vol. 60, no. 1, pp. 105–113, Jan. 1990.
[34] R. J. Samulski, L. S. Chang, and T. Shenk, “A recombinant plasmid from which an infectious adeno-associated virus genome can be excised in vitro and its use to study viral replication,” *J. Virol.*, vol. 61, no. 10, pp. 3096–3101, Oct. 1987.
[35] S. K. McLaughlin, P. Collis, P. L. Hermonat, and N. Muzyczka, “Adeno-associated virus general transduction vectors: analysis of proviral structures,” *J. Virol.*, vol. 62, no. 6, pp. 1963–1973, Jun. 1988.
[36] M. A. Labow and K. I. Berns, “The adeno-associated virus rep gene inhibits replication of an adeno-associated virus/simian virus 40 hybrid genome in cos-7 cells,” *J. Virol.*, vol. 62, no. 5, pp. 1705–1712, May 1988.
[37] N. Chejanovsky and B. J. Carter, “Replication of a human parvovirus nonsense mutant in mammalian cells containing an inducible amber suppressor,” *Virology*, vol. 171, no. 1, pp. 239–247, Jul. 1989.

[38] R. Dubielzig, J. A. King, S. Weger, A. Kern, and J. A. Kleinschmidt, “Adeno-associated virus type 2 protein interactions: formation of pre-encapsidation complexes,” *J. Virol.*, vol. 73, no. 11, pp. 8989–8998, Nov. 1999.

[39] J. A. King, “DNA helicase-mediated packaging of adeno-associated virus type 2 genomes into preformed capsids,” *EMBO J.*, vol. 20, no. 12, pp. 3282–3291, Jun. 2001.

[40] D. E. Smith, S. J. Tans, S. B. Smith, S. Grimes, D. L. Anderson, and C. Bustamante, “The bacteriophage straight phi29 portal motor can package DNA against a large internal force,” *Nature*, vol. 413, no. 6857, pp. 748–752, Oct. 2001.

[41] F. Sonntag, K. Schmidt, and J. A. Kleinschmidt, “A viral assembly factor promotes AAV2 capsid formation in the nucleolus,” *Proc. Natl. Acad. Sci.*, vol. 107, no. 22, pp. 10220–10225, Jun. 2010.

[42] F. Sonntag, K. Kother, K. Schmidt, M. Weghofer, C. Raupp, K. Nieto, A. Kuck, B. Gerlach, B. Bottcher, O. J. Muller, K. Lux, M. Horer, and J. A. Kleinschmidt, “The Assembly-Activating Protein Promotes Capsid Assembly of Different Adeno-Associated Virus Serotypes,” *J. Virol.*, vol. 85, no. 23, pp. 12686–12697, Dec. 2011.

[43] S. P. Becerra, J. A. Rose, M. Hardy, B. M. Baroudy, and C. W. Anderson, “Direct mapping of adeno-associated virus capsid proteins B and C: a possible ACG initiation codon,” *Proc. Natl. Acad. Sci. U. S. A.*, vol. 82, no. 23, pp. 7919–7923, Dec. 1985.

[44] S. P. Becerra, F. Koczot, P. Fabisch, and J. A. Rose, “Synthesis of adeno-associated virus structural proteins requires both alternative mRNA splicing and alternative initiations from a single transcript,” *J. Virol.*, vol. 62, no. 8, pp. 2745–2754, Aug. 1988.

[45] J. A. Kleinschmidt, M. Ried, A. Girod, K. Leike, C. E. Wobus, M. Hallek, P. Tijssen, and Z. Zádori, “The VP1 capsid protein of adeno-associated virus type 2 is carrying a phospholipase A2 domain required for virus infectivity,” *J. Gen. Virol.*, vol. 83, no. 5, pp. 973–978, May 2002.

[46] S. Bleker, F. Sonntag, and J. A. Kleinschmidt, “Mutational Analysis of Narrow Pores at the Fivefold Symmetry Axes of Adeno-Associated Virus Type 2 Capsids Reveals a Dual Role in Genome Packaging and Activation of Phospholipase A2 Activity,” *J. Virol.*, vol. 79, no. 4, pp. 2528–2540, Feb. 2005.

[47] S. Kronenberg, B. Bottcher, C. W. von der Lieth, S. Bleker, and J. A. Kleinschmidt, “A Conformational Change in the Adeno-Associated Virus Type 2 Capsid Leads to the Exposure of Hidden VP1 N Termini,” *J. Virol.*, vol. 79, no. 9, pp. 5296–5303, May 2005.

[48] B. L. Gurda, C. Raupp, R. Popa-Wagner, M. Naumer, N. H. Olson, R. Ng, R. McKenna, T. S. Baker, J. A. Kleinschmidt, and M. Agbandje-McKenna, “Mapping a Neutralizing Epitope onto the Capsid of Adeno-Associated Virus Serotype 8,” *J. Virol.*, vol. 86, no. 15, pp. 7739–7751, Aug. 2012.

[49] M. A. DiMattia, H.-J. Nam, K. Van Vliet, M. Mitchell, A. Bennett, B. L. Gurda, R. McKenna, N. H. Olson, R. S. Sinkovits, M. Potter, B. J. Byrne, G. Aslanidi, S. Zolotukhin, N. Muzyczka, T. S. Baker, and M. Agbandje-McKenna, “Structural Insight into the Unique Properties of Adeno-Associated Virus Serotype 9,” *J. Virol.*, vol. 86, no. 12, pp. 6947–6958, Jun. 2012.

[50] B. L. Gurda, M. A. DiMattia, E. B. Miller, A. Bennett, R. McKenna, W. S. Weichert, C. D. Nelson, W. -j. Chen, N. Muzyczka, N. H. Olson, R. S. Sinkovits, J. A. Chiorini, S. Zolotutkhin, O. G. Kozyreva, R. J. Samulski, T. S. Baker, C. R. Parrish, and M. Agbandje-McKenna, “Capsid Antibodies to Different Adeno-Associated Virus Serotypes Bind Common Regions,” *J. Virol.*, vol. 87, no. 16, pp. 9111–9124, Aug. 2013.

[51] H.-J. Nam, B. L. Gurda, R. McKenna, M. Potter, B. Byrne, M. Salganik, N. Muzyczka, and M. Agbandje-McKenna, “Structural Studies of Adeno-Associated Virus Serotype 8 Capsid Transitions Associated with Endosomal Trafficking,” *J. Virol.*, vol. 85, no. 22, pp. 11791–11799, Nov. 2011.

[52] R. Ng, L. Govindasamy, B. L. Gurda, R. McKenna, O. G. Kozyreva, R. J. Samulski, K. N. Parent, T. S. Baker, and M. Agbandje-McKenna, “Structural Characterization of the Dual Glycan Binding Adeno-Associated Virus Serotype 6,” *J. Virol.*, vol. 84, no. 24, pp. 12945–12957, Dec. 2010.

[53] L. Govindasamy, E. Padron, R. McKenna, N. Muzyczka, N. Kaludov, J. A. Chiorini, and M. Agbandje-McKenna, “Structurally Mapping the Diverse Phenotype of Adeno-Associated Virus Serotype 4,” *J. Virol.*, vol. 80, no. 23, pp. 11556–11570, Dec. 2006.

[54] Q. Xie, W. Bu, S. Bhatia, J. Hare, T. Somasundaram, A. Azzi, and M. S. Chapman, “The atomic structure of adeno-associated virus (AAV-2), a vector for human gene therapy,” *Proc. Natl. Acad. Sci.*, vol. 99, no. 16, pp. 10405–10410, Aug. 2002.
[55] Y.-S. Tseng and M. Agbandje-McKenna, “Mapping the AAV Capsid Host Antibody Response toward the Development of Second Generation Gene Delivery Vectors,” *Front. Immunol.*, vol. 5, 2014.
[56] S. R. Opie, K. H. Warrington, M. Agbandje-McKenna, S. Zolotukhin, and N. Muzyczka, “Identification of Amino Acid Residues in the Capsid Proteins of Adeno-Associated Virus Type 2 That Contribute to Heparan Sulfate Proteoglycan Binding,” *J. Virol.*, vol. 77, no. 12, pp. 6995–7006, Jun. 2003.
[57] L. M. Drouin and M. Agbandje-McKenna, “Adeno-associated virus structural biology as a tool in vector development,” *Future Virol.*, vol. 8, no. 12, pp. 1183–1199, Dec. 2013.
[58] E. Zinn and L. H. Vandenberghe, “Adeno-associated virus: fit to serve,” *Curr. Opin. Virol.*, vol. 8, pp. 90–97, Oct. 2014.
[59] S. Kronenberg, J. A. Kleinschmidt, and B. Böttcher, “Electron cryo-microscopy and image reconstruction of adeno-associated virus type 2 empty capsids,” *EMBO Rep.*, vol. 2, no. 11, pp. 997–1002, Nov. 2001.
[60] W. H. Roos, R. Bruinsma, and G. J. L. Wuite, “Physical virology,” *Nat. Phys.*, vol. 6, no. 10, pp. 733–743, Oct. 2010.
[61] I. L. Ivanovska, P. J. de Pablo, B. Ibarra, G. Sgalari, F. C. MacKintosh, J. L. Carrascosa, C. F. Schmidt, and G. J. L. Wuite, “Bacteriophage capsids: Tough nanoshells with complex elastic properties,” *Proc. Natl. Acad. Sci.*, vol. 101, no. 20, pp. 7600–7605, May 2004.
[62] I. Ivanovska, G. Wuite, B. Jonsson, and A. Evilevitch, “Internal DNA pressure modifies stability of WT phage,” *Proc. Natl. Acad. Sci.*, vol. 104, no. 23, pp. 9603–9608, Jun. 2007.
[63] U. Sae-Ueng, D. Li, X. Zuo, J. B. Huffman, F. L. Homa, D. Rau, and A. Evilevitch, “Solid-to-fluid DNA transition inside HSV-1 capsid close to the temperature of infection,” *Nat. Chem. Biol.*, vol. 10, no. 10, pp. 861–867, Sep. 2014.
[64] C. Carrasco, A. Carreira, I. A. T. Schaap, P. A. Serena, J. Gomez-Herrero, M. G. Mateu, and P. J. de Pablo, “DNA-mediated anisotropic mechanical reinforcement of a virus,” *Proc. Natl. Acad. Sci.*, vol. 103, no. 37, pp. 13706–13711, Sep. 2006.
[65] C. Carrasco, M. Castellanos, P. J. de Pablo, and M. G. Mateu, “Manipulation of the mechanical properties of a virus by protein engineering,” *Proc. Natl. Acad. Sci.*, vol. 105, no. 11, pp. 4150–4155, Mar. 2008.
[66] V. Rayaprolu, S. Kruse, R. Kant, B. Venkatakrishnan, N. Movahed, D. Brooke, B. Lins, A. Bennett, T. Potter, R. McKenna, M. Agbandje-McKenna, and B. Bothner, “Comparative Analysis of Adeno-Associated Virus Capsid Stability and Dynamics,” *J. Virol.*, vol. 87, no. 24, pp. 13150–13160, Dec. 2013.
[67] E. D. Horowitz, K. S. Rahman, B. D. Bower, D. J. Dismuke, M. R. Falvo, J. D. Griffith, S. C. Harvey, and A. Asokan, “Biophysical and Ultrastructural Characterization of Adeno-Associated Virus Capsid Uncoating and Genome Release,” *J. Virol.*, vol. 87, no. 6, pp. 2994–3002, Mar. 2013.
[68] M. Salganik, F. Aydemir, H.-J. Nam, R. McKenna, M. Agbandje-McKenna, and N. Muzyczka, “Adeno-Associated Virus Capsid Proteins May Play a Role in Transcription and Second-Strand Synthesis of Recombinant Genomes,” *J. Virol.*, vol. 88, no. 2, pp. 1071–1079, Jan. 2014.
[69] J. Zhu, X. Huang, and Y. Yang, “The TLR9-MyD88 pathway is critical for adaptive immune responses to adeno-associated virus gene therapy vectors in mice,” *J. Clin. Invest.*, vol. 119, no. 8, pp. 2388–2398, Aug. 2009.
[70] G. L. Rogers, M. Suzuki, I. Zolotukhin, D. M. Markusic, L. M. Morel, B. Lee, H. C. J. Ertl, and R. W. Herzog, “Unique Roles of TLR9- and MyD88-Dependent and -Independent Pathways in Adaptive Immune Responses to AAV-Mediated Gene Transfer,” *J. Innate Immun.*, vol. 7, no. 3, pp. 302–314, Jan. 2015.

[71] E. Zinn, S. Pacouret, V. Khaychuk, H. T. Turunen, L. S. Carvalho, E. Andres-Mateos, S. Shah, R. Shelke, A. C. Maurer, E. Plovie, R. Xiao, and L. H. Vandenberghe, "In Silico Reconstruction of the Viral Evolutionary Lineage Yields a Potent Gene Therapy Vector," *Cell Rep.*, vol. 12, no. 6, pp. 1056–1068, Aug. 2015.
[72] W. Ding, L. Zhang, Z. Yan, and J. F. Engelhardt, "Intracellular trafficking of adeno-associated viral vectors," *Gene Ther.*, vol. 12, no. 11, pp. 873–880, Jun. 2005.
[73] C. Summerford and R. J. Samulski, "Membrane-associated heparan sulfate proteoglycan is a receptor for adeno-associated virus type 2 virions," *J. Virol.*, vol. 72, no. 2, pp. 1438–1445, Feb. 1998.
[74] A. Kern, K. Schmidt, C. Leder, O. J. Muller, C. E. Wobus, K. Bettinger, C. W. Von der Lieth, J. A. King, and J. A. Kleinschmidt, "Identification of a Heparin-Binding Motif on Adeno-Associated Virus Type 2 Capsids," *J. Virol.*, vol. 77, no. 20, pp. 11072–11081, Oct. 2003.
[75] K. Qing, C. Mah, J. Hansen, S. Zhou, V. Dwarki, and A. Srivastava, "Human fibroblast growth factor receptor 1 is a co-receptor for infection by adeno-associated virus 2," *Nat. Med.*, vol. 5, no. 1, pp. 71–77, Jan. 1999.
[76] C. Summerford, J. S. Bartlett, and R. J. Samulski, "AlphaVbeta5 integrin: a co-receptor for adeno-associated virus type 2 infection," *Nat. Med.*, vol. 5, no. 1, pp. 78–82, Jan. 1999.
[77] B. Akache, D. Grimm, K. Pandey, S. R. Yant, H. Xu, and M. A. Kay, "The 37/67-Kilodalton Laminin Receptor Is a Receptor for Adeno-Associated Virus Serotypes 8, 2, 3, and 9," *J. Virol.*, vol. 80, no. 19, pp. 9831–9836, Oct. 2006.
[78] Y. Kashiwakura, K. Tamayose, K. Iwabuchi, Y. Hirai, T. Shimada, K. Matsumoto, T. Nakamura, M. Watanabe, K. Oshimi, and H. Daida, "Hepatocyte Growth Factor Receptor Is a Coreceptor for Adeno-Associated Virus Type 2 Infection," *J. Virol.*, vol. 79, no. 1, pp. 609–614, Jan. 2005.
[79] G. Seisenberger, "Real-Time Single-Molecule Imaging of the Infection Pathway of an Adeno-Associated Virus," *Science*, vol. 294, no. 5548, pp. 1929–1932, Nov. 2001.
[80] H. C. Levy, V. D. Bowman, L. Govindasamy, R. McKenna, K. Nash, K. Warrington, W. Chen, N. Muzyczka, X. Yan, T. S. Baker, and M. Agbandje-McKenna, "Heparin binding induces conformational changes in Adeno-associated virus serotype 2," *J. Struct. Biol.*, vol. 165, no. 3, pp. 146–156, Mar. 2009.
[81] A. Asokan, J. B. Hamra, L. Govindasamy, M. Agbandje-McKenna, and R. J. Samulski, "Adeno-Associated Virus Type 2 Contains an Integrin 5 1 Binding Domain Essential for Viral Cell Entry," *J. Virol.*, vol. 80, no. 18, pp. 8961–8969, Sep. 2006.
[82] J. Qiu and K. E. Brown, "Integrin αVβ5 Is Not Involved in Adeno-Associated Virus Type 2 (AAV2) Infection," *Virology*, vol. 264, no. 2, pp. 436–440, Nov. 1999.
[83] D. Duan, Y. Yue, Z. Yan, J. Yang, and J. F. Engelhardt, "Endosomal processing limits gene transfer to polarized airway epithelia by adeno-associated virus," *J. Clin. Invest.*, vol. 105, no. 11, pp. 1573–1587, Jun. 2000.
[84] C.-L. Chen, R. L. Jensen, B. C. Schnepp, M. J. Connell, R. Shell, T. J. Sferra, J. S. Bartlett, K. R. Clark, and P. R. Johnson, "Molecular characterization of adeno-associated viruses infecting children," *J. Virol.*, vol. 79, no. 23, pp. 14781–14792, Dec. 2005.
[85] G. J. Doherty and H. T. McMahon, "Mechanisms of endocytosis," *Annu. Rev. Biochem.*, vol. 78, pp. 857–902, 2009.
[86] S. Mayor and R. E. Pagano, "Pathways of clathrin-independent endocytosis," *Nat. Rev. Mol. Cell Biol.*, vol. 8, no. 8, pp. 603–612, Aug. 2007.
[87] J. S. Blum, P. A. Wearsch, and P. Cresswell, "Pathways of Antigen Processing," *Annu. Rev. Immunol.*, vol. 31, no. 1, pp. 443–473, Mar. 2013.
[88] D. Duan, Q. Li, A. W. Kao, Y. Yue, J. E. Pessin, and J. F. Engelhardt, "Dynamin is required for recombinant adeno-associated virus type 2 infection," *J. Virol.*, vol. 73, no. 12, pp. 10371–10376, Dec. 1999.

[89] S. Uhrig, O. Coutelle, T. Wiehe, L. Perabo, M. Hallek, and H. Büning, “Successful target cell transduction of capsid-engineered rAAV vectors requires clathrin-dependent endocytosis,” *Gene Ther.*, vol. 19, no. 2, pp. 210–218, Feb. 2012.
[90] S. Sanlioglu, P. K. Benson, J. Yang, E. M. Atkinson, T. Reynolds, and J. F. Engelhardt, “Endocytosis and nuclear trafficking of adeno-associated virus type 2 are controlled by rac1 and phosphatidylinositol-3 kinase activation,” *J. Virol.*, vol. 74, no. 19, pp. 9184–9196, Oct. 2000.
[91] M. Nonnenmacher and T. Weber, “Adeno-associated virus 2 infection requires endocytosis through the CLIC/GEEC pathway,” *Cell Host Microbe*, vol. 10, no. 6, pp. 563–576, Dec. 2011.
[92] G. Di Pasquale, N. Kaludov, M. Agbandje-McKenna, and J. A. Chiorini, “BAAV transcytosis requires an interaction with beta-1-4 linked- glucosamine and gp96,” *PloS One*, vol. 5, no. 3, p. e9336, 2010.
[93] G. Di Pasquale and J. A. Chiorini, “AAV transcytosis through barrier epithelia and endothelium,” *Mol. Ther. J. Am. Soc. Gene Ther.*, vol. 13, no. 3, pp. 506–516, Mar. 2006.
[94] C. Zincarelli, S. Soltys, G. Rengo, and J. E. Rabinowitz, “Analysis of AAV Serotypes 1–9 Mediated Gene Expression and Tropism in Mice After Systemic Injection,” *Mol. Ther.*, vol. 16, no. 6, pp. 1073–1080, Jun. 2008.
[95] C. Zincarelli, S. Soltys, G. Rengo, W. J. Koch, and J. E. Rabinowitz, “Comparative cardiac gene delivery of adeno-associated virus serotypes 1-9 reveals that AAV6 mediates the most efficient transduction in mouse heart,” *Clin. Transl. Sci.*, vol. 3, no. 3, pp. 81–89, Jun. 2010.
[96] F. Sonntag, S. Bleker, B. Leuchs, R. Fischer, and J. A. Kleinschmidt, “Adeno-Associated Virus Type 2 Capsids with Externalized VP1/VP2 Trafficking Domains Are Generated prior to Passage through the Cytoplasm and Are Maintained until Uncoating Occurs in the Nucleus,” *J. Virol.*, vol. 80, no. 22, pp. 11040–11054, Nov. 2006.
[97] B. Akache, D. Grimm, X. Shen, S. Fuess, S. R. Yant, D. S. Glazer, J. Park, and M. A. Kay, “A Two-hybrid Screen Identifies Cathepsins B and L as Uncoating Factors for Adeno-associated Virus 2 and 8,” *Mol. Ther.*, vol. 15, no. 2, pp. 330–339, Feb. 2007.
[98] M. Zerial and H. McBride, “Rab proteins as membrane organizers,” *Nat. Rev. Mol. Cell Biol.*, vol. 2, no. 2, pp. 107–117, Feb. 2001.
[99] S. R. Pfeffer, “Rab GTPases: specifying and deciphering organelle identity and function,” *Trends Cell Biol.*, vol. 11, no. 12, pp. 487–491, Dec. 2001.
[100] W. Ding, L. Zhang, C. Yeaman, and J. Engelhardt, “rAAV2 traffics through both the late and the recycling endosomes in a dose-dependent fashion,” *Mol. Ther.*, vol. 13, no. 4, pp. 671–682, Apr. 2006.
[101] M. E. Nonnenmacher, J.-C. Cintrat, D. Gillet, and T. Weber, “Syntaxin 5-dependent retrograde transport to the trans-Golgi network is required for adeno-associated virus transduction,” *J. Virol.*, vol. 89, no. 3, pp. 1673–1687, Feb. 2015.
[102] W. Xiao, K. H. Warrington, P. Hearing, J. Hughes, and N. Muzyczka, “Adenovirus-Facilitated Nuclear Translocation of Adeno-Associated Virus Type 2,” *J. Virol.*, vol. 76, no. 22, pp. 11505–11517, Nov. 2002.
[103] P.-J. Xiao and R. J. Samulski, “Cytoplasmic Trafficking, Endosomal Escape, and Perinuclear Accumulation of Adeno-Associated Virus Type 2 Particles Are Facilitated by Microtubule Network,” *J. Virol.*, vol. 86, no. 19, pp. 10462–10473, Oct. 2012.
[104] S. Chitra, G. Nalini, and G. Rajasekhar, “The ubiquitin proteasome system and efficacy of proteasome inhibitors in diseases,” *Int. J. Rheum. Dis.*, vol. 15, no. 3, pp. 249–260, Jun. 2012.
[105] L. Zhong, B. Li, G. Jayandharan, C. S. Mah, L. Govindasamy, M. Agbandje-McKenna, R. W. Herzog, K. A. Weigel-Van Aken, J. A. Hobbs, S. Zolotukhin, N. Muzyczka, and A. Srivastava, “Tyrosine-phosphorylation of AAV2 vectors and its consequences on viral intracellular trafficking and transgene expression,” *Virology*, vol. 381, no. 2, pp. 194–202, Nov. 2008.
[106] J. Qiu and K. E. Brown, “A 110-kDa nuclear shuttle protein, nucleolin, specifically binds to adeno-associated virus type 2 (AAV-2) capsid,” *Virology*, vol. 257, no. 2, pp. 373–382, May 1999.

[107] J. S. Johnson, C. Li, N. DiPrimio, M. S. Weinberg, T. J. McCown, and R. J. Samulski, “Mutagenesis of Adeno-Associated Virus Type 2 Capsid Protein VP1 Uncovers New Roles for Basic Amino Acids in Trafficking and Cell-Specific Transduction,” *J. Virol.*, vol. 84, no. 17, pp. 8888–8902, Sep. 2010.
[108] Z. Yan, R. Zak, G. W. G. Luxton, T. C. Ritchie, U. Bantel-Schaal, and J. F. Engelhardt, “Ubiquitination of both Adeno-Associated Virus Type 2 and 5 Capsid Proteins Affects the Transduction Efficiency of Recombinant Vectors,” *J. Virol.*, vol. 76, no. 5, pp. 2043–2053, Mar. 2002.
[109] S. Stahnke, K. Lux, S. Uhrig, F. Kreppel, M. Hösel, O. Coutelle, M. Ogris, M. Hallek, and H. Büning, “Intrinsic phospholipase A2 activity of adeno-associated virus is involved in endosomal escape of incoming particles,” *Virology*, vol. 409, no. 1, pp. 77–83, Jan. 2011.
[110] J. S. Bartlett, R. Wilcher, and R. J. Samulski, “Infectious Entry Pathway of Adeno-Associated Virus and Adeno-Associated Virus Vectors,” *J. Virol.*, vol. 74, no. 6, pp. 2777–2785, Mar. 2000.
[111] K. Lux, N. Goerlitz, S. Schlemminger, L. Perabo, D. Goldnau, J. Endell, K. Leike, D. M. Kofler, S. Finke, M. Hallek, and H. Buning, “Green Fluorescent Protein-Tagged Adeno-Associated Virus Particles Allow the Study of Cytosolic and Nuclear Trafficking,” *J. Virol.*, vol. 79, no. 18, pp. 11776–11787, Sep. 2005.
[112] J. C. Grieger, S. Snowdy, and R. J. Samulski, “Separate Basic Region Motifs within the Adeno-Associated Virus Capsid Proteins Are Essential for Infectivity and Assembly,” *J. Virol.*, vol. 80, no. 11, pp. 5199–5210, Jun. 2006.
[113] S. C. Nicolson and R. J. Samulski, “Recombinant adeno-associated virus utilizes host cell nuclear import machinery to enter the nucleus,” *J. Virol.*, vol. 88, no. 8, pp. 4132–4144, Apr. 2014.
[114] J. M. Kelich, J. Ma, B. Dong, Q. Wang, M. Chin, C. M. Magura, W. Xiao, and W. Yang, “Super-resolution imaging of nuclear import of adeno-associated virus in live cells,” *Mol. Ther. Methods Clin. Dev.*, vol. 2, p. 15047, 2015.
[115] S. Cohen, A. K. Marr, P. Garcin, and N. Panté, “Nuclear envelope disruption involving host caspases plays a role in the parvovirus replication cycle,” *J. Virol.*, vol. 85, no. 10, pp. 4863–4874, May 2011.
[116] M. Porwal, S. Cohen, K. Snoussi, R. Popa-Wagner, F. Anderson, N. Dugot-Senant, H. Wodrich, C. Dinsart, Jã¼. A. Kleinschmidt, N. PantÃ©, and M. Kann, “Parvoviruses Cause Nuclear Envelope Breakdown by Activating Key Enzymes of Mitosis,” *PLoS Pathog.*, vol. 9, no. 10, p. e1003671, Oct. 2013.
[117] J. Hansen, “Infection of Purified Nuclei by Adeno-associated Virus 2,” *Mol. Ther.*, vol. 4, no. 4, pp. 289–296, Oct. 2001.
[118] C. E. Thomas, T. A. Storm, Z. Huang, and M. A. Kay, “Rapid uncoating of vector genomes is the key to efficient liver transduction with pseudotyped adeno-associated virus vectors,” *J. Virol.*, vol. 78, no. 6, pp. 3110–3122, Mar. 2004.
[119] I. Sipo, H. Fechner, S. Pinkert, L. Suckau, X. Wang, S. Weger, and W. Poller, “Differential internalization and nuclear uncoating of self-complementary adeno-associated virus pseudotype vectors as determinants of cardiac cell transduction,” *Gene Ther.*, Jul. 2007.
[120] J. S. Johnson and R. J. Samulski, “Enhancement of Adeno-Associated Virus Infection by Mobilizing Capsids into and Out of the Nucleolus,” *J. Virol.*, vol. 83, no. 6, pp. 2632–2644, Mar. 2009.
[121] J. M. Bevington, P. G. Needham, K. C. Verrill, R. F. Collaco, V. Basrur, and J. P. Trempe, “Adeno-associated virus interactions with B23/Nucleophosmin: identification of sub-nucleolar virion regions,” *Virology*, vol. 357, no. 1, pp. 102–113, Jan. 2007.
[122] T. R. Flotte and K. I. Berns, “Adeno-Associated Virus: A Ubiquitous Commensal of Mammals,” *Hum. Gene Ther.*, vol. 16, no. 4, pp. 401–407, Apr. 2005.
[123] R. M. Kotin, “Prospects for the use of adeno-associated virus as a vector for human gene therapy,” *Hum. Gene Ther.*, vol. 5, no. 7, pp. 793–801, Jul. 1994.
[124] F. K. Ferrari, T. Samulski, T. Shenk, and R. J. Samulski, “Second-strand synthesis is a rate-limiting step for efficient transduction by recombinant adeno-associated virus vectors,” *J. Virol.*, vol. 70, no. 5, pp. 3227–3234, May 1996.

[125] C. R. Parrish, “Structures and functions of parvovirus capsids and the process of cell infection,” *Curr. Top. Microbiol. Immunol.*, vol. 343, pp. 149–176, 2010.
[126] R. J. Samulski, X. Zhu, X. Xiao, J. D. Brook, D. E. Housman, N. Epstein, and L. A. Hunter, “Targeted integration of adeno-associated virus (AAV) into human chromosome 19,” *EMBO J.*, vol. 10, no. 12, pp. 3941–3950, Dec. 1991.
[127] C. C. Yang, X. Xiao, X. Zhu, D. C. Ansardi, N. D. Epstein, M. R. Frey, A. G. Matera, and R. J. Samulski, “Cellular recombination pathways and viral terminal repeat hairpin structures are sufficient for adeno-associated virus integration in vivo and in vitro,” *J. Virol.*, vol. 71, no. 12, pp. 9231–9247, Dec. 1997.
[128] B. R. Schultz and J. S. Chamberlain, “Recombinant Adeno-associated Virus Transduction and Integration,” *Mol. Ther.*, vol. 16, no. 7, pp. 1189–1199, Jul. 2008.
[129] J. R. Brister and N. Muzyczka, “Mechanism of Rep-mediated adeno-associated virus origin nicking,” *J. Virol.*, vol. 74, no. 17, pp. 7762–7771, Sep. 2000.
[130] B. E. Redemann, E. Mendelson, and B. J. Carter, “Adeno-associated virus rep protein synthesis during productive infection,” *J. Virol.*, vol. 63, no. 2, pp. 873–882, Feb. 1989.
[131] M. A. Labow, L. H. Graf, and K. I. Berns, “Adeno-associated virus gene expression inhibits cellular transformation by heterologous genes,” *Mol. Cell. Biol.*, vol. 7, no. 4, pp. 1320–1325, Apr. 1987.
[132] M.-C. Geoffroy and A. Salvetti, “Helper functions required for wild type and recombinant adeno-associated virus growth,” *Curr. Gene Ther.*, vol. 5, no. 3, pp. 265–271, Jun. 2005.
[133] J. Timpe, J. Bevington, J. Casper, J. D. Dignam, and J. P. Trempe, “Mechanisms of adeno-associated virus genome encapsidation,” *Curr. Gene Ther.*, vol. 5, no. 3, pp. 273–284, Jun. 2005.
[134] N. Muzyczka and K. H. Warrington, “Custom Adeno-Associated Virus Capsids: The Next Generation of Recombinant Vectors with Novel Tropism,” *Hum. Gene Ther.*, vol. 16, no. 4, pp. 408–416, Apr. 2005.
[135] C. J. Buchholz, T. Friedel, and H. Büning, “Surface-Engineered Viral Vectors for Selective and Cell Type-Specific Gene Delivery,” *Trends Biotechnol.*, vol. 33, no. 12, pp. 777–790, Dec. 2015.
[136] T. Wirth, N. Parker, and S. Ylä-Herttuala, “History of gene therapy,” *Gene*, vol. 525, no. 2, pp. 162–169, Aug. 2013.
[137] L. Roberts, “Human gene transfer test approved,” *Science*, vol. 243, no. 4890, p. 473, Jan. 1989.
[138] S. A. Rosenberg, P. Aebersold, K. Cornetta, A. Kasid, R. A. Morgan, R. Moen, E. M. Karson, M. T. Lotze, J. C. Yang, S. L. Topalian, M. J. Merino, K. Culver, A. D. Miller, R. M. Blaese, and W. F. Anderson, “Gene Transfer into Humans — Immunotherapy of Patients with Advanced Melanoma, Using Tumor-Infiltrating Lymphocytes Modified by Retroviral Gene Transduction,” *N. Engl. J. Med.*, vol. 323, no. 9, pp. 570–578, Aug. 1990.
[139] R. M. Blaese, K. W. Culver, A. D. Miller, C. S. Carter, T. Fleisher, M. Clerici, G. Shearer, L. Chang, Y. Chiang, P. Tolstoshev, J. J. Greenblatt, S. A. Rosenberg, H. Klein, M. Berger, C. A. Mullen, W. J. Ramsey, L. Muul, R. A. Morgan, and W. F. Anderson, “T lymphocyte-directed gene therapy for ADA- SCID: initial trial results after 4 years,” *Science*, vol. 270, no. 5235, pp. 475–480, Oct. 1995.
[140] C. Y. Kuo and D. B. Kohn, “Gene Therapy for the Treatment of Primary Immune Deficiencies,” *Curr. Allergy Asthma Rep.*, vol. 16, no. 5, May 2016.
[141] E. L. Scheller and P. H. Krebsbach, “Gene Therapy: Design and Prospects for Craniofacial Regeneration,” *J. Dent. Res.*, vol. 88, no. 7, pp. 585–596, Jul. 2009.
[142] C. Mueller and T. R. Flotte, “Clinical gene therapy using recombinant adeno-associated virus vectors,” *Gene Ther.*, vol. 15, no. 11, pp. 858–863, Jun. 2008.
[143] M. L. Hirsch, M. Salganik, and R. J. Samulski, “Adeno-associated Virus as a Mammalian DNA Vector,” *Microbiol. Spectr.*, vol. 3, no. 4, Aug. 2015.
[144] F. Mingozzi, X. M. Anguela, G. Pavani, Y. Chen, R. J. Davidson, D. J. Hui, M. Yazicioglu, L. Elkouby, C. J. Hinderer, A. Faella, C. Howard, A. Tai, G. M. Podsakoff, S. Zhou, E. Basner-Tschakarjan, J. F. Wright, and K. A. High, “Overcoming Preexisting Humoral Immunity to AAV Using Capsid Decoys,” *Sci. Transl. Med.*, vol. 5, no. 194, pp. 194ra92–194ra92, Jul. 2013.

[145] A. C. Nathwani, E. G. D. Tuddenham, S. Rangarajan, C. Rosales, J. McIntosh, D. C. Linch, P. Chowdary, A. Riddell, A. J. Pie, C. Harrington, J. O'Beirne, K. Smith, J. Pasi, B. Glader, P. Rustagi, C. Y. C. Ng, M. A. Kay, J. Zhou, Y. Spence, C. L. Morton, J. Allay, J. Coleman, S. Sleep, J. M. Cunningham, D. Srivastava, E. Basner-Tschakarjan, F. Mingozzi, K. A. High, J. T. Gray, U. M. Reiss, A. W. Nienhuis, and A. M. Davidoff, "Adenovirus-Associated Virus Vector–Mediated Gene Transfer in Hemophilia B," *N. Engl. J. Med.*, vol. 365, no. 25, pp. 2357–2365, Dec. 2011.

[146] A. Ploquin, J. Szecsi, C. Mathieu, V. Guillaume, V. Barateau, K. C. Ong, K. T. Wong, F.-L. Cosset, B. Horvat, and A. Salvetti, "Protection Against Henipavirus Infection by Use of Recombinant Adeno-Associated Virus-Vector Vaccines," *J. Infect. Dis.*, vol. 207, no. 3, pp. 469–478, Feb. 2013.

[147] K. Nieto and A. Salvetti, "AAV Vectors Vaccines Against Infectious Diseases," *Front. Immunol.*, vol. 5, 2014.

[148] W. C. Manning, X. Paliard, S. Zhou, M. Pat Bland, A. Y. Lee, K. Hong, C. M. Walker, J. A. Escobedo, and V. Dwarki, "Genetic immunization with adeno-associated virus vectors expressing herpes simplex virus type 2 glycoproteins B and D," *J. Virol.*, vol. 71, no. 10, pp. 7960–7962, Oct. 1997.

[149] K.-Q. Xin, M. Urabe, J. Yang, K. Nomiyama, H. Mizukami, K. Hamajima, H. Nomiyama, T. Saito, M. Imai, J. Monahan, K. Okuda, K. Ozawa, and K. Okuda, "A Novel Recombinant Adeno-Associated Virus Vaccine Induces a Long-Term Humoral Immune Response to Human Immunodeficiency Virus," *Hum. Gene Ther.*, vol. 12, no. 9, pp. 1047–1061, Jun. 2001.

[150] E. Basner-Tschakarjan and F. Mingozzi, "Cell-Mediated Immunity to AAV Vectors, Evolving Concepts and Potential Solutions," *Front. Immunol.*, vol. 5, Jul. 2014.

[151] M. L. Hirsch, M. Agbandje-McKenna, and R. Jude Samulski, "Little Vector, Big Gene Transduction: Fragmented Genome Reassembly of Adeno-associated Virus," *Mol. Ther.*, vol. 18, no. 1, pp. 6–8, Jan. 2010.

[152] Z. Yan, Y. Zhang, D. Duan, and J. F. Engelhardt, "Trans-splicing vectors expand the utility of adeno-associated virus for gene therapy," *Proc. Natl. Acad. Sci. U. S. A.*, vol. 97, no. 12, pp. 6716–6721, Jun. 2000.

[153] Z. Wu, H. Yang, and P. Colosi, "Effect of Genome Size on AAV Vector Packaging," *Mol. Ther.*, vol. 18, no. 1, pp. 80–86, Jan. 2010.

[154] M. L. Hirsch, S. J. Wolf, and R. J. Samulski, "Delivering Transgenic DNA Exceeding the Carrying Capacity of AAV Vectors," in *Gene Therapy for Neurological Disorders*, vol. 1382, F. P. Manfredsson, Ed. New York, NY: Springer New York, 2016, pp. 21–39.

[155] D. M. McCarty, P. E. Monahan, and R. J. Samulski, "Self-complementary recombinant adeno-associated virus (scAAV) vectors promote efficient transduction independently of DNA synthesis," *Gene Ther.*, vol. 8, no. 16, pp. 1248–1254, Aug. 2001.

[156] J. Wu, W. Zhao, L. Zhong, Z. Han, B. Li, W. Ma, K. A. Weigel-Kelley, K. H. Warrington, and A. Srivastava, "Self-Complementary Recombinant Adeno-Associated Viral Vectors: Packaging Capacity And The Role of Rep Proteins in Vector Purity," *Hum. Gene Ther.*, vol. 18, no. 2, pp. 171–182, Feb. 2007.

[157] E. D. Papadakis, S. A. Nicklin, A. H. Baker, and S. J. White, "Promoters and control elements: designing expression cassettes for gene therapy," *Curr. Gene Ther.*, vol. 4, no. 1, pp. 89–113, Mar. 2004.

[158] Y. Kim, T. Kim, J. K. Rhee, D. Lee, K. Tanaka-Yamamoto, and Y. Yamamoto, "Selective transgene expression in cerebellar Purkinje cells and granule cells using adeno-associated viruses together with specific promoters," *Brain Res.*, vol. 1620, pp. 1–16, Sep. 2015.

[159] H. S. Gompf, E. A. Budygin, P. M. Fuller, and C. E. Bass, "Targeted genetic manipulations of neuronal subtypes using promoter-specific combinatorial AAVs in wild-type animals," *Front. Behav. Neurosci.*, vol. 9, Jul. 2015.

[160] Q. Lu, T. H. Ganjawala, E. Ivanova, J. G. Cheng, D. Troilo, and Z.-H. Pan, "AAV-mediated transduction and targeting of retinal bipolar cells with improved mGluR6 promoters in rodents and primates," *Gene Ther.*, May 2016.

[161] B. Hauck, L. Chen, and W. Xiao, “Generation and characterization of chimeric recombinant AAV vectors,” *Mol. Ther. J. Am. Soc. Gene Ther.*, vol. 7, no. 3, pp. 419–425, Mar. 2003.
[162] J. E. Rabinowitz, D. E. Bowles, S. M. Faust, J. G. Ledford, S. E. Cunningham, and R. J. Samulski, “Cross-dressing the virion: the transcapsidation of adeno-associated virus serotypes functionally defines subgroups,” *J. Virol.*, vol. 78, no. 9, pp. 4421–4432, May 2004.
[163] D. E. Bowles, J. E. Rabinowitz, and R. J. Samulski, “Marker rescue of adeno-associated virus (AAV) capsid mutants: a novel approach for chimeric AAV production,” *J. Virol.*, vol. 77, no. 1, pp. 423–432, Jan. 2003.
[164] X. Shen, T. Storm, and M. A. Kay, “Characterization of the Relationship of AAV Capsid Domain Swapping to Liver Transduction Efficiency,” *Mol. Ther.*, vol. 15, no. 11, pp. 1955–1962, Nov. 2007.
[165] L. Perabo, J. Endell, S. King, K. Lux, D. Goldnau, M. Hallek, and H. Büning, “Combinatorial engineering of a gene therapy vector: directed evolution of adeno-associated virus,” *J. Gene Med.*, vol. 8, no. 2, pp. 155–162, Feb. 2006.
[166] N. Maheshri, J. T. Koerber, B. K. Kaspar, and D. V. Schaffer, “Directed evolution of adeno-associated virus yields enhanced gene delivery vectors,” *Nat. Biotechnol.*, vol. 24, no. 2, pp. 198–204, Feb. 2006.
[167] H. Büning, A. Huber, L. Zhang, N. Meumann, and U. Hacker, “Engineering the AAV capsid to optimize vector–host-interactions,” *Curr. Opin. Pharmacol.*, vol. 24, pp. 94–104, Oct. 2015.
[168] L. Perabo, A. Huber, S. Märsch, M. Hallek, and H. Büning, “Artificial evolution with adeno-associated viral libraries,” *Comb. Chem. High Throughput Screen.*, vol. 11, no. 2, pp. 118–126, Feb. 2008.
[169] G. L. Rogers, A. T. Martino, G. V. Aslanidi, G. R. Jayandharan, A. Srivastava, and R. W. Herzog, “Innate Immune Responses to AAV Vectors,” *Front. Microbiol.*, vol. 2, 2011.
[170] E. S. Trombetta and I. Mellman, “CELL BIOLOGY OF ANTIGEN PROCESSING IN VITRO AND IN VIVO,” *Annu. Rev. Immunol.*, vol. 23, no. 1, pp. 975–1028, Apr. 2005.
[171] G. E. Hammer and A. Ma, “Molecular Control of Steady-State Dendritic Cell Maturation and Immune Homeostasis,” *Annu. Rev. Immunol.*, vol. 31, no. 1, pp. 743–791, Mar. 2013.
[172] A.-K. Zaiss, Q. Liu, G. P. Bowen, N. C. W. Wong, J. S. Bartlett, and D. A. Muruve, “Differential activation of innate immune responses by adenovirus and adeno-associated virus vectors,” *J. Virol.*, vol. 76, no. 9, pp. 4580–4590, May 2002.
[173] A. K. Zaiss, M. J. Cotter, L. R. White, S. A. Clark, N. C. W. Wong, V. M. Holers, J. S. Bartlett, and D. A. Muruve, “Complement is an essential component of the immune response to adeno-associated virus vectors,” *J. Virol.*, vol. 82, no. 6, pp. 2727–2740, Mar. 2008.
[174] M. Hösel, M. Broxtermann, H. Janicki, K. Esser, S. Arzberger, P. Hartmann, S. Gillen, J. Kleeff, D. Stabenow, M. Odenthal, P. Knolle, M. Hallek, U. Protzer, and H. Büning, “Toll-like receptor 2-mediated innate immune response in human nonparenchymal liver cells toward adeno-associated viral vectors,” *Hepatology*, vol. 55, no. 1, pp. 287–297, Jan. 2012.
[175] A. T. Martino, M. Suzuki, D. M. Markusic, I. Zolotukhin, R. C. Ryals, B. Moghimi, H. C. J. Ertl, D. A. Muruve, B. Lee, and R. W. Herzog, “The genome of self-complementary adeno-associated viral vectors increases Toll-like receptor 9-dependent innate immune responses in the liver,” *Blood*, vol. 117, no. 24, pp. 6459–6468, Jun. 2011.
[176] C. Li, Y. He, S. Nicolson, M. Hirsch, M. S. Weinberg, P. Zhang, T. Kafri, and R. J. Samulski, “Adeno-associated virus capsid antigen presentation is dependent on endosomal escape,” *J. Clin. Invest.*, vol. 123, no. 3, pp. 1390–1401, Mar. 2013.
[177] G. C. Pien, E. Basner-Tschakarjan, D. J. Hui, A. N. Mentlik, J. D. Finn, N. C. Hasbrouck, S. Zhou, S. L. Murphy, M. V. Maus, F. Mingozzi, J. S. Orange, and K. A. High, “Capsid antigen presentation flags human hepatocytes for destruction after transduction by adeno-associated viral vectors,” *J. Clin. Invest.*, vol. 119, no. 6, pp. 1688–1695, Jun. 2009.
[178] J. D. Finn, D. Hui, H. D. Downey, D. Dunn, G. C. Pien, F. Mingozzi, S. Zhou, and K. A. High, “Proteasome inhibitors decrease AAV2 capsid derived peptide epitope presentation on MHC

class I following transduction," *Mol. Ther. J. Am. Soc. Gene Ther.*, vol. 18, no. 1, pp. 135–142, Jan. 2010.
[179] L. E. Mays and J. M. Wilson, "The complex and evolving story of T cell activation to AAV vector-encoded transgene products," *Mol. Ther. J. Am. Soc. Gene Ther.*, vol. 19, no. 1, pp. 16–27, Jan. 2011.
[180] K. Erles, P. Sebökovà, and J. R. Schlehofer, "Update on the prevalence of serum antibodies (IgG and IgM) to adeno-associated virus (AAV)," *J. Med. Virol.*, vol. 59, no. 3, pp. 406–411, Nov. 1999.
[181] C. Li, N. Narkbunnam, R. J. Samulski, A. Asokan, G. Hu, L. J. Jacobson, M. J. Manco-Johnson, and P. E. Monahan, "Neutralizing antibodies against adeno-associated virus examined prospectively in pediatric patients with hemophilia," *Gene Ther.*, vol. 19, no. 3, pp. 288–294, Mar. 2012.
[182] R. Calcedo, H. Morizono, L. Wang, R. McCarter, J. He, D. Jones, M. L. Batshaw, and J. M. Wilson, "Adeno-associated virus antibody profiles in newborns, children, and adolescents," *Clin. Vaccine Immunol. CVI*, vol. 18, no. 9, pp. 1586–1588, Sep. 2011.
[183] F. Mingozzi and K. A. High, "Immune responses to AAV vectors: overcoming barriers to successful gene therapy," *Blood*, vol. 122, no. 1, pp. 23–36, Jul. 2013.
[184] C. S. Manno, V. R. Arruda, G. F. Pierce, B. Glader, M. Ragni, J. Rasko, M. C. Ozelo, K. Hoots, P. Blatt, B. Konkle, M. Dake, R. Kaye, M. Razavi, A. Zajko, J. Zehnder, H. Nakai, A. Chew, D. Leonard, J. F. Wright, R. R. Lessard, J. M. Sommer, M. Tigges, D. Sabatino, A. Luk, H. Jiang, F. Mingozzi, L. Couto, H. C. Ertl, K. A. High, and M. A. Kay, "Successful transduction of liver in hemophilia by AAV-Factor IX and limitations imposed by the host immune response," *Nat. Med.*, vol. 12, no. 3, pp. 342–347, Mar. 2006.
[185] F. Mingozzi and K. A. High, "Therapeutic in vivo gene transfer for genetic disease using AAV: progress and challenges," *Nat. Rev. Genet.*, vol. 12, no. 5, pp. 341–355, May 2011.
[186] A. T. Martino, E. Basner-Tschakarjan, D. M. Markusic, J. D. Finn, C. Hinderer, S. Zhou, D. A. Ostrov, A. Srivastava, H. C. J. Ertl, C. Terhorst, K. A. High, F. Mingozzi, and R. W. Herzog, "Engineered AAV vector minimizes in vivo targeting of transduced hepatocytes by capsid-specific CD8+ T cells," *Blood*, vol. 121, no. 12, pp. 2224–2233, Mar. 2013.
[187] F. Mingozzi, J. J. Meulenberg, D. J. Hui, E. Basner-Tschakarjan, N. C. Hasbrouck, S. A. Edmonson, N. A. Hutnick, M. R. Betts, J. J. Kastelein, E. S. Stroes, and K. A. High, "AAV-1-mediated gene transfer to skeletal muscle in humans results in dose-dependent activation of capsid-specific T cells," *Blood*, vol. 114, no. 10, pp. 2077–2086, Sep. 2009.
[188] K. Willett and J. Bennett, "Immunology of AAV-Mediated Gene Transfer in the Eye," *Front. Immunol.*, vol. 4, 2013.
[189] L. Zhong, B. Li, C. S. Mah, L. Govindasamy, M. Agbandje-McKenna, M. Cooper, R. W. Herzog, I. Zolotukhin, K. H. Warrington, K. A. Weigel-Van Aken, J. A. Hobbs, S. Zolotukhin, N. Muzyczka, and A. Srivastava, "Next generation of adeno-associated virus 2 vectors: Point mutations in tyrosines lead to high-efficiency transduction at lower doses," *Proc. Natl. Acad. Sci.*, vol. 105, no. 22, pp. 7827–7832, Jun. 2008.
[190] D. J. Hui, E. Basner-Tschakarjan, Y. Chen, R. J. Davidson, G. Buchlis, M. Yazicioglu, G. C. Pien, J. D. Finn, V. Haurigot, A. Tai, D. W. Scott, L. P. Cousens, S. Zhou, A. S. De Groot, and F. Mingozzi, "Modulation of CD8+ T cell responses to AAV vectors with IgG-derived MHC class II epitopes," *Mol. Ther.*, vol. 21, no. 9, Sep. 2013.
[191] A. S. De Groot, L. Moise, J. A. McMurry, E. Wambre, L. Van Overtvelt, P. Moingeon, D. W. Scott, and W. Martin, "Activation of natural regulatory T cells by IgG Fc-derived peptide 'Tregitopes,'" *Blood*, vol. 112, no. 8, pp. 3303–3311, Oct. 2008.
[192] E. Dobrzynski, "Induction of antigen-specific CD4+ T-cell anergy and deletion by in vivo viral gene transfer," *Blood*, vol. 104, no. 4, pp. 969–977, Apr. 2004.
[193] F. Mingozzi, Y.-L. Liu, E. Dobrzynski, A. Kaufhold, J. H. Liu, Y. Wang, V. R. Arruda, K. A. High, and R. W. Herzog, "Induction of immune tolerance to coagulation factor IX antigen by in vivo hepatic gene transfer," *J. Clin. Invest.*, vol. 111, no. 9, pp. 1347–1356, May 2003.

[194] O. Cao, E. Dobrzynski, L. Wang, S. Nayak, B. Mingle, C. Terhorst, and R. W. Herzog, “Induction and role of regulatory CD4+CD25+ T cells in tolerance to the transgene product following hepatic in vivo gene transfer,” *Blood*, vol. 110, no. 4, pp. 1132–1140, Aug. 2007.

[195] F. Mingozzi, N. C. Hasbrouck, E. Basner-Tschakarjan, S. A. Edmonson, D. J. Hui, D. E. Sabatino, S. Zhou, J. F. Wright, H. Jiang, G. F. Pierce, V. R. Arruda, and K. A. High, “Modulation of tolerance to the transgene product in a nonhuman primate model of AAV-mediated gene transfer to liver,” *Blood*, vol. 110, no. 7, pp. 2334–2341, Oct. 2007.

[196] A. W. Thomson and P. A. Knolle, “Antigen-presenting cell function in the tolerogenic liver environment,” *Nat. Rev. Immunol.*, vol. 10, no. 11, pp. 753–766, Nov. 2010.

[197] L. Franco, B. Sun, X. Yang, A. Bird, H. Zhang, A. Schneider, T. Brown, S. Young, T. Clay, and A. Amalfitano, “Evasion of Immune Responses to Introduced Human Acid α-Glucosidase by Liver-Restricted Expression in Glycogen Storage Disease Type II,” *Mol. Ther.*, vol. 12, no. 5, pp. 876–884, Nov. 2005.

[198] R. Ziegler, “AAV2 Vector Harboring a Liver-Restricted Promoter Facilitates Sustained Expression of Therapeutic Levels of α-Galactosidase A and the Induction of Immune Tolerance in Fabry Mice,” *Mol. Ther.*, vol. 9, no. 2, pp. 231–240, Feb. 2004.

[199] J. R. Mendell, K. Campbell, L. Rodino-Klapac, Z. Sahenk, C. Shilling, S. Lewis, D. Bowles, S. Gray, C. Li, G. Galloway, V. Malik, B. Coley, K. R. Clark, J. Li, X. Xiao, J. Samulski, S. W. McPhee, R. J. Samulski, and C. M. Walker, “Dystrophin Immunity in Duchenne’s Muscular Dystrophy,” *N. Engl. J. Med.*, vol. 363, no. 15, pp. 1429–1437, Oct. 2010.

[200] V. R. Arruda, J. Schuettrumpf, R. W. Herzog, T. C. Nichols, N. Robinson, Y. Lotfi, F. Mingozzi, W. Xiao, L. B. Couto, and K. A. High, “Safety and efficacy of factor IX gene transfer to skeletal muscle in murine and canine hemophilia B models by adeno-associated viral vector serotype 1,” *Blood*, vol. 103, no. 1, pp. 85–92, Jan. 2004.

[201] R. W. Herzog, P. A. Fields, V. R. Arruda, J. O. Brubaker, E. Armstrong, D. McClintock, D. A. Bellinger, L. B. Couto, T. C. Nichols, and K. A. High, “Influence of Vector Dose on Factor IX-Specific T and B Cell Responses in Muscle-Directed Gene Therapy,” *Hum. Gene Ther.*, vol. 13, no. 11, pp. 1281–1291, Jul. 2002.

[202] R. Herzog, “Muscle-Directed Gene Transfer and Transient Immune Suppression Result in Sustained Partial Correction of Canine Hemophilia B Caused by a Null Mutation,” *Mol. Ther.*, vol. 4, no. 3, pp. 192–200, Sep. 2001.

[203] F. Granucci, M. Foti, and P. Ricciardi-Castagnoli, “Dendritic cell biology,” *Adv. Immunol.*, vol. 88, pp. 193–233, 2005.

[204] R. M. Steinman and H. Hemmi, “Dendritic cells: translating innate to adaptive immunity,” *Curr. Top. Microbiol. Immunol.*, vol. 311, pp. 17–58, 2006.

[205] M. F. Lipscomb and B. J. Masten, “Dendritic Cells: Immune Regulators in Health and Disease,” *Physiol. Rev.*, vol. 82, no. 1, pp. 97–130, Jan. 2002.

[206] P. Veron, V. Allo, C. Riviere, J. Bernard, A.-M. Douar, and C. Masurier, “Major Subsets of Human Dendritic Cells Are Efficiently Transduced by Self-Complementary Adeno-Associated Virus Vectors 1 and 2,” *J. Virol.*, vol. 81, no. 10, pp. 5385–5394, May 2007.

[207] Y. Zhang, N. Chirmule, G. p Gao, and J. Wilson, “CD40 ligand-dependent activation of cytotoxic T lymphocytes by adeno-associated virus vectors in vivo: role of immature dendritic cells,” *J. Virol.*, vol. 74, no. 17, pp. 8003–8010, Sep. 2000.

[208] S. Ponnazhagan, G. Mahendra, D. T. Curiel, and D. R. Shaw, “Adeno-associated virus type 2-mediated transduction of human monocyte-derived dendritic cells: implications for ex vivo immunotherapy,” *J. Virol.*, vol. 75, no. 19, pp. 9493–9501, Oct. 2001.

[209] O. Shin, S. J. Kim, W. I. Lee, J. Y. Kim, and H. Lee, “Effective transduction by self-complementary adeno-associated viruses of human dendritic cells with no alteration of their natural characteristics,” *J. Gene Med.*, vol. 10, no. 7, pp. 762–769, Jul. 2008.

[210] K.-Q. Xin, H. Mizukami, M. Urabe, Y. Toda, K. Shinoda, A. Yoshida, K. Oomura, Y. Kojima, M. Ichino, D. Klinman, K. Ozawa, and K. Okuda, “Induction of Robust Immune Responses against Human

Immunodeficiency Virus Is Supported by the Inherent Tropism of Adeno-Associated Virus Type 5 for Dendritic Cells," *J. Virol.*, vol. 80, no. 24, pp. 11899–11910, Dec. 2006.

[211] G. V. Aslanidi, A. E. Rivers, L. Ortiz, L. Govindasamy, C. Ling, G. R. Jayandharan, S. Zolotukhin, M. Agbandje-McKenna, and A. Srivastava, "High-efficiency transduction of human monocyte-derived dendritic cells by capsid-modified recombinant AAV2 vectors," *Vaccine*, vol. 30, no. 26, pp. 3908–3917, Jun. 2012.

[212] R. Sayroo, D. Nolasco, Z. Yin, Y. Colon-Cortes, M. Pandya, C. Ling, and G. Aslanidi, "Development of novel AAV serotype 6 based vectors with selective tropism for human cancer cells," *Gene Ther.*, vol. 23, no. 1, pp. 18–25, Jan. 2016.

[213] M. Pandya, K. Britt, B. Hoffman, C. Ling, and G. V. Aslanidi, "Reprogramming Immune Response With Capsid-Optimized AAV6 Vectors for Immunotherapy of Cancer:," *J. Immunother.*, vol. 38, no. 7, pp. 292–298, Sep. 2015.

[214] G. Gernoux, M. Guilbaud, L. Dubreil, T. Larcher, C. Babarit, M. Ledevin, N. Jaulin, P. Planel, P. Moullier, and O. Adjali, "Early Interaction of Adeno-Associated Virus Serotype 8 Vector with the Host Immune System Following Intramuscular Delivery Results in Weak but Detectable Lymphocyte and Dendritic Cell Transduction," *Hum. Gene Ther.*, vol. 26, no. 1, pp. 1–13, Jan. 2015.

[215] L. E. Mays, L. Wang, J. Lin, P. Bell, A. Crawford, E. J. Wherry, and J. M. Wilson, "AAV8 Induces Tolerance in Murine Muscle as a Result of Poor APC Transduction, T Cell Exhaustion, and Minimal MHCI Upregulation on Target Cells," *Mol. Ther.*, vol. 22, no. 1, pp. 28–41, Jan. 2014.

[216] X. Xiao, J. Li, and R. J. Samulski, "Production of high-titer recombinant adeno-associated virus vectors in the absence of helper adenovirus," *J. Virol.*, vol. 72, no. 3, pp. 2224–2232, Mar. 1998.

[217] A. Salvetti, S. Orève, G. Chadeuf, D. Favre, Y. Cherel, P. Champion-Arnaud, J. David-Ameline, and P. Moullier, "Factors Influencing Recombinant Adeno-Associated Virus Production," *Hum. Gene Ther.*, vol. 9, no. 5, pp. 695–706, Mar. 1998.

[218] S. Zolotukhin, B. J. Byrne, E. Mason, I. Zolotukhin, M. Potter, K. Chesnut, C. Summerford, R. J. Samulski, and N. Muzyczka, "Recombinant adeno-associated virus purification using novel methods improves infectious titer and yield," *Gene Ther.*, vol. 6, no. 6, pp. 973–985, Jun. 1999.

[219] null Girod, null Ried, null Wobus, null Lahm, null Leike, null Kleinschmidt, null Deléage, and null Hallek, "Genetic capsid modifications allow efficient re-targeting of adeno-associated virus type 2," *Nat. Med.*, vol. 5, no. 12, p. 1438, Dec. 1999.

[220] S. Nicklin, "Efficient and Selective AAV2-Mediated Gene Transfer Directed to Human Vascular Endothelial Cells," *Mol. Ther.*, vol. 4, no. 3, pp. 174–181, Sep. 2001.

[221] M. Carpentier, S. Lorain, P. Chappert, M. Lalfer, R. Hardet, D. Urbain, C. Peccate, S. Adriouch, L. Garcia, J. Davoust, and D.-A. Gross, "Intrinsic transgene immunogenicity gears CD8(+) T-cell priming after rAAV-mediated muscle gene transfer," *Mol. Ther. J. Am. Soc. Gene Ther.*, vol. 23, no. 4, pp. 697–706, Apr. 2015.

[222] L. Perabo, "In vitro selection of viral vectors with modified tropism: the adeno-associated virus display," *Mol. Ther.*, vol. 8, no. 1, pp. 151–157, Jul. 2003.

[223] C. E. Wobus, B. Hügle-Dörr, A. Girod, G. Petersen, M. Hallek, and J. A. Kleinschmidt, "Monoclonal antibodies against the adeno-associated virus type 2 (AAV-2) capsid: epitope mapping and identification of capsid domains involved in AAV-2-cell interaction and neutralization of AAV-2 infection," *J. Virol.*, vol. 74, no. 19, pp. 9281–9293, Oct. 2000.

[224] R. Hardet, B. Chevalier, L. Dupaty, Y. Naïmi, G. Riou, L. Drouot, L. Jean, A. Salvetti, O. Boyer, and S. Adriouch, "Oral-tolerization Prevents Immune Responses and Improves Transgene Persistence Following Gene Transfer Mediated by Adeno-associated Viral Vector," *Mol. Ther.*, vol. 24, no. 1, pp. 87–95, Jan. 2016.

[225] K. C. McCullough, N. Ruggli, and A. Summerfield, "Dendritic cells—At the front-line of pathogen attack," *Vet. Immunol. Immunopathol.*, vol. 128, no. 1–3, pp. 7–15, Mar. 2009.

[226] L. Delamarre, "Differential Lysosomal Proteolysis in Antigen-Presenting Cells Determines Antigen Fate," *Science*, vol. 307, no. 5715, pp. 1630–1634, Mar. 2005.

[227] R. Liberman, S. Bond, M. G. Shainheit, M. J. Stadecker, and M. Forgac, “Regulated Assembly of Vacuolar ATPase Is Increased during Cluster Disruption-induced Maturation of Dendritic Cells through a Phosphatidylinositol 3-Kinase/mTOR-dependent Pathway,” *J. Biol. Chem.*, vol. 289, no. 3, pp. 1355–1363, Jan. 2014.

[228] A. Savina and S. Amigorena, “Phagocytosis and antigen presentation in dendritic cells,” *Immunol. Rev.*, vol. 219, no. 1, pp. 143–156, Oct. 2007.

[229] A. Savina, C. Jancic, S. Hugues, P. Guermonprez, P. Vargas, I. C. Moura, A.-M. Lennon-Duménil, M. C. Seabra, G. Raposo, and S. Amigorena, “NOX2 Controls Phagosomal pH to Regulate Antigen Processing during Crosspresentation by Dendritic Cells,” *Cell*, vol. 126, no. 1, pp. 205–218, Jul. 2006.

[230] A. Savina, A. Peres, I. Cebrian, N. Carmo, C. Moita, N. Hacohen, L. F. Moita, and S. Amigorena, “The Small GTPase Rac2 Controls Phagosomal Alkalinization and Antigen Crosspresentation Selectively in CD8+ Dendritic Cells,” *Immunity*, vol. 30, no. 4, pp. 544–555, Apr. 2009.

[231] B. C. Schnepp, K. R. Clark, D. L. Klemanski, C. A. Pacak, and P. R. Johnson, “Genetic Fate of Recombinant Adeno-Associated Virus Vector Genomes in Muscle,” *J. Virol.*, vol. 77, no. 6, pp. 3495–3504, Mar. 2003.

[232] P. J. de Pablo and M. Carrión-Vázquez, “Imaging Biological Samples with Atomic Force Microscopy,” *Cold Spring Harb. Protoc.*, vol. 2014, no. 2, p. pdb.top080473, Feb. 2014.

[233] T. Zhu, “Sustained Whole-Body Functional Rescue in Congestive Heart Failure and Muscular Dystrophy Hamsters by Systemic Gene Transfer,” *Circulation*, vol. 112, no. 17, pp. 2650–2659, Oct. 2005.

[234] Z. Wang, T. Zhu, C. Qiao, L. Zhou, B. Wang, J. Zhang, C. Chen, J. Li, and X. Xiao, “Adeno-associated virus serotype 8 efficiently delivers genes to muscle and heart,” *Nat. Biotechnol.*, vol. 23, no. 3, pp. 321–328, Mar. 2005.

[235] K. Inagaki, S. Fuess, T. A. Storm, G. A. Gibson, C. F. Mctiernan, M. A. Kay, and H. Nakai, “Robust systemic transduction with AAV9 vectors in mice: efficient global cardiac gene transfer superior to that of AAV8,” *Mol. Ther. J. Am. Soc. Gene Ther.*, vol. 14, no. 1, pp. 45–53, Jul. 2006.

[236] N. M. Kotchey, K. Adachi, M. Zahid, K. Inagaki, R. Charan, R. S. Parker, and H. Nakai, “A potential role of distinctively delayed blood clearance of recombinant adeno-associated virus serotype 9 in robust cardiac transduction,” *Mol. Ther. J. Am. Soc. Gene Ther.*, vol. 19, no. 6, pp. 1079–1089, Jun. 2011.

[237] Y. S. Gwak, J. Kang, J. W. Leem, and C. E. Hulsebosch, “Spinal AMPA receptor inhibition attenuates mechanical allodynia and neuronal hyperexcitability following spinal cord injury in rats,” *J. Neurosci. Res.*, vol. 85, no. 11, pp. 2352–2359, Aug. 2007.

[238] M. Antonietta Ajmone-Cat, M. Mancini, R. De Simone, P. Cilli, and L. Minghetti, “Microglial polarization and plasticity: Evidence from organotypic hippocampal slice cultures: Microglial Polarization and Tolerization,” *Glia*, vol. 61, no. 10, pp. 1698–1711, Oct. 2013.

[239] S. Hashemian, F. Marschinke, S. af Bjerkén, and I. Strömberg, “Degradation of proteoglycans affects astrocytes and neurite formation in organotypic tissue cultures,” *Brain Res.*, vol. 1564, pp. 22–32, May 2014.

[240] I. Spitzbarth, A. Cana, K. Hahn, F. Hansmann, and W. Baumgärtner, “Associated occurrence of p75 neurotrophin receptor expressing aldynoglia and microglia/macrophages in long term organotypic murine brain slice cultures,” *Brain Res.*, vol. 1595, pp. 29–42, Jan. 2015.

[241] W. P. Duprex, F. M. Collins, and B. K. Rima, “Modulating the Function of the Measles Virus RNA-Dependent RNA Polymerase by Insertion of Green Fluorescent Protein into the Open Reading Frame,” *J. Virol.*, vol. 76, no. 14, pp. 7322–7328, Jul. 2002.

VII. Acknowledgments

L'ensemble de mon travail de doctorat, ainsi que la proposition de ce manuscrit résultent d'une interaction constante avec un environnement scientifique et humain, riche et favorable. Je souhaite par ces quelques lignes remercier l'ensemble des personnes qui, au cours de ce long et fastidieux travail, ont su avec leurs mots et/ou leurs mains rendre cette aventure si passionnante.

Je tiens donc à remercier en premier lieu le Dr Anna Salvetti, qui m'a soutenu, le plus souvent contre moi-même, du premier au dernier jour de mon doctorat. Ses qualités de chercheuse, sa grande maitrise des techniques de laboratoire ainsi que sa bienveillance ont été d'une importance décisive dans l'avancement de ce projet.

I also want to thank my co-supervisor, PhD Hildegard Büning for having taken the risk to welcome in her laboratory a young French master student who never spoke English before. Her important knowledge, and her patience were also critical for the good execution of my project.

I really appreciated to do my PhD project under their supervision, indeed both of them let me conduct my project as I wanted to, without any limitation. I also could count on their full support for my popularization project. They were always available for my scientific or professional interrogations. I cannot imagine better conditions for my PhD.

Parmi les membres de l'équipe d'Anna, je voudrais d'abord remercier Ludovic Aillot et Célia Gallien qui ont travaillé avec moi sur ce projet. Ludovic est une personne stoïque, passionnée et possédant une parfaite technicité. Travailler avec lui fut pour moi un réel plaisir, j'espère avoir de nouvelles occasions de partager avec lui de si bons moments scientifiques. J'aimerais remercier Celia pour son enthousiasme qui fut déterminant dans mon choix de continuer en thèse. J'aimerais également remercier les autres membres de cette équipe : Hélène C, Héloïse A, Rachel M, Aurélie P, Alberto E, Anna G et Véronique B, pour leur soutien, inestimable dans les moments difficiles.

From the Hildegard's team, I want to thank Li-Ang Zhang who welcomed me in Cologne during my master and helped me a lot for my experiments. I learned a lot from him about science, life and humanity, and I would like to thank him for having taught me English, I just regret to keep his Chinese accent. I also want to thank the other members of the team who rendered my missions more interesting and pleasant: Anke H, Franciso JRR, Hanna J and Mariana H.

J'aimerais remercier les membres de mon comité de suivi de thèse, Dr Hélène Dutartre, Dr Marlène Dreux et Dr Sahil Adriouch qui ont su, par leur précieux conseils et interrogations, m'aider à orienter correctement ce projet. Les différentes conversations que j'ai pu avoir avec eux m'ont également aidées à voir plus clair dans ce milieu opaque qu'est le monde de la recherche scientifique.

I also want to thank my rapporteurs, PhD Dirk Grimm and PhD Jean Davoust who accepted to evaluate and criticize my research project. Their accurate reviewing allowed me to improve my PhD thesis.

Le travail de recherche que je propose ici, ne serait que l'ombre de lui-même sans les différentes collaborations que j'ai eu la chance de réaliser au cours de mon doctorat.

Je souhaite donc remercier le laboratoire de physique de l'ENS de Lyon, plus précisément le Dr Cendrine Moskalenko et son équipe qui m'ont permis d'aborder des thématiques transdisciplinaires que je trouve passionnantes. J'aimerais donc remercier Cendrine, Julien Bernaud, Anny Fis et Jorge Rodriguez Ramos pour leur enthousiasme à étudier les propriétés physiques et mécaniques des vecteurs AAV. Je reste convaincu que ces travaux auront d'importantes conséquences sur la manière de designer les vecteurs viraux à l'avenir.

Je souhaite également remercier l'institut de recherche et d'innovation biomédicale (iRiB), plus précisément le Dr Sahil Adriouch et Léa Dupaty pour leur importante contribution dans la caractérisation immunologique *in vivo* du mutant sélectionné. Je voudrais les remercier pour les différents échanges passionnants que nous avons eus ces derniers mois.

Je souhaite également remercier le Centre International de Recherche en Infectiologie (CIRI), plus précisément Jérémy Welsch pour l'initiation de la collaboration sur le modèle de culture *ex vivo* de cerveau de souris. L'enthousiasme de Jérémy et sa grande réactivité ont rendu cette prometteuse collaboration très enrichissante pour moi. J'ai hâte de suivre la poursuite de ces travaux.

Pour finir je souhaite remercier le collectif Mauvaise Foi, plus précisément Rémy Mattei (qui ne sait peut-être pas encore complètement dans quoi il a mis les pieds) pour notre projet de vulgarisation scientifique, portant sur le transfert de gène médié par les vecteurs viraux en bande dessinée. Je remercie donc Rémy pour son implication. Sa rapidité à comprendre les concepts biologique et son immense talent d'illustrateur permettront, j'en suis sûr, de mener à bien ce projet. Dans le cadre de cette collaboration je voudrais également remercier Isabelle Grosjean et Nancy Willkomm sans qui je n'aurai surement pas eu le financement de la Région Rhône-Alpes pour initier ce projet.

I also want to thank my personal proofreader, Manon Grosmaire for the hard work she have executed to read, understand and correct my manuscript.

J'aimerais remercier l'association des doctorants du CIRI (CIRI'Pamp), plus précisément Thibaut Deschamps, Vincent Grass, Chloé Mengardi et Sonia Assil toujours motivés, disponibles et enthousiastes pour initier de nouvelles collaborations ou se lancer dans des initiatives estudiantines diverses et variées. Leur présence au sein du CIRI a permis, en ce qui me concerne, de créer une dynamique que je n'aurais pas retrouvée sans eux.

J'aimerais remercier l'ensemble des personnes que le doctorat a mis sur mon chemin, et avec qui j'ai pu au détour d'un couloir, partager un café (ou une cigarette) et refaire le monde : Eloise T, Mohamed I, Delphine B, Jérôme S, Baptiste P, Gerges R, Philipe M, Emiliano R, Amandine P, Fabrice M, Brian W, Steven M, Claire B, Romain B, Erica U, Agnès N, Emma R, François R, Roulio B, Natali AS, Anaïs C, Charlotte S, Baptiste G, Roxane L, Roberta M, Valentin A, Sandrine A, Julie S.

Cette liste serait incomplète si je ne remerciais pas les personnes qui compte le plus pour moi, l'ensemble des personnes qui font que je me tiens encore debout aujourd'hui et que j'aime le plus, ma famille et mon « sanctuaire », sans eux qui me suivent depuis plusieurs années, la question de devenir ou non Docteur ne se serait certainement jamais posée.

Je souhaite également remercier l'accueil du Dr Théophile Ohlmann et du Dr François-Loïc Cosset qui m'ont permis de finir ma thèse au sein du CIRI.

J'aimerais finaliser mes remerciements en citant la Région Rhône-Alpes (ARC-1 : Infectiologie) pour avoir financé mon projet de recherche ainsi que mon projet de vulgarisation scientifique.

IX. Publications